A COMPARATIVE STUDY ON STABILITY AND OVERTOPPING PERFORMANCES OF RESHAPING BERM BREAKWATERS

A THESIS SUBMITTED TO
THE GRADUATE SCHOOL OF NATURAL AND APPLIED SCIENCES
OF
MIDDLE EAST TECHNICAL UNIVERSITY

BY

SEMİH BEZAZOĞLU

IN PARTIAL FULFILLMENT OF THE REQUIREMENTS
FOR
THE DEGREE OF MASTER OF SCIENCE
IN
CIVIL ENGINEERING

SEPTEMBER 2016

Approval of the thesis:

A COMPARATIVE STUDY ON STABILITY AND OVERTOPPING PERFORMANCES OF RESHAPING BERM BREAKWATERS

submitted by **SEMİH BEZAZOĞLU** in partial fulfillment of the requirements for the degree of **Master of Science in Civil Engineering Department, Middle East Technical University** by,

Prof. Dr. Gülbin Dural Ünver
Dean, Graduate School of **Natural and Applied Sciences** _____

Prof. Dr. İsmail Özgür Yaman
Head of Department, **Civil Engineering** _____

Asst. Prof. Dr. Cüneyt Baykal
Supervisor, **Civil Engineering Department, METU** _____

Dr. Işıkhan Güler
Co-Supervisor, **Civil Engineering Department, METU** _____

Examining Committee Members:

Prof. Dr. Ahmet Cevdet Yalçıner _____
Civil Eng. Dept., METU

Asst. Prof. Dr. Cüneyt Baykal _____
Civil Eng. Dept., METU

Prof. Dr. Melih Yanmaz _____
Civil Eng. Dept., METU

Asst. Prof. Dr. Gülizar Özyurt Tarakcıoğlu _____
Civil Eng. Dept., METU

Assoc. Prof. Dr. Kubilay Cihan _____
Civil Eng. Dept., Kırıkkale University

Date: 06.09.2016

I hereby declare that all information in this document has been obtained and presented in accordance with academic rules and ethical conduct. I also declare that, as required by these rules and conduct, I have fully cited and referenced all material and results that are not original to this work.

Name, Last Name : Semih Bezazoğlu

Signature :

ABSTRACT

A COMPARATIVE STUDY ON STABILITY AND OVERTOPPING PERFORMANCES OF RESHAPING BERM BREAKWATERS

Bezazoğlu, Semih

M.S., Department of Civil Engineering

Supervisor: Asst. Prof. Dr. Cüneyt Baykal

Co-Supervisor: Dr. Işıkhan Güler

September 2016, 127 pages

Berm type rubble mound breakwaters are preferred by engineers due to their relative advantages in economy and implementation compared to conventional rubble mound breakwaters. In this study, a previously constructed hardly reshaping berm breakwater protecting a filling area used as an airport between Ordu and Giresun cities in the Black Sea Region is compared to several alternative reshaping (partly or fully) models under the same stability and serviceability conditions by physical model experiments.

In the first part of the study, results of physical model experiments are discussed in terms of damage parameter and recession, which are found to be in agreement with the findings given in the literature. In the second part, serviceability conditions of the

selected models are investigated by analysing wave overtopping discharges and comparing overtopping results with available design formulations. In the final part of the study, the cumulative damage development on the alternative cross-sections is studied. Moreover, the relation between the damage and wave overtopping is examined under the cumulative damage condition of models. According to cumulative damage analysis, cross-sections reach equilibrium approximately at the end of 8000 waves. According to the results when the damage increases on the structure, overtopping discharges do not change significantly. Results of this study show that Ordu-Giresun hardly reshaping berm breakwater might be designed as a reshaping berm breakwater with the same stability and serviceability conditions.

Keywords: berm breakwaters, recession, wave overtopping, cumulative damage, physical model experiments

ÖZ

ŞEKİL DEĞİŞTİREN BASAMAK TİPİ DALGAKIRANLARIN DENGE VE DALGA AŞMASI BAŞARIMLARI ÜZERİNE KARŞILAŞTIRMALI BİR ÇALIŞMA

Bezazoğlu, Semih

Yüksek Lisans, İnşaat Mühendisliği Bölümü

Tez Yöneticisi: Yrd. Doç. Dr. Cüneyt Baykal

Ortak Tez Yöneticisi: Dr. Işıkhan Güler

Eylül 2016, 127 sayfa

Basamak tipi taş dolgu dalgakıranlar ekonomi ve uygulamadaki avantajları nedeniyle mühendisler tarafından tercih edilmektedir. Bu çalışmada daha önce Karadeniz Bölgesi'nde, Ordu ve Giresun şehirleri arasında havalimanı olarak kullanılan dolgu alanını koruyan zor şekil değiştiren basamak tipi dalgakıran olarak inşa edilmiş dalgakıran aynı denge ve dalga aşması koşulları altında fiziksel model deneyleri vasıtasıyla şekil değiştirebilen (kısmen ya da tamamen) çeşitli alternatif kesit modelleri ile karşılaştırılmıştır.

Çalışmanın ilk kısmında fiziksel model deneylerinin sonuçları hasar ve geri çekilme parametreleri açısından tartışılmıştır. Sonuçlar literatürde verilen kaynaklarla uyumlu

bulunmuştur. Çalışmanın ikinci kısmında seçilmiş modellerin işletilebilirlik koşulları aşan dalga debilerinin analizi ve aşma sonuçlarının mevcut tasarım formülleriyle kıyaslanması yoluyla incelenmiştir. Çalışmanın son kısmında alternatif kesitlerdeki birikimli hasar oluşumu çalışılmıştır. Ayrıca modellerin birikimli hasar durumunda, hasar ve dalga aşması arasındaki ilişkisi de incelenmiştir. Birikimli hasar analizine göre kesitler yaklaşık olarak 8000 dalga sonunda dengeye ulaşmaktadır. Sonuçlara göre yapıdaki hasar artarsa yapının üzerinden aşan debi belirgin bir şekilde değişmemektedir. Bu çalışmanın sonuçları göstermektedir ki Ordu-Giresun zor şekil değiştiren basamak tipi dalgakıranı aynı denge ve işletilebilirlik şartları altında şekil değiştirebilen basamak tipi dalgakıran olarak tasarlanabilmektedir.

Anahtar Kelimeler: basamak tipi dalgakıranlar, geri çekilme, dalga aşması, birikimli hasar, fiziksel model deneyleri

To my beloved family…

ACKNOWLEDGEMENTS

I would like to begin with expressing my deepest gratitude to Prof. Dr. Ayşen Ergin. She was encouraging at each step of my studies and she enlightened my way as showing how to be an optimistic person.

I would like to extend my sincere thanks to Prof. Dr. Ahmet Cevdet Yalçıner. He always guided me in my graduate program.

It is a great chance to be a student of Assist. Prof. Dr. Cüneyt Baykal. I appreciate his help and guidance throughout my studies. His practical experience taught me a lot in the discussions of this study.

I am thankful to Assist. Prof. Dr. Gülizar Özyurt Tarakcıoğlu. I appreciate her advice and encouragement throughout the research.

I would like to express my gratitude to Dr. Işıkhan Güler for his continuous support and discussions on my study. He always shared his experience.

I would like to express my sincere thanks to Gökhan Güler, throughout the years of my graduate study he offered his welcome all the time and his scholarly advice whenever I asked for. For all, I will always be grateful. Without his encouragement and insightful comments, this thesis would not have been completed.

It is a pleasure to be a part of Coastal and Ocean Engineering Lab Family. I would like to thank my friends Çağıl Kirezci, Ebru Demirci, Duha Metin, Ezgi Çınar, and Deniz Can Aydın for both cheerful and challenging times we shared through 3 years.

I would like to express my sincere thanks to our lab staff Arif Kayışlı, Yusuf Korkut and Nuray Sefa.

I would like to extend my deepest thanks to Doğukan Atak that we actually walk in this way together. It would be impossible to finish this study without him.

I would like to thank my friends Duygu Simser, Deniz Kenan Kılıç, Cüneyt Ercan, Mert Özdemir, and Gürsel Demir. They supported, encouraged, helped me and shared every important moment of this period.

I am sincerely thankful to Özgür Akarsu for his understanding and patience. During the course of my master studies, his kindness and generosity prevented me from falling to pieces and helped me to finish my study.

I would like to thank my father Zafer Bezazoğlu who always wanted me to get a master's degree. I know he is always watching me. Finally, I would like to thank my mother Türkan Bezazoğlu. She always supported me more than enough. I owe her everything I could succeed.

TABLE OF CONTENTS

LIST OF TABLES

LIST OF FIGURES

LIST OF SYMBOLS

H_s	Incident significant wave height
Δ	Relative buoyant density of the stone
ρ_a	Density of stone
ρ_w	Density of water
D_{n50}	Nominal diameter of the armour stone
M_{50}	Median stone mass
S_d	Damage parameter
Rec	Recession of the berm
T_m	Mean wave period
f_g	Gradation factor
f_d	Depth factor
d	Water depth in front of the breakwater
D_{n15}	Diameter of the armour stone assuming a 15% cumulative distribution
D_{n85}	Diameter of the armour stone assuming a 85% cumulative distribution
g	Gravitational acceleration
N	Number of waves
h_{br}	Berm elevation above still water level

B	Berm width
f_{H0}	Influence of stability index including wave period
α	Front slope angle
f_N	Influence of number of waves
$f_{grading}$	Influence of stone gradation
h_b	Height of berm
f_β	Influence of wave direction
β	Angle between the wave direction and the breakwater trunk centreline
f_{hb}	Influence of berm height
h_s	Step height
S_{0m}	Wave steepness
h_t	Water depth above toe
q	Average wave overtopping discharge per unit width
ξ_0	Breaker parameter
R_c	Free crest height above still water line
γ_b	Influence factor for influence of berm
γ_f	Influence factor for roughness elements
γ_β	Influence factor for angle of wave attack
γ_v	Influence factor for vertical wall on slope
$T_{m-1,0}$	Spectral wave period at the toe of the structure

CHAPTER 1

INTRODUCTION

Coastal areas have vital importance on the development of the civilization since they provide people's needs in both materially and spiritually. Therefore, it is a need for people to protect coastal areas by coastal defence structures. Breakwaters, one of the most common coastal defence structures, can be divided into different categories such as rubble mound, piled, vertical wall, and floating breakwaters. Rubble mound breakwaters are the most popular breakwaters around the world due to its construction convenience. Although the construction process is easier than the other types of breakwaters, in certain conditions, such as the bathymetrical conditions in terms of increasing water depth, the lack of the available quarries, severe wave conditions, and environmental conditions, the construction of a conventional rubble mound breakwater might be challenging for engineers. Therefore, scientists have searched for new techniques to overcome this challenging situation. In the early 1980s, a new type of rubble mound breakwater, berm breakwater, has entered to the coastal engineering profession and the popularity of berm breakwaters has increased day by day (Sigurdarson et al., 2011). The biggest advantage of a berm breakwater compared to a conventional breakwater is the provision of the stability condition with smaller size of stones while a conventional breakwater needs larger stone sizes. Therefore, this situation results in the construction of more economical breakwaters having same service conditions. The construction of breakwaters with larger stone sizes requires much more money and labour force. Moreover, the procurement of larger stones instead of smaller stones is also a challenging issue. Therefore,

structures with smaller sizes gain a vital importance among the rubble mound breakwaters.

The construction of berm breakwaters increases around the world, and one of the examples of berm breakwaters constructed in Turkey is namely Ordu-Giresun berm breakwater, designed as an airport protection structure. Ordu-Giresun berm breakwater is a “Hardly Reshaping” berm breakwater which means that the damage on the armour layer of the cross-section is very limited under 100-years design wave condition according to the classification criteria. The main purpose of this study is to test the feasibility of existing Ordu-Giresun berm breakwater whether it would be constructed cheaper or not. In other words, it is aimed to investigate Ordu-Giresun berm breakwater by designing alternative sections with smaller stone sizes whether the alternative sections provide the same stability and serviceability conditions of Ordu-Giresun berm breakwater or not.

There are several formulations that are used to design berm breakwaters. However, physical modelling is highly recommended to complete design work and to observe the performance of the design section under design wave conditions; thus, it helps engineer to optimize the design. In this study, physical modelling of alternative sections for Ordu-Giresun berm breakwater is conducted in order to observe the structural behaviour, and in order to propose a more economic design.

In Chapter 2, the previous studies for berm breakwater concept are presented. Types of berm breakwaters and main parameters that are considered in the design of berm breakwaters are discussed. Moreover, the formulations which are used for the determination of wave overtopping are discussed.

The importance of hydraulic modelling and model scale calculations are presented at the beginning of Chapter 3. The experimental setup used in the wave flume of Middle East Technical University Coastal and Harbour Engineering Laboratory, information on the wave generation, wave, profile, and overtopping measurements is given. Furthermore, studied cross sections are presented at the end of Chapter 3.

In Chapter 4, the results obtained from both experiments and calculations are presented. Stability investigations of the alternative models are presented in terms of damage parameter and recession. Cumulative damage analyses of alternative sections are presented as a result of video recording assessments. Wave overtopping measurements are compared with calculations according to well-known design formulations, and results are discussed in this chapter. Moreover, the relationship between wave overtopping and stability is investigated at the end of this chapter.

In Chapter 5, the conclusions and future recommendations are given.

CHAPTER 2

LITERATURE SURVEY

In coastal engineering, rubble mound breakwaters have great importance as being one of the most common types of coastal defence structures. Rubble mound breakwaters are composed of mainly two types, conventional rubble mound breakwaters and berm breakwaters. Conventional breakwaters are single sloped breakwaters; on the other hand, berm breakwaters can have multiple slopes and have a berm above or below the water on the seaside. Berm breakwaters have gained significant popularity in the last decades. In time, several researchers and engineers have studied berm breakwaters, and concluded their advantages such as:

- Stability condition can be satisfied with smaller armour stones.
- As a result of smaller stone sizes, the cost of construction decreases.
- Berm reduces wave run up and overtopping. The berm breakwater concept is also studied by Ergin et al. (1989) and the results of the study indicates that the damage and wave run up values of the berm type sections are lower than the single sloped sections.
- Wave reflection is reduced in the narrow port entrances; and thus, navigational safety is increased.
- Berm type cross-sections can be used as a repair method for damaged conventional rubble mound breakwaters. To illustrate, a berm construction is determined as a repair method for Samandağ fishing port in order to prevent the collapse of the breakwater (Günbak et al., 1988).

Abovementioned advantages of berm breakwaters motive researchers and engineers to develop the berm breakwater concept and with time the construction of berm breakwaters has spread all around the world. Constructed berm breakwaters around the world by year 2006 are presented in Table 2.1. Moreover, Sirevag berm breakwater in Norway and Ordu-Giresun berm breakwater in Turkey are given as examples in Figure 2.1, and Figure 2.2, respectively.

Table 2.1: List of constructed berm breakwaters (BB), (Sigurdarson et al., 2006)

Country	Number of constructed BB	The year the construction of the first BB finished
Iceland	29	1984
Canada	5	1984
USA	4	1984
Australia	4	1986
Brazil	2	1990
Norway	6	1991
Faroe Islands	1	1992
Iran	8	1996
Madeira	1	1996
China	1	1999
India	1	2003
Denmark	1	2003

Figure 2.1: Sirevag berm breakwater in Norway.

(Adopted from www.researchgate.net/figure/266260481_fig4_Figure-5)

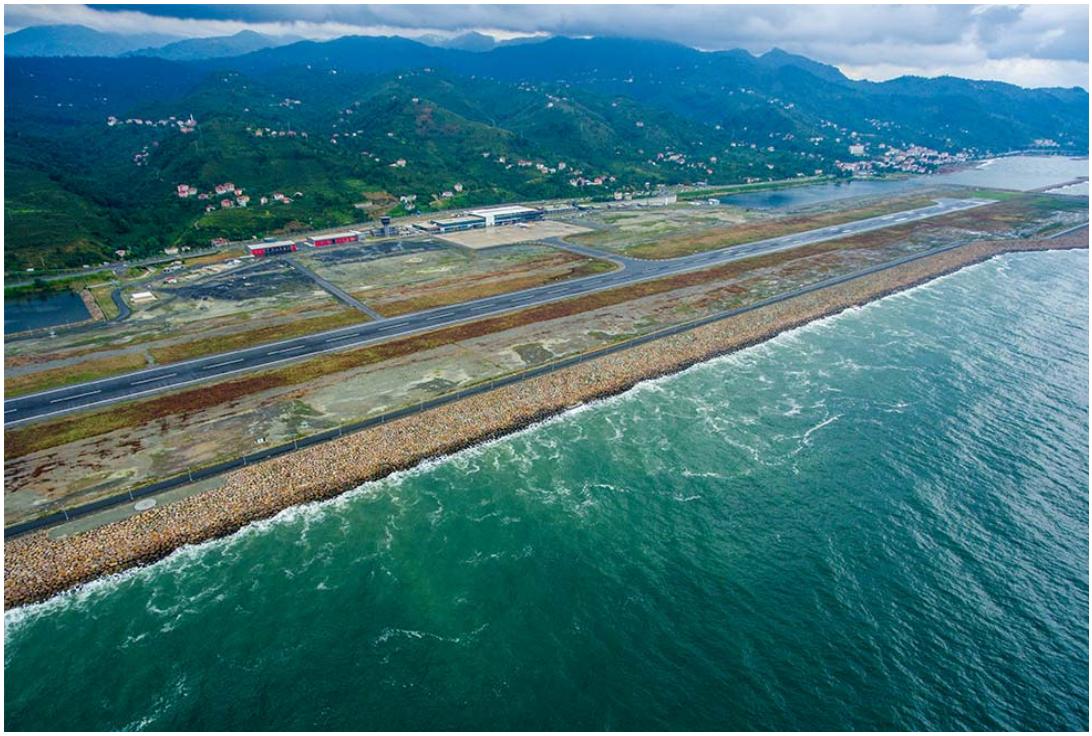

Figure 2.2: Ordu-Giresun berm breakwater in Turkey.

(Adopted from www.dhmi.gov.tr/fotogaleri.aspx?hv=54#.)

2.1. Classification of the Berm Breakwaters

Berm breakwaters are divided into different categories by different authors during the development period. PIANC (2003) divided the berm breakwaters into three categories:

- Statically stable non-reshaped.
- Statically stable reshaped.
- Dynamically stable reshaped.

Since PIANC (2003) classification focused only on the reshaping behaviour of the berm breakwaters, some modifications were necessary to improve the classification. Sigurdarson and Van der Meer (2012) modified the PIANC (2003) classification by focusing on the structural behaviour. As a result of the modification, classification introduces two types at the beginning, mass armoured, MA, and Icelandic-type, IC, berm breakwaters. Mass armoured berm breakwaters are commonly composed of one stone class with a wide range; however, Icelandic-type berm breakwaters are composed of more than one stone class with a narrow range. After that, the classification involves the structural behaviour due to reshaping difference of these two types. Therefore, Sigurdarson and Van der Meer (2012) conclude the classification into four types of berm breakwaters:

- Hardly reshaping Icelandic-type berm breakwater HR-IC
- Partly reshaping Icelandic-type berm breakwater PR-IC
- Partly reshaping mass armoured berm breakwater PR-MA
- Fully reshaping mass armoured berm breakwater FR-MA

Table 2.2 shows the classification for berm breakwaters stated by Sigurdarson and Van der Meer (2012).

Table 2.2: Classification of berm breakwaters based on 100-years wave condition

	Abbreviation	$H_s/\Delta D_{n50}$	S_d	Rec/D_{n50}
Hardly reshaping Icelandic-type berm breakwater	HR-IC	1.7 - 2.0	2 - 8	0.5 - 2
Partly reshaping Icelandic-type berm breakwater	PR-IC	2.0 - 2.5	10 - 20	1 - 5
Partly reshaping mass armoured berm breakwater	PR-MA	2.0 -2.5	10 - 20	1 - 5
Fully reshaping mass armoured berm breakwater	FR-MA	2.5 - 3.0	-	3 - 10

In Table 2.2, $H_s/\Delta D_{n50}$ is the stability number, H_s is the incident significant wave height, Δ is the relative buoyant density of the stone ($\Delta = (\rho_a/\rho_w)-1$), ρ_a is the density of stone, ρ_w is the density of water, D_{n50} is the nominal diameter of the armour stone ($D_{n50} = (M_{50}/\rho_a)^{1/3}$), M_{50} is the median stone mass, S_d is the damage parameter, and Rec is the recession of the berm.

2.2. Design of the Berm Breakwaters

Berm breakwaters include several geometrical parameters in the design period; however, mainly two parameters govern the design named as recession and overtopping.

2.2.1. Recession at Berm Breakwaters

Recession has a great importance in the stability investigation of the berm breakwaters. Researchers defined the recession as the reduction in the width of the berm. Recession for a berm breakwater is shown in Figure 2.3.

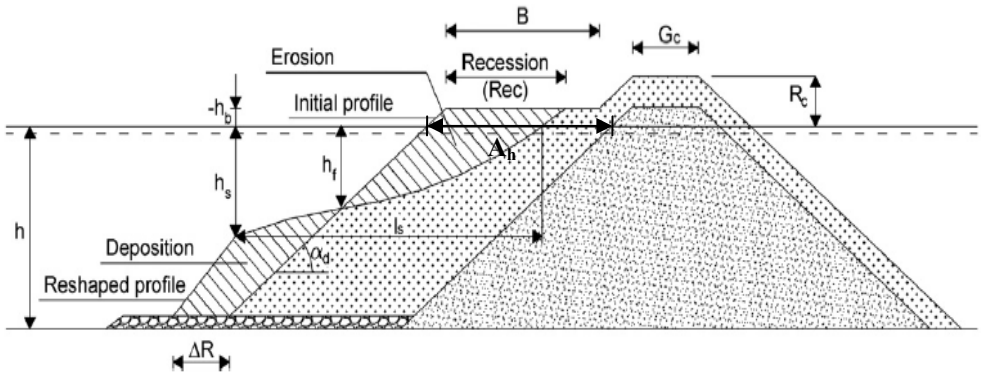

Figure 2.3: Demonstration of recession for a berm breakwater (Lykke Andersen et al., 2010)

Van der Meer (1988), Torum and Krogh (2000), Moghim et al. (2011), and Shekari et al. (2012) studied and presented formulas for recession in the development of berm breakwater concept. Furthermore, Lykke Andersen et al. (2014) have presented a formula to calculate the recession for berm breakwaters that considers more parameters than the other formulas. The validation area of Lykke Andersen et al. (2014) formulae is larger than the other formulas and the formula provides usually reliable results. Moreover, Lykke Andersen et al. (2014) formula provides a solution for the application in the very deep water situations.

Formulas proposed by Torum and Krogh (2000) for breaking waves are presented in Equations [2.1]-[2.6] and parameters related to formulas are given in Table 2.3.

$$\frac{\mathrm{Re}\,c}{D_{n50}} = 2.7 \cdot 10^{-6} (H_0 T_0)^3 + 9 \cdot 10^{-6} (H_0 T_0)^2 + 0.11 (H_0 T_0) - f_{grading} - f_d \qquad [2.1]$$

$$H_0 = \frac{H_s}{\Delta D_{n50}} \qquad [2.2]$$

$$T_0 = T_m \sqrt{\frac{g}{D_{n50}}} \qquad [2.3]$$

$$f_{grading} = \left(-9.9 f_g^{\ 2} + 23.9 f_g - 10.5\right) \quad [2.4]$$

$$f_g = \frac{D_{n85}}{D_{n15}} \quad [2.5]$$

$$f_d = -0.16\left(\frac{d}{D_{n50}}\right) + 4 \quad [2.6]$$

Table 2.3: Parameters in Torum and Krogh (2000) formula

Symbol	**Parameter**
H_s	Significant wave height
Δ	Relative buoyant density
T_m	Mean wave period
f_g	Gradation factor
f_d	Depth factor
d	Water depth in front of the breakwater
D_{n50}	Nominal diameter of the armour stone
D_{n15}	Diameter of the armour stone assuming a 15% cumulative distribution
D_{n85}	Diameter of the armour stone assuming a 85% cumulative distribution
g	Gravitational acceleration

Formulas proposed by Moghim et al. (2011) are presented in Equations [2.7]-[2.10] and parameters related to formulas are given in Table 2.4.

For $H_0\sqrt{T_0} < 17$:

$$\frac{\mathrm{Re}c}{D_{n50}} = \left(10.4\left(H_0\sqrt{T_0}\right)^{0.14} - 13.6\right)\cdot\left(1.61 - \exp\left[-2.2\frac{N}{3000}\right]\right)\cdot\left(\frac{h_{br}}{H_s}\right)^{-0.2}\cdot\left(\frac{d}{D_{n50}}\right)^{0.56} \quad [2.7]$$

For $H_0\sqrt{T_0} \geq 17$:

$$\frac{\mathrm{Re}c}{D_{n50}} = \left(0.089H_0\sqrt{T_0} + 0.49\right)\cdot\left(1.61 - \exp\left[-2.2\frac{N}{3000}\right]\right)\cdot\left(\frac{h_{br}}{H_s}\right)^{-0.2}\cdot\left(\frac{d}{D_{n50}}\right)^{0.56} \quad [2.8]$$

$$H_0 = \frac{H_s}{\Delta D_{n50}} \quad [2.9]$$

$$T_0 = T_m\sqrt{\frac{g}{D_{n50}}} \quad [2.10]$$

Table 2.4: Parameters in Moghim et al. (2011) formula

Symbol	**Parameter**
H_s	Significant wave height
Δ	Relative buoyant density
T_m	Mean wave period
N	Number of waves
h_{br}	Berm elevation above SWL
d	Water depth in front of the breakwater
D_{n50}	Nominal diameter of the armour stone
g	Gravitational acceleration

Formulas proposed by Shekari et al. (2012) are presented in Equations [2.11]-[2.13] and parameters related to formulas are given in Table 2.5.

$$\frac{\mathrm{Re}c}{D_{n50}} = \left(-0.016\left(H_0\sqrt{T_0}\right)^2 + 1.59H_0\sqrt{T_0} - 9.86\right)\cdot\left(1.72 - \exp\left[-2.19\frac{N}{3000}\right]\right)$$

$$\left(\frac{h_{br}}{H_s}\right)^{-0.21}\cdot\left(\frac{B}{D_{n50}}\right)^{-0.15} \qquad [2.11]$$

$$H_0 = \frac{H_s}{\Delta D_{n50}} \qquad [2.12]$$

$$T_0 = T_m\sqrt{\frac{g}{D_{n50}}} \qquad [2.13]$$

Table 2.5: Parameters in Shekari et al. (2012) formula

Symbol	**Parameter**
H_s	Significant wave height
Δ	Relative buoyant density
T_m	Mean wave period
N	Number of waves
h_{br}	Berm elevation above SWL
B	Berm width
D_{n50}	Nominal diameter of the armour stone
g	Gravitational acceleration

Formulas proposed by Lykke Andersen et al. (2014) are presented in Equations [2.14]-[2.25] and parameters related to formulas are given in Table 2.6.

$$\frac{\mathrm{Re}c}{D_{n50}} = f_{hb}\left[\frac{2.2h_t^* - 1.2h_s}{h_t^* - h_b} f_N f_\beta f_{H0} f_{grading} + \frac{[\cot(\alpha) - 1.05]}{2D_{n50}} \times \left[h_b - h_t^*\right]\right] \qquad [2.14]$$

$$h_s = 0.65 H_{m0} S_{0m}^{-0.3} f_N f_\beta \qquad [2.15]$$

$$f_N = \left(\frac{N}{3000}\right)^{\varphi} \qquad \varphi = \begin{cases} 0.30 & for \quad H_0\sqrt{T_0} \le 24 \\ 0.64 - 0.0143 H_0\sqrt{T_0} & for \quad 24 > H_0\sqrt{T_0} > 40 \\ 0.07 & for \quad H_0\sqrt{T_0} \ge 40 \end{cases} \qquad [2.16]$$

$$f_\beta = \cos(\beta) \qquad [2.17]$$

$$\begin{aligned} f_{grading} &= 1 && for \quad f_g \le 1.5 \\ f_{grading} &= 0.43 f_g + 0.355 && for \quad 1.5 < f_g \le 2.5 \\ f_{grading} &= 1.43 && for \quad f_g > 2.5 \end{aligned} \qquad [2.18]$$

$$f_{H0} = \min\left(\begin{array}{c} -4.7\times10^{-5}\left(H_0\sqrt{T_0}\right)^4 + 1.6\times10^{-3}\left(H_0\sqrt{T_0}\right)^3 + 2.2\times10^{-2}\left(H_0\sqrt{T_0}\right)^2 + 3.8\times10^{-2} H_0\sqrt{T_0} \\ 0.429 H_0\sqrt{T_0} + 12 \end{array} \right) \qquad [2.19]$$

$$f_{hb} = \begin{cases} 1 & for \quad \dfrac{h_b}{H_{m0}} \le 0.1 \\ 1.18 \times \exp\left(-1.64 \times \dfrac{h_b}{H_{m0}}\right) & for \quad \dfrac{h_b}{H_{m0}} > 0.1 \end{cases} \qquad [2.20]$$

$$h_t^* = \min\left(h_t \ ; \ \sqrt{\frac{2\,\mathrm{Re}\,c_1}{\cot(\alpha_d) - 1.05} \times \left[1.2 h_s - 2.2 h_{b*}\right] + h_{b*}^{\ 2}} \right) \qquad [2.21]$$

$$h_{b*} = \min\left(h_b \ ; \ 0.0\right) \qquad [2.22]$$

$$\frac{\mathrm{Re}\,c_1}{D_{n50}} = f_{H0} \cdot f_\beta \cdot f_N \cdot f_{grading} \qquad [2.23]$$

$$H_0 = \frac{H_s}{\Delta D_{n50}} \qquad [2.24]$$

$$T_0 = T_m \sqrt{\frac{g}{D_{n50}}} \qquad [2.25]$$

Table 2.6: Parameters in Lykke Andersen et al. (2014) formula

Symbol	**Parameter**
f_{H0}	Influence of stability index including wave period
d	Water depth
α	Front slope angle
f_N	Influence of number of waves
$f_{grading}$	Influence of stone gradation
h_b	Height of berm
f_β	Influence of wave direction
β	Angle between the wave direction and the breakwater trunk centreline
f_{hb}	Influence of berm height
h_s	Step height
S_{0m}	Wave steepness
N	Number of waves
h_t	Water depth above toe
f_g	Influence of stone grading (D_{n85} / D_{n15})
H_s	Significant wave height
Δ	Relative buoyant density
T_m	Mean wave period
D_{n15}	Diameter of the armour stone assuming a 15% cumulative distribution
D_{n85}	Diameter of the armour stone assuming a 85% cumulative distribution
g	Gravitational acceleration

2.2.2. Overtopping at Berm Breakwaters

Another important parameter in the design of berm breakwaters is wave overtopping. In the literature, several methods are given by design manuals to compute mean overtopping discharge. TAW (2002) is one of the manuals used for wave overtopping. Equation [2.26] is the formula given for rubble mound structures with a single slope (TAW, 2002).

$$\frac{q}{\sqrt{g\,H_{m0}^{\;3}}} = \frac{0.067}{\sqrt{\tan\alpha}} \cdot \gamma_b \cdot \zeta_0 \cdot \exp\left(-4.3 \frac{R_c}{H_{m0}} \frac{1}{\zeta_0 \cdot \gamma_b \cdot \gamma_f \cdot \gamma_\beta \cdot \gamma_v} \right) \qquad [2.26]$$

The parameters related to TAW (2002) formula are given in Table 2.7.

Table 2.7: Parameters in TAW (2002) formula

Symbol	**Parameter**
q	Average wave overtopping discharge per unit width
g	Acceleration due to gravity
H_{m0}	Significant wave height at the toe of the structure
tanα	Slope
ξ_0	Breaker parameter
s_0	Wave steepness
R_c	Free crest height above still water line
γ_b	Influence factor for influence of berm
γ_f	Influence factor for roughness elements
γ_β	Influence factor for angle of wave attack
γ_v	Influence factor for vertical wall on slope

Another wave overtopping calculation manual is EurOtop Manual (2007). Equation [2.27] is the formula for rubble mound structures with a single slope given in EurOtop Manual (2007).

$$\frac{q}{\sqrt{g\,H_{m0}^{\;3}}} = \frac{0.067}{\sqrt{\tan\alpha}} \cdot \gamma_b \cdot \zeta_{m-1,0} \cdot \exp\left(-4.75 \frac{R_c}{H_{m0}} \frac{1}{\zeta_{m-1,0} \cdot \gamma_b \cdot \gamma_f \cdot \gamma_\beta \cdot \gamma_v} \right) \qquad [2.27]$$

The parameters related to EurOtop Manual (2007) formula are given in Table 2.8.

Table 2.8: Parameters in EurOtop Manual (2007) formula

Symbol	**Parameter**
q	Average wave overtopping discharge per unit width
g	Acceleration due to gravity
H_{m0}	Significant wave height at the toe of the structure
tanα	Slope
$\xi_{m-1,0}$	Breaker parameter
s_0	Wave steepness
R_c	Free crest height above still water line
γ_b	Influence factor for influence of berm
γ_f	Influence factor for roughness elements
γ_β	Influence factor for angle of wave attack
γ_v	Influence factor for vertical wall on slope

Moreover, EurOtop Manual (2007) leads the designer to use the Neural Network named as CLASH (Verhaeghe et al., 2005) for the prediction of the overtopping at berm breakwaters. CLASH is the database including about 10000 overtopping results of tests collected from several laboratories (Van Gent et al., 2006). Since a large number of parameters are included in CLASH, parameters are divided into two

groups named as wave field and geometrical shape of the structure. The spectral significant wave height at the toe of the structure (H_{m0}), the mean spectral wave period at the toe of the structure ($T_{m-1,0}$), and the direction of wave attack (β), are the parameters related to the description of the wave field. Furthermore, the water depth in front of the structure (h), the water depth at the toe of the structure (h_t), the width of the toe (B_t), the roughness of the armour layer (γ_f), the slope of the structure downward of the berm ($\cot\alpha_d$), the slope of the structure upward of the berm ($\cot\alpha_u$), the width of the berm (B), the water depth on the berm (h_b), the slope of the berm ($\tan\alpha_b$), the crest freeboard of the structure (R_c), the armour crest freeboard of the structure (A_c), and the crest width of the structure (G_c) (Van Gent et al., 2006). CLASH (Verhaeghe, et al., 2005) covers more geometrical parameters for the determination of overtopping, thus, it can give more reliable results rather than TAW (2002) and EurOtop Manual (2007) for berm breakwaters.

The input parameters used in CLASH (Verhaeghe et al., 2005) is shown in detail in Figure 2.4.

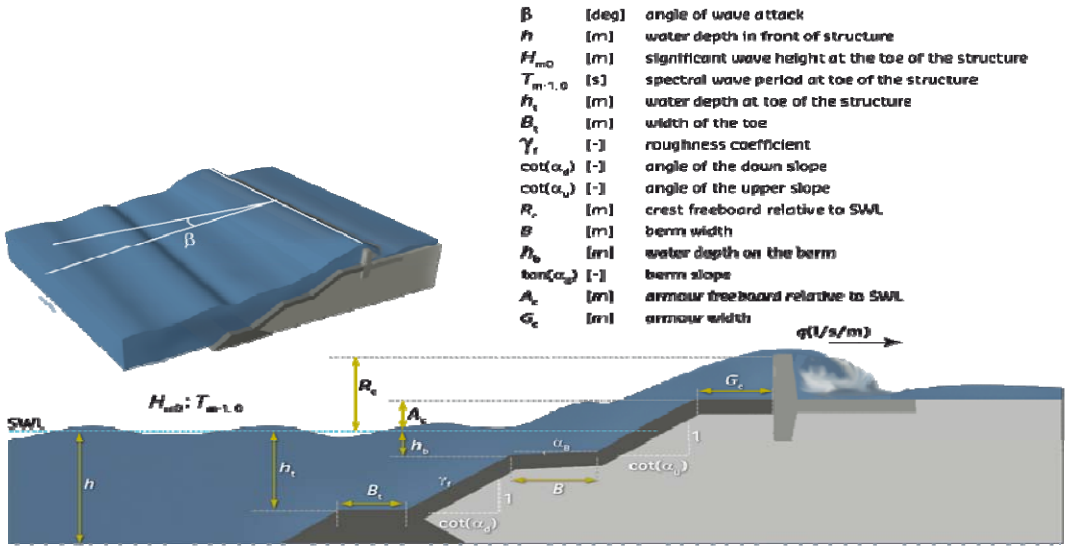

Figure 2.4: Input parameters for wave overtopping in CLASH (Verhaeghe, 2005) (Adopted from www.nn-overtopping.deltares.nl)

In addition to these available overtopping calculation guidelines, Sigurdarson and Van der Meer (2012) have developed a formula for berm breakwaters.

Formula proposed by Sigurdarson and Van der Meer (2012) is presented in Equations [2.28]-[2.30].

$$\frac{q}{\sqrt{g\,H_{m0}^{\;3}}} = 0.2 \cdot \exp\left(-2.6\,\frac{R_c}{H_{m0} \cdot \gamma_{BB} \cdot \gamma_{\beta}} \right) \qquad [2.28]$$

$\gamma_{BB} = 0.68 - 4.5s_{op} - 0.05B/H_s$ for HR and PR [2.29]

$\gamma_{BB} = 0.70 - 9.0s_{op}$ for FR [2.30]

The parameters in the formula proposed by Sigurdarson and Van der Meer (2012) are given in Table 2.9.

Table 2.9: Parameters in formula proposed by Sigurdarson and Van der Meer (2012)

Symbol	**Parameter**
q	Average wave overtopping discharge per unit width
g	Acceleration due to gravity
H_{m0}	Significant wave height at the toe of the structure
S_{op}	Peak wave steepness
R_c	Free crest height above still water line
B	Berm width
γ_{BB}	Influence factor for berm breakwater
γ_{β}	Influence factor for angle of wave attack

The main difference of Sigurdarson and Van der Meer (2012) overtopping formula is the influence factor for berm breakwater (γ_{BB}). The influence factor for berm

breakwater considers the reshaping of the breakwater and its effect to the wave overtopping while other methods do not include.

CHAPTER 3

PHYSICAL MODEL EXPERIMENTS

Hydraulic modelling plays an important role on the design and development of the coastal structures. The definition of the physical model may vary from engineer to engineer. A physical model is a physical system reproduced usually with a small-scale; thus, main forces acting on the system are represented in the model in correct proportion to the actual physical system (Hughes, 1993).

3.1. Advantages and Disadvantages of Physical Model Experiments

There are some advantages and disadvantages of physical experiments in terms of laboratory and modelling conditions.

Hughes (1993) summarizes the advantages of the physical model experiments by taking the discussions of Dalrymple (1985), Kamphius (1991), and Le Mehaute (1990) into consideration as follows:

- Data collection of the small size models reduces the cost while prototype data collection is more expensive and difficult to achieve (Dalrymple, 1985).
- Integration of the appropriate equations governing the process without assumptions in analytical or numerical models is provided with physical models (Dalrymple, 1985).

- Observation of a physical model during operation helps the researcher to improve a qualitative impression for understanding of the physical processes (Kamphius, 1991).
- Considering the size of the coastal projects model studies are cost effective. Moreover, in the decision making process physical models increase the reliability (Le Mehaute, 1990).
- Physical relationships in modelling will be well-understood with improving technology (Le Mehaute, 1990).
- Physical models let one to control and measure the physics in a controlled environment (Le Mehaute, 1990).
- Physical modelling helps engineer to develop more creative solutions (Le Mehaute, 1990).
- Complex boundary conditions are reproduced by physical models beyond the accuracy of finite step differences (Le Mehaute, 1990).

On the other hand, there are also disadvantages of physical models, and these are summarized by Hughes (1993) as follows:

- Scale effects occur due to the differences between model and prototype if all relevant variables are not simulated in correct relationship (Le Mehaute, 1990). Inaccurately scaled parameters, such as fluid density, may cause serious problems in the reflection of forces in the nature.
- Since it is impossible to simulate the natural environment in the laboratory, laboratory effects may affect the physical experiment results (Hughes, 1993).
- In the physical models, it may be impossible to act all forces to the models, such as wind force (Hughes, 1993).
- Numerical model simulations are cheaper than the physical model experiments (Hughes, 1993).

3.2. Model Scale

In most of the coastal engineering problems, viscosity and surface tension forces do not play significant roles while the inertia and gravitational forces are governing forces. Therefore, Froude Law is often applied to coastal engineering physical models (Hughes, 1993). Froude Law indicates that Froude numbers of both model (m) and prototype (p) must be equal to each other. Froude number is expressed in Equation [3.1]:

$$F_r^{\,2} = \frac{u^2}{gd} \qquad [3.1]$$

In Equation [3.1], u is the velocity of water particle, g is the gravitational acceleration, and d is the water depth.

The condition between the model and the prototype is given in Equation [3.2].

$$(F_r)_p = (F_r)_m \qquad [3.2]$$

Length scale (λ_L) is the ratio of the length in model (L_m) to the real length of the prototype (L_p) and given by Equation [3.3]. Time scale (λ_T) is also given by Equation [3.4].

$$\lambda_L = \frac{L_m}{L_p} \qquad [3.3]$$

$$\lambda_T = \sqrt{\lambda_L} \qquad [3.4]$$

In order to define the weight scale of armour units correctly, stability numbers in both prototype and model must be equal to each other (Hudson et al., 1979). Weight scale (λ_W) is presented in Equation [3.5].

$$\lambda_W = \left(\lambda_L{}^3\right)\frac{(\gamma_r)_m}{(\gamma_r)_p}\left[\frac{(\gamma_r)_p/(\gamma_w)_p - 1}{(\gamma_r)_m/(\gamma_w)_m - 1}\right]^3 \qquad [3.5]$$

$(\gamma_r)_m$ = unit weight of stone used in model, 2.7 t/m³

$(\gamma_r)_p$ = unit weight of stone used in prototype, 2.55 t/m³

$(\gamma_w)_m$ = unit weight of water used in model, 1.0 t/m³

$(\gamma_w)_p$ = unit weight of water used in prototype, 1.025 t/m³

There are several limitations affecting the selection of the model scale such as depth of water at wave flume and available stone sizes. After taking into consideration these factors, length scale is determined as 1:32.8625. Time and weight scales are determined accordingly using the equations given above. Model scale factors are given in Table 3.1.

Table 3.1: Scale factors used in models

Length	λ_L = 1:32.8625
Time	λ_T = 1:5.7326
Weight	λ_W = 1:50002

3.3. Experimental Setup

In this study, Ordu-Giresun hardly reshaping berm breakwater is compared to alternative cross-sections of fully and partly reshaping berm breakwaters focusing on damage and wave overtopping. Physical model experiments are conducted in the wave flume of Middle East Technical University (METU) Coastal and Harbour Engineering Laboratory. Wave channel is 28.8 meters in length, 6.2 meters in width

and 1.0 meter in depth. An inner channel is constructed by glass and plywood walls in the wave flume to reduce the size of the cross-section and the reflection effects occurring due to side walls of bigger channel. The inner channel is composed of two channels 18.0 meters in length, 0.75 meter in width and 1.0 meter in depth, separated by plywood walls. A piston type wave generator which is capable of producing irregular waves is placed at one end of the wave channel. Moreover, on the other end wave absorbers are placed to reduce the effect of reflected waves. Layout of the wave channel is given in Figure 3.1.

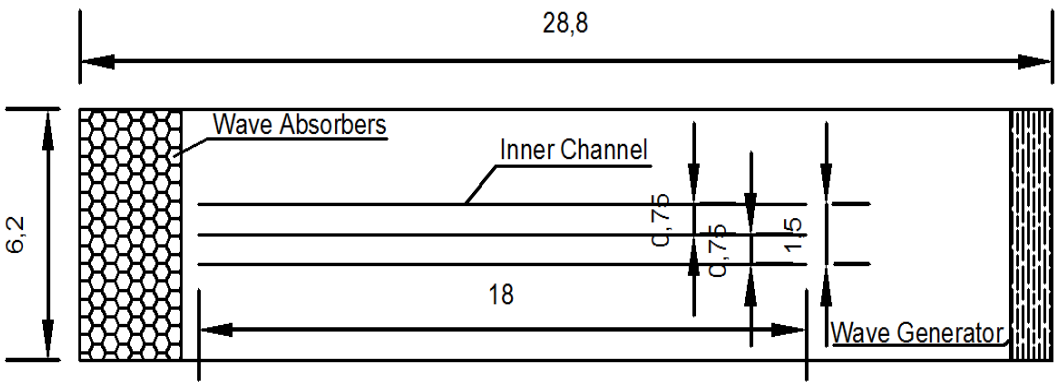

Figure 3.1: Layout of the wave channel

(Dimensions are in meters and figure is not to scale.)

In Figure 3.2, the wave flume of METU Coastal and Harbour Engineering Laboratory, the inner channel of the wave flume, and wave absorbers at the end of the channel are shown. The piston type wave generator and a wave gauge are given in Figure 3.3.

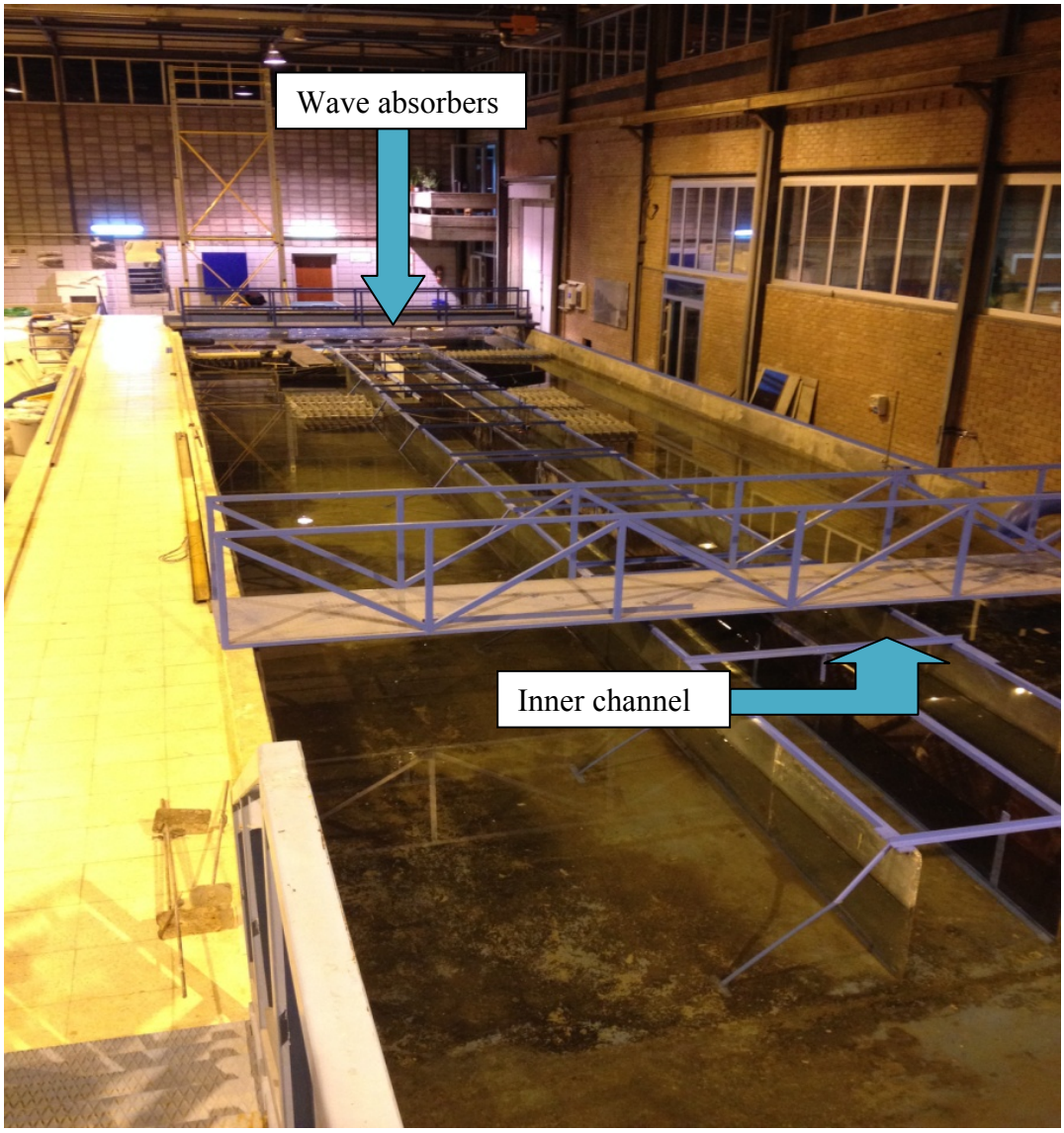

Figure 3.2: Wave channel, inner channel and wave absorbers

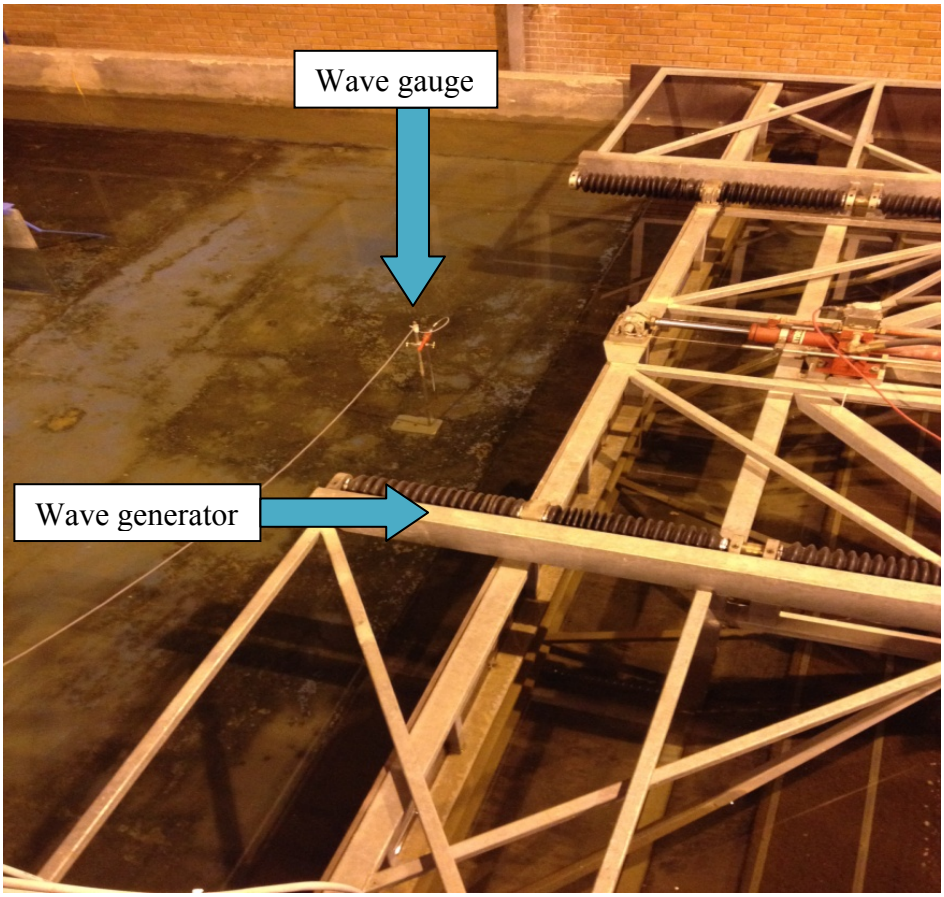

Figure 3.3: Piston type wave generator and wave gauge

In order to calibrate the test wave conditions in the channel and to observe the effects of reflection in the channel without the structures, first, a 1:20 sea bottom slope is constructed in both inner channels of 0.75 m in width. The wave gauges which will be used to measure the wave heights at the toe of the structure are placed at the onshore end of the bottom slope in both channels. The test wave conditions are generated and measured in the empty channels with the sea bottom slope only. Figure 3.4 and Figure 3.5 show the locations of the wave gauges and the sea bottom slope as a sketch of the channel and as a photo, respectively. After the test wave conditions are calibrated in the empty channels, the cross-sections that will be tested are constructed in one of the inner channels and tested one by one in that channel,

while keeping the other inner channel empty with the slope only. The placement of one of the test cross-sections and overtopping water collection system, the conduit and the tank, is given in Figure 3.6.

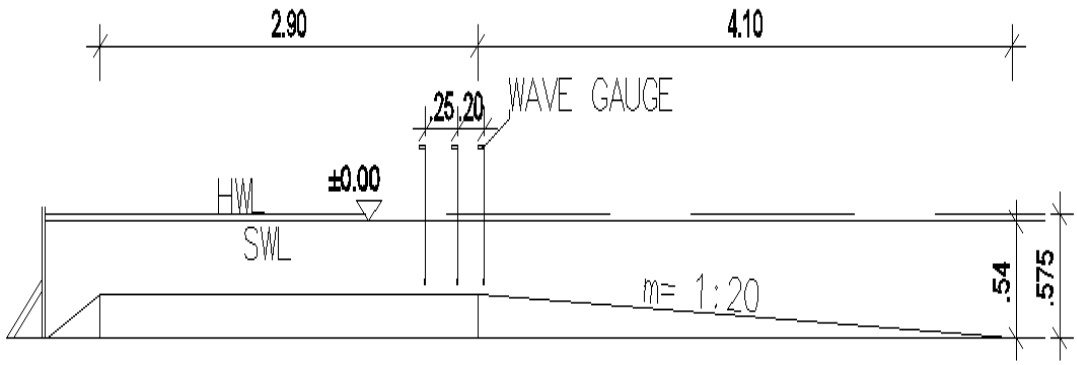

Figure 3.4: Sea bottom slope placement to the empty wave channel (without any structure)

(Dimensions are in meters and figure is not to scale.)

Figure 3.5: 1:20 slope in the wave channel

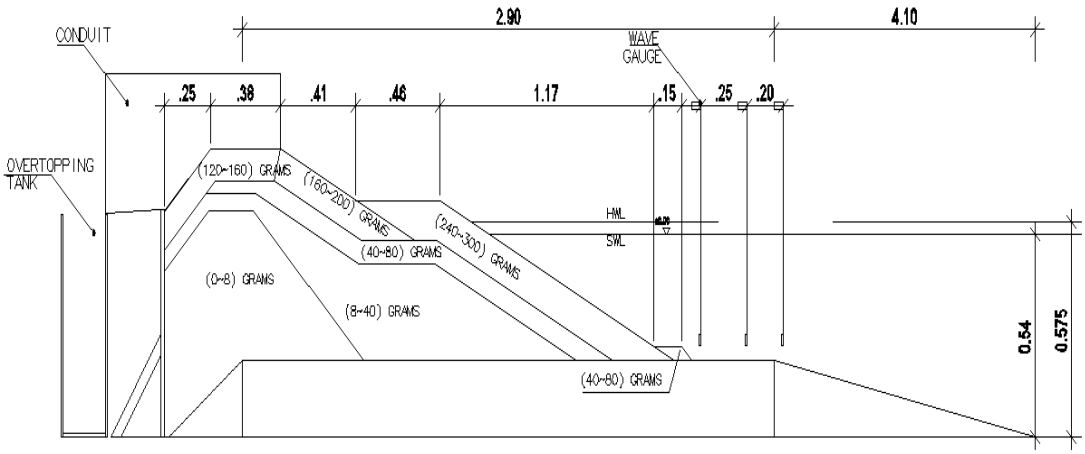

Figure 3.6: Sea bottom slope placement to wave channel with structure (Model 1)

(Dimensions are in meters and figure is not to scale.)

Wave Generator

Piston type wave generator has mainly three parts. First of all, wave synthesizer is the software that controls the wave generator. It converts to digital wave motion data to analog data. Secondly, converted analog signals are transferred to the piston by hydraulic servo actuator. Thirdly, the piston pressure is maintained by hydraulic power pack.

Wave Gauges and Water Level Measurements

The objectives of wave gauge are to measure the hydraulic waves and water level. The wave gauge has two parallel steel rods measuring the voltage differences. These voltage measurements are transmitted and recorded in the computer as a ".txt" file by the software written by TDG Scientific Measuring Ltd. (2016). The gauges must be placed vertical with respect to bottom and immersed by approximately half length of the gauge relative to the water level to get reliable results. Moreover, gauges must be placed well away from the channel boundaries to eliminate the boundary effects from sides and all gauges must be cleaned before the test to remove any possible substances (lime, etc.) remained on the measuring rods.

In the physical model experiments, eleven DHI-202 type wave gauges (60 cm long) are used to measure water level fluctuations. One of the gauges is placed in front of the wave generator to measure the wave properties at the generation. Three gauges are placed to the channel at the offshore end of bottom slope to observe reflection at deeper water conditions. Three gauges are placed in front of the structure to measure the wave characteristics acting on the structure. Four gauges are placed in the other inner channel to observe the reflection effects. The gauges are placed as groups for the analysis of the wave reflection given by Goda and Suzuki (1976).

In order to define the relationship between the recorded voltage measurements and water surface elevation calibration must be conducted. Three point (above still water

level (+), at still water level (0), below still water level (-)) calibration procedure is done in the model experiments at the beginning of each test. The process can be summarized as follows:

- Fill the channel above the still water level used in the physical models. Ensure the water level is stabilized and record the data.
- Discharge the channel until it reaches to the still water level. Ensure the water level is stabilized and record the data.
- Discharge the channel under the still water level. Ensure the water level is stabilized and record the data.

After completion of the procedure stated above, calibration coefficients are obtained by MATLAB. According to the voltage measurements which are recorded at three points for the calibration process are analyzed in MATLAB. Every voltage record is matched with the related water levels. After repeating this process for three points a calibration line is composed and calibration coefficients are obtained.

Profile Measurements

To measure the damage in the breakwater cross-sections, profile measurements have been carried out along the cross-section. In the profile measurements, the change in the height of the cross-section with respect to a reference point and along a line perpendicular to wave action is measured. Profile measurements are conducted at the beginning and at the end of each test. The profiles are measured with a laser meter at 5 cm intervals along three lines for Model 1 and 2 cm intervals along three lines for other models.

Eroded area (A_e) is the areal difference between the profile measurements carried out before and after the test. From the profile measurements, eroded areas for the sections are obtained and thus, damage parameter (S) is determined. Area erosion example is given in Figure 3.7.

Van der Meer (1988) defines the damage parameter by using Broderick's study (1984) in Equation [3.6]:

$$S = \frac{A_e}{D_{n50}^{\ 2}} \qquad [3.6]$$

In Equation [3.6], S is the damage parameter, A_e is the eroded area of the section, and D_{n50} is the nominal diameter of the armour stone.

In the calculations, damage parameter is obtained by averaging the damage parameters of all three lines.

Moreover, photos of the sections are taken at the beginning and at the end of each test in order to observe the change in the sections visually. In addition, video records are taken from the side view of the sections for all of the tests.

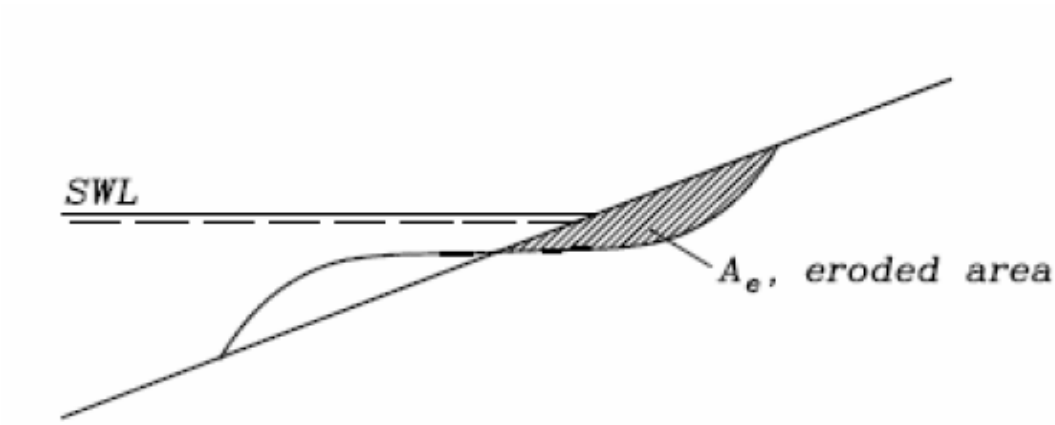

Figure 3.7: An example of eroded area (Coastal Engineering Manual, 2003)

Overtopping Measurements

In the model experiments, a conduit (Figure 3.8) of 25 cm in width is placed on the crest of berm breakwater and an overtopping tank is placed behind the breakwater so

that overtopping water is collected via the conduit. Overtopping quantities are determined by measuring the mass of the overtopping water. Later, the overtopped volume is converted to the wave overtopping discharge.

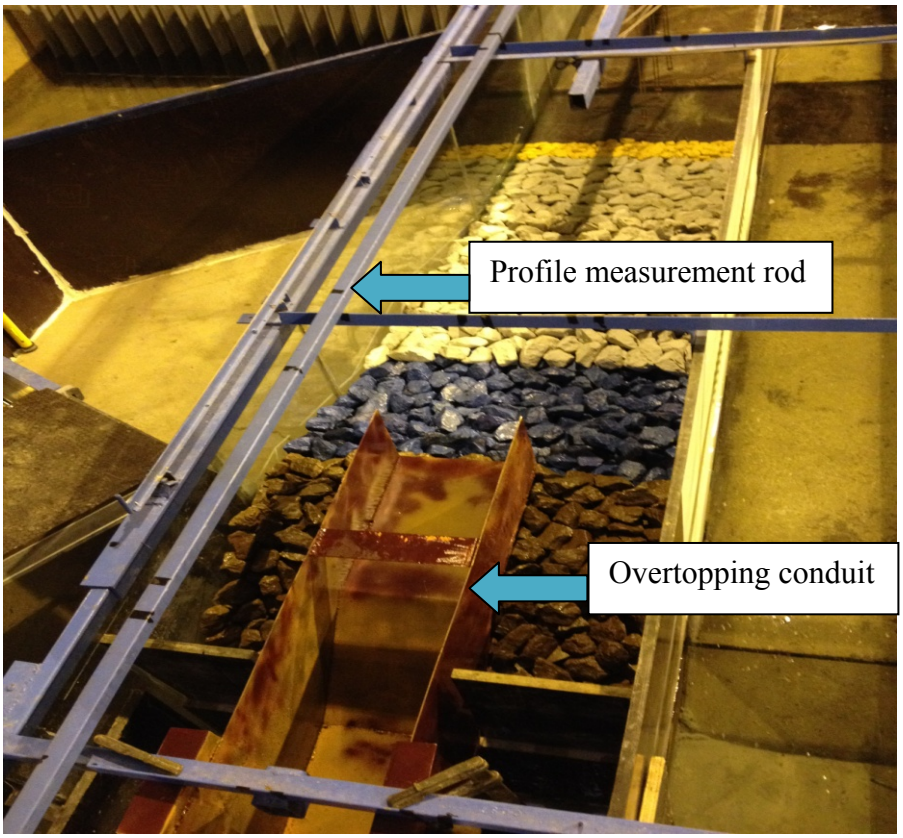

Figure 3.8: Overtopping conduit and profile measurement rod

3.4. Generation and Analysis of Waves

In the physical model experiments, a 6 m long piston type wave generator is used. The wave generator has a vertical paddle which makes a user-defined random or regular oscillatory motion in one horizontal direction depending on the type of waves

to be generated. In order to obtain the desired wave characteristics, a digital signal, time series of paddle position, is inputted to the software, the wave generation system transforms this digital signal to an analog signal followed by the paddle.

In the generation of the irregular waves, firstly, a target frequency spectrum must be determined. In the physical models, the time series of water level fluctuations and thus, the time series of paddle position for the generation of random waves are computed in MATLAB. In this study, Bretschneider-Mitsuyasu type spectrum is chosen as the target wave spectrum, given by Equation [3.7]. Computed spectral density values associated with wave series are converted to the spectral density values associated with piston movement time series. Finally, the spectral density values associated with piston movement time series are converted to piston movement time series. During this procedure, the spectral density values associated with wave series are also converted to a wave time series, and analyzed in order to check computations (CE 593 Lecture Notes, 2014).

$$S(f) = 0.257\, H_{1/3}{}^{2}\, T_{1/3}{}^{-4}\, f^{-5} \exp\left\{-1.03\left(T_{1/3}\, f\right)^{-4}\right\} \qquad [3.7]$$

In Equation [3.7], $H_{1/3}$ is significant wave height, $T_{1/3}$ is significant wave period, f is wave frequency, and S is spectral wave energy.

After the calculation of the time series and generation of waves in the flume, the water level fluctuations measured by the wave gauges during the tests should be analyzed. The analysis of the raw data is performed by zero-up crossing method.

In Section 3.3, it is stated that wave gauges are placed as couples to analyze the wave reflection. Wave reflection is an important concept in physical model experiments, especially in the experiments of reflective or impervious structures such as vertical quay walls, caisson type breakwaters, and in cases where an active wave absorption system is not present in the wave generation system and therefore, multi wave reflection occurs in the wave channel. In this study, the wave generation system lacks an active wave absorption system and the cross-sections tested have a vertical wall

behind the section representing the fill area behind the actual breakwater of Ordu-Giresun airport. The incident and reflected wave heights are determined via MATLAB according to the method given by Goda and Suzuki (1976).

In the physical model experiments, 1 set is defined as 1000 waves and all models are tested with minimum two sets. Moreover, some models are tested for 10000 waves to observe the cumulative damage development.

3.5. Construction of the Models

Stone weights are determined after the scaling calculations. Quarry run material is first sieved for the elimination of the unrelated quarry material. After the sieve process is completed, all stones are weighed individually. According to the breakwater cross-sections tested in the experiments, stones are determined whether they are in the weight scale range or not. All stone ranges are painted with a different colour to ease the detection of stone movements. The cross-sections are drawn to the glass wall (Figure 3.9) of the wave flume by a correction fluid in order to place the stones correctly. Stones are placed randomly to the wave flume as they are placed to original prototype breakwater cross-section and stone placement is conducted carefully in order to avoid from the compaction.

Figure 3.9: Location of cross-section in the empty wave flume

3.6. Test Cross-Sections

Five cross-sections including the constructed cross-section of Ordu-Giresun berm breakwater trunk section at 11 m water depth are tested in the physical model experiments. Four of cross-sections are designed as alternative cross-sections for the constructed section. In these alternative models, some parameters are left same as in the constructed section. These parameters are the height and stone weight of toe structure, the core material of the structure, the height of the berm and the crest, sea bottom slope, water depth and design wave characteristics. Alternative cross-sections are designed using a computational tool developed in MS Excel environment in scope of this study based on the formulas proposed by Lykke Andersen et al. (2014)

and Sigurdarson and Van der Meer (2012) described in Chapter 2. This computational tool is capable of classifying the berm breakwater type, and calculating the recession and overtopping of berm breakwaters from the given inputs of significant wave height at the toe of the structure (H_s), spectral wave period at the toe of the structure ($T_{m-1,0}$), water depth in front of the structure (d), angle of wave attack (β), front slope of the structure (α), median stone weight (W_{50}), density of stone (ρ_s) and water (ρ_w), number of waves (N), height of berm (h_b), water depth above toe (h_t), and crest level (R_c) with respect to HWL.

Moreover, front slope of the models are selected as 1/1.5 instead of 1/3, the front slope of the constructed section.

Water depth at the toe of Ordu-Giresun berm breakwater is 12.12 m for highest water level (HWL). Therefore, in the models the water level at the toe of the structures is determined as 0.37 m. Moreover, significant wave height at the toe of the structure is 6.68 m and significant wave period is 10.80 sec. As mentioned above, the core, filter and toe material heights are kept same in all sections. The prototype weights of the core layer, filter layer and toe structure are 0-0.4 tons, 0.4-2 tons, 2-4 tons respectively. Model weights are determined as stated in Section 3.2 as 0-8 grams, 8-40 grams, 40-80 grams. Moreover, the prototype nominal diameters of the core layer, filter layer and toe structure are 0.428 m, 0.778 m and 1.056 m respectively. Model nominal diameters are 1.1 cm, 2.1 cm and 2.8 cm. Different armour stone classes are used in the experiments. Prototype and model properties for all stones used in the experiments are presented in Table 3.2.

Table 3.2: Model and prototype stone diameters and weights

Prototype Stone Class Range (tons)	Prototype Stone Class Diameter (m)	Model Stone Class Range (grams)	Model Stone Class Diameter (cm)
0-0.4	0-0.539	0-8	0-1.4
0.4-2	0.539-0.922	8-40	1.4-2.5
2-4	0.922-1.162	40-80	2.5-3.1
2-8	0.922-1.464	40-160	2.5-3.9
6-10	1.330-1.577	120-200	3.5-4.2
6-8	1.330-1.464	120-160	3.5-3.9
8-10	1.464-1.577	160-200	3.9-4.2
12-15	1.676-1.805	240-300	4.5-4.8

3.6.1. Model 1

Model 1 is the constructed Ordu-Giresun berm breakwater trunk cross-section. Armour layer stone range is 240-300 grams in model and 12-15 tons in prototype. The breakwater is a hardly reshaping (HR) Icelandic type berm breakwater. In the model, 120-160 grams and 160-200 grams stone ranges are used which correspond to 6-8 tons and 8-10 tons in prototype, respectively. The nominal diameters of armour stones are 4.6 cm for 240-300 grams stones, 3.7 cm for 120-160 grams stones and 4.1 cm for 160-200 grams stones. In addition, the nominal diameters of armour stones are 1.743 m for 12-15 tons stones, 1.4 m for 6-8 tons stones and 1.523 m for 8-10 tons stones in the prototype scale. Cross-section of Model 1 is shown in Figure 3.10.

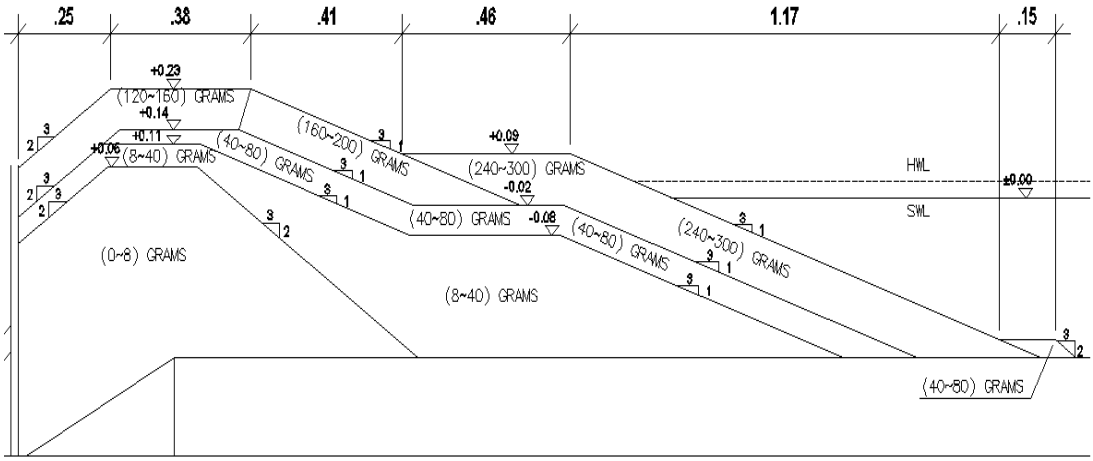

Figure 3.10: Cross-section of Model 1

(Dimensions are in meters and figure is not to scale.)

3.6.2. Model 2

Model 2 is the first alternative section for Ordu-Giresun berm breakwater cross-section. The model cross-section is a fully reshaping (FR) mass armoured berm breakwater section. Berm width of the cross-section is determined as the minimum berm width which satisfying the serviceability criteria calculated by CLASH (Verhaeghe et al., 2005). Model 2 has the minimum cross-sectional area among the tested cross-sections in the physical model experiments. The aim of testing Model 2 is the observation of damage development at the smallest cross-section. Armour layer stone range is 40-80 grams in model and 2-4 tons in prototype. The nominal diameters of armour stones are 2.8 cm for 40-80 grams stones and 1.056 m for 2-4 tons prototype. Cross-section of Model 2 is shown in Figure 3.11.

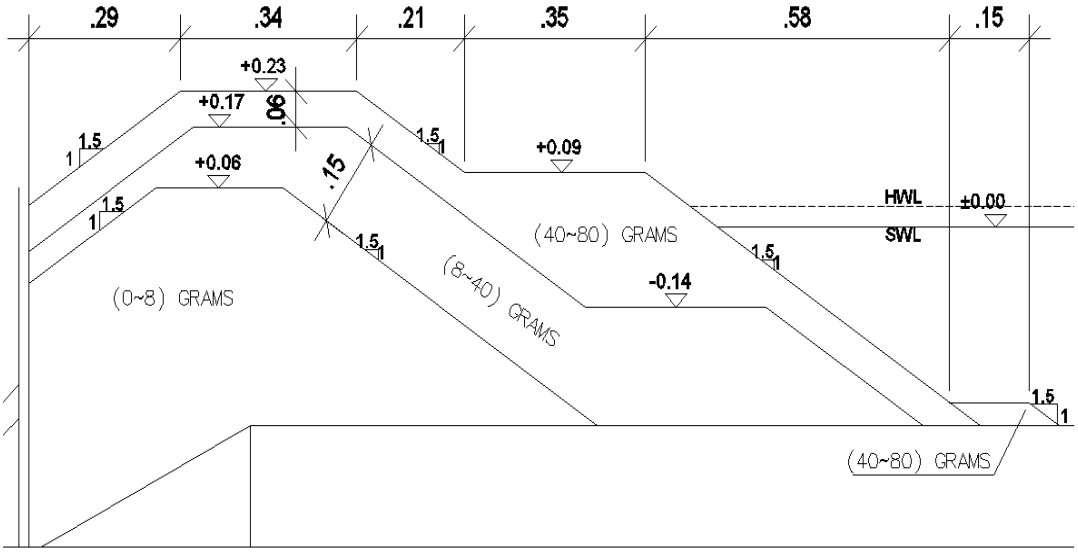

Figure 3.11: Cross-section of Model 2

(Dimensions are in meters and figure is not to scale.)

3.6.3. Model 3

Model 3 is the second alternative cross-section for Ordu-Giresun berm breakwater trunk cross-section. The model cross-section is a fully reshaping (FR) mass armoured berm breakwater cross-section. The difference between Model 3 from Model 2 is the width of the berm. Berm width of Model 3 is 44 cm longer than Model 2 which corresponds to approximately 14.5 m in prototype. Since the serviceability criterion is not satisfied with the berm width of Model 2, berm width of Model 3 is determined according to the formulations given by Sigurdarson and Van der Meer (2014).

$A_h/H_s = 2H_s/\Delta D_{n50}$ (See Fig. 2.3) [3.8]

Where A_h is the horizontal armour width, H_s is the incident significant wave height, Δ is the relative buoyant density of the stone, D_{n50} is the nominal diameter of the armour stone.

The aim of testing Model 3 is the observation of berm width effect on the berm breakwater. Armour layer stone range is 40-80 grams in model and 2-4 tons in prototype. The nominal diameters of armour stones are 2.8 cm for 40-80 grams stones and 1.056 m for 2-4 tons prototype. Cross-section of Model 3 is shown in Figure 3.12.

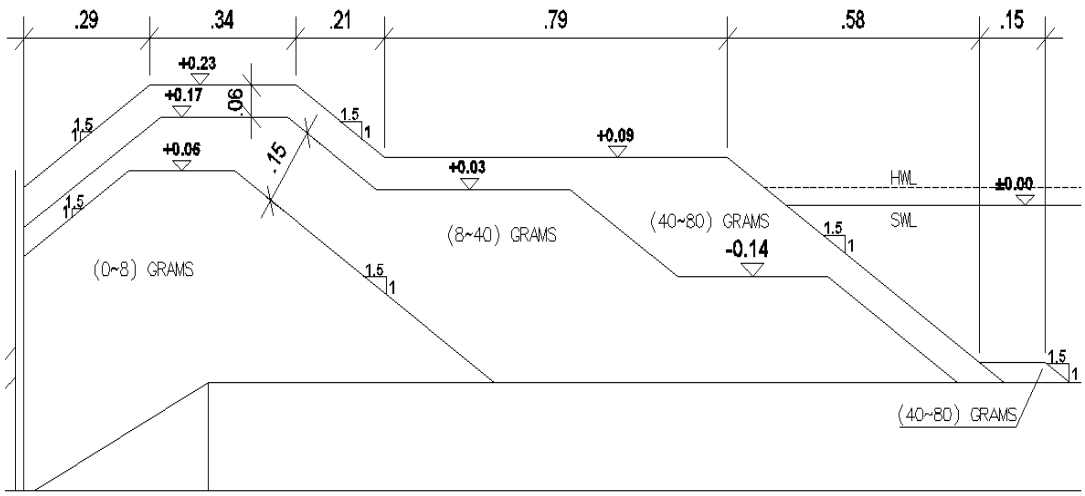

Figure 3.12: Cross-section of Model 3

(Dimensions are in meters and figure is not to scale.)

3.6.4. Model 4

Model 4 is the second alternative cross-section for Ordu-Giresun berm breakwater trunk cross-section. The model cross-section is a fully reshaping (FR) mass armoured

berm breakwater cross-section. The difference between Model 4 from Model 3 is the armour stone range. The aim of testing Model 4 is the observation of stone gradation effect on the berm breakwater. Model 4 is wider grading compared to Model 3. Armour layer stone range is 40-160 grams in model and 2-8 tons in prototype. The nominal diameters of armour stones are 3.3 cm for 40-160 grams stones and 1.252 m for 2-8 tons prototype. Cross-section is composed of 2-4 tons, 4-6 tons, and 6-8 tons stone range with the ratio of 37%, 29%, and 34%, respectively. Cross-section of Model 4 is shown in Figure 3.13.

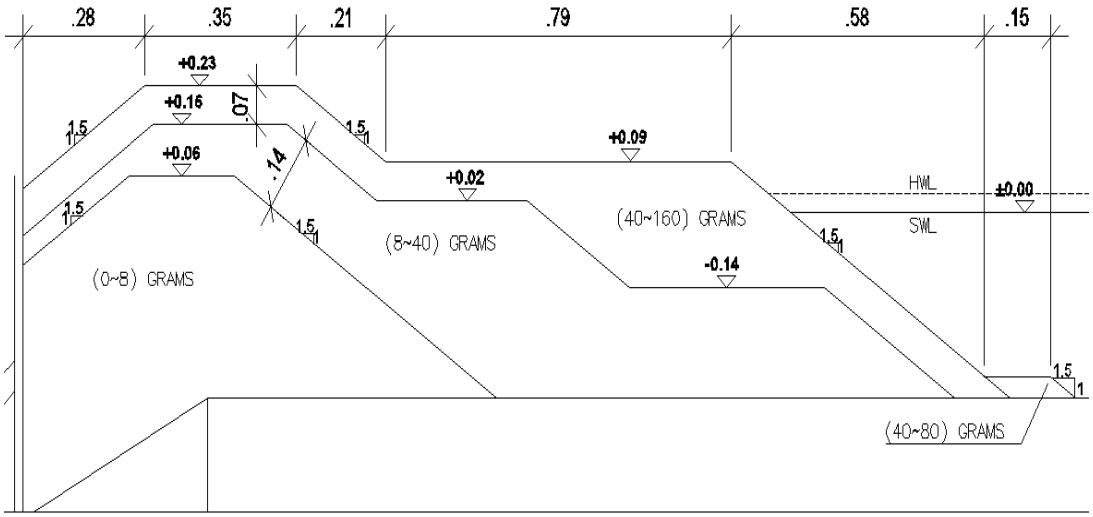

Figure 3.13: Cross-section of Model 4

(Dimensions are in meters and figure is not to scale.)

3.6.5. Model 5

Model 5 is the second alternative cross-section for Ordu-Giresun berm breakwater trunk cross-section. The model cross-section is a partly reshaping (PR) mass

armoured berm breakwater cross-section. The differences between Model 5 from Model 4 are the armour stone size and range. The aim of testing Model 5 is the observation of stone gradation and size effect on the berm breakwater. Armour layer stone range is 120-200 grams in model and 6-10 tons in prototype. The nominal diameters of armour stones are 3.9 cm for 120-200 grams stones and 1.464 m for 6-10 tons prototype. Cross-section is composed of 6-8 tons, and 8-10 tons stone range with the ratio of 47%, and 53%, respectively. Cross-section of Model 5 is shown in Figure 3.14.

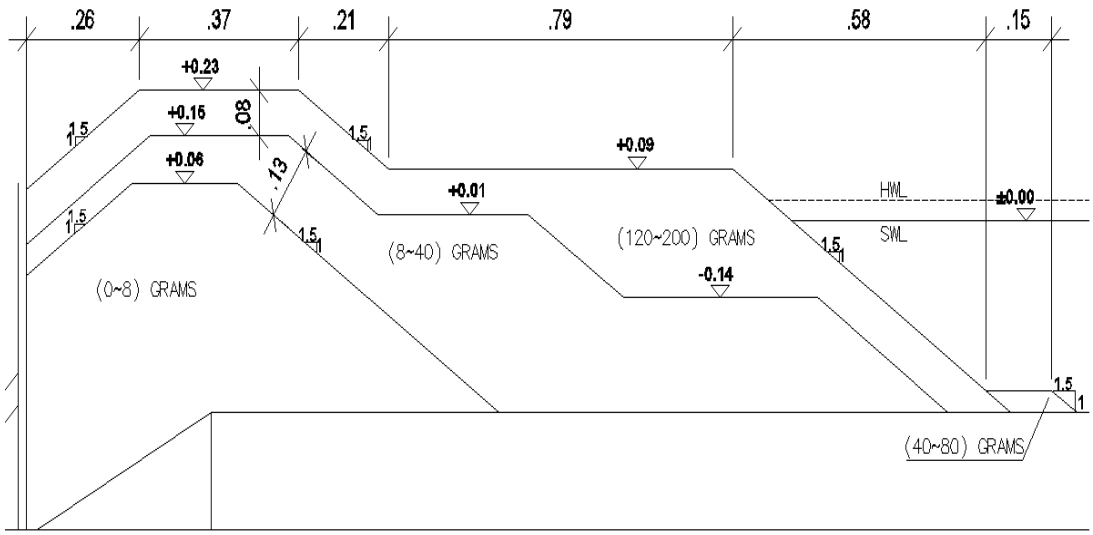

Figure 3.14: Cross-section of Model 5

(Dimensions are in meters and figure is not to scale.)

3.7. Test Program

In the physical model experiments, three different wave series of 500 waves having same wave characteristics are determined and used in the sets. Model 1 is tested

using these three different wave series. Set 1 and 2 are conducted for 1000 waves. Section is repaired at the end of each set. Set 3 is conducted for 10000 waves in order to observe the cumulative damage on the section without any repair and maintenance between each 500 waves. Wave overtopping is recorded at the end of each 500 waves. Profile measurements are conducted at the end of 1000 waves for Set 1 and 2. For Set 3, profile measurements are conducted at the end of 1000, 3000, 5000, 7000, and 10000 waves.

Model 2 is tested for three sets. All sets are conducted for 1000 waves and section is repaired at the end of each set. Wave overtopping is recorded at the end of each 500 waves. Profile measurements are conducted at the end of the 1000 waves for all sets.

Model 3 is tested for two sets. Set 1 is conducted for 1000 waves and section is repaired at the end of the set. Set 2 is tested for 10000 waves in order to observe the cumulative damage on the section without any repair. Wave overtopping is recorded at the end of each 500 waves. Profile measurement is conducted at the end of 1000 waves for Set 1. For Set 2, profile measurements are taken at the end of 1000, and 10000 waves.

Model 4 is tested for three sets. Set 1 and 2 are conducted for 1000 waves and section is repaired at the end of each set. Set 3 is tested for 10000 waves in order to observe the cumulative damage on the section without any repair. Wave overtopping is recorded at the end of each 500 waves. Profile measurements are conducted at the end of 1000 waves for Set 1 and 2. For Set 3, profile measurements are taken at the end of 1000, 4000, 8000, and 10000 waves.

Model 5 is tested for two sets. Set 1 is tested for 10000 waves in order to observe the cumulative damage on the section without any repair. Set 2 is conducted for 1000 waves and section is repaired at the end of the set. Wave overtopping is recorded at the end of each 500 waves. Profile measurements are conducted at the end of 1000, 4000, 7000, and 10000 waves for Set 1. For Set 2, profile measurement is taken at the end of 1000 waves.

The model properties and test program summary is presented in Table 3.3.

Detailed information about the wave heights and wave periods measured in the physical model experiments for all models is presented in Appendix-A.

Table 3.3: Summary of the model properties and test program

Name	Set No	Number of Waves Profile Measured	Number of Waves Overtopping Measured	Berm Width (cm)	Model Stone Class Range (grams)	Model Stone Class Diameter (cm)
Model 1	Set-1	1000	At the end of each 500 waves	46	240-300	4.5-4.8
	Set-2	1000				
	Set-3	1000				
		3000				
		5000				
		7000				
		10000				
Model 2	Set-1	1000	At the end of each 500 waves	35	40-80	2.5-3.1
	Set-2	1000				
	Set-3	1000				
Model 3	Set-1	1000	At the end of each 500 waves	79	40-80	2.5-3.1
	Set-2	1000				
		10000				
Model 4	Set-1	1000	At the end of each 500 waves	79	40-160	2.5-3.9
	Set-2	1000				
	Set-3	1000				
		4000				
		8000				
		10000				
Model 5	Set-1	1000	At the end of each 500 waves	79	120-200	3.5-4.2
		4000				
		7000				
		10000				
	Set-2	1000				

CHAPTER 4

RESULTS AND DISCUSSIONS

There are two main concerns governing the design of berm type rubble mound breakwaters namely, stability and serviceability of the structures. This chapter presents the results of the experiments in terms of the stability investigation and serviceability of the structures. Stability condition is implied by the deformation of the armour layer of the structures. Moreover, serviceability condition of the structures is implied by the wave overtopping. Since Model 1 is the constructed trunk cross-section of Ordu-Giresun berm breakwater, it is tested in order to form the base for this study and compare to the alternative models.

4.1. Stability Investigation of the Structures

A breakwater has to be stable enough to fulfil its purpose of construction. Therefore, in the design of breakwaters, stability of the structure has a great importance. In Section 2.1, it is stated that the classification of the berm breakwaters are determined according to the deformation of the armour layer of the structures. According to the damage parameter, the berm breakwaters are divided as “Hardly Reshaping”, “Partly Reshaping”, and “Fully Reshaping” (Sigurdarson and Van der Meer, 2012). Deformation of the armour layer is defined by recession parameter, Rec, and damage parameter, S. In the model tests, both recession and damage parameters of the structures are determined and compared to each other whether there are any conflicts

between them or not. Stability analyses of the structures are conducted by the help of profile measurement and video recording techniques.

4.1.1. Damage Parameter and Recession

Profile measurement technique is used in the model experiments in order to measure the damage and recession on the armour layer of the structure.

The initial profile measurement is conducted at the beginning of each set for all models. Moreover, the final profile measurement is conducted at the end of 1000 waves for the sets which are conducted for only 1000 waves. However, the profile measurements are conducted at various time steps of sets of cumulative damage tests conducted for 10000 waves. The detailed information about the test program for all of the models is stated in Section 3.7.

Eroded area is the areal difference between the profile measurements carried out before and after the test. A definitional sketch of area erosion is presented in Figure 3.7. For damage analysis, profile measurements are conducted before and after each test with certain increments along x-axis as stated in the description of experiments along at least three lines (sides and middle). Average of the measurements along these lines is used as profile measurements data to include the effect of whole cross-section. Eroded area along the cross-section and damage parameter given by Van der Meer's formula (1988) as stated in Equation [3.6] are calculated using a MATLAB code from the profile measurements in order to interpret magnitude of the damage. In the computations, a reference height is chosen, and the measurements are subtracted from this reference height to present the results in more understandable manner. In the model experiments, reference height is chosen as 100 cm for all models. Therefore, in the profile measurement graphs, the minimum value of vertical axis is 10 cm because of the distance between crest level and measuring rod. Linear lines

are assumed between the measured data points to get a continuous data for numerical integration. Eroded area is computed checking whether there is erosion or not by comparing the measurements at every successive interpolated data points, and using trapezoidal rule as the numerical integration method. In order to have precise calculations, distance between each successive interpolated data point is taken as 0.001 cm.

Another important issue affecting the stability of berm breakwaters is recession. Recession on the armour layer of the models is also determined by profile measurement technique. Moreover, Lykke Andersen et al. (2014) are used to calculate the expected recession on the armour layer of the models given in Equations [2.14]-[2.23]. On the other hand, the effect of the number of waves (N) is relatively small for larger N than 1000 and the formula is valid up to 3000 waves (Lykke Andersen and Burcharth, 2010). Therefore, in the recession calculations, the recession value is taken constant after 3000 waves.

Figure 4.1 and Figure 4.2 show the average profile measurement graphs for Set-1 and Set-2 of Model 1, respectively. Figure 4.3 shows the average profile measurement graph for Set-3 of Model 1 including cumulative damage. Moreover, damage parameters, calculated and measured recession values obtained from the profile measurement for Model 1 are presented in Table 4.1.

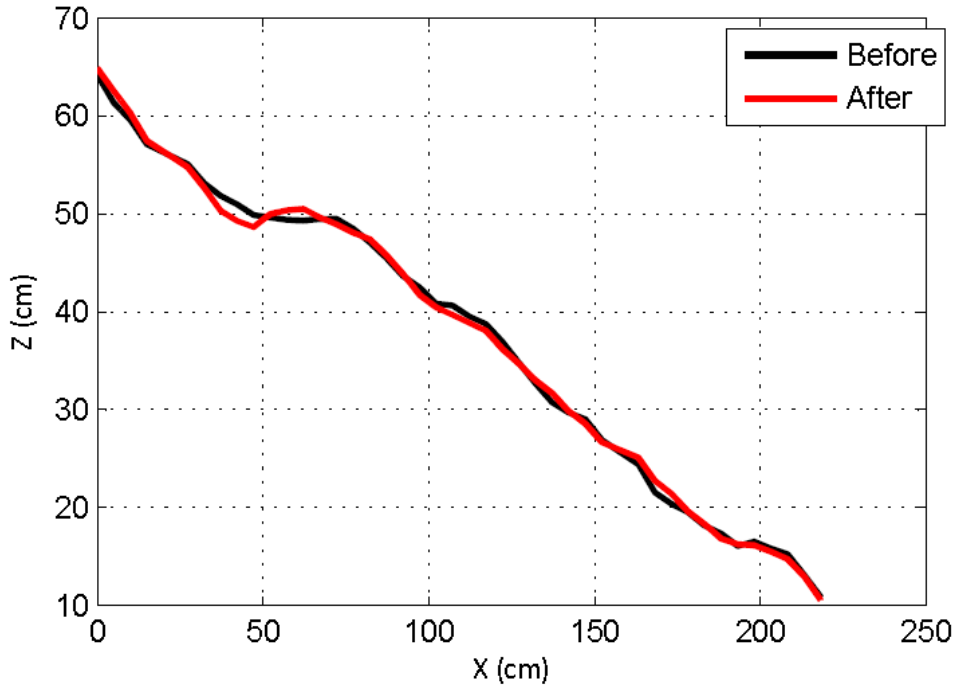

Figure 4.1: Average profile measurement graph for Set-1 of Model 1

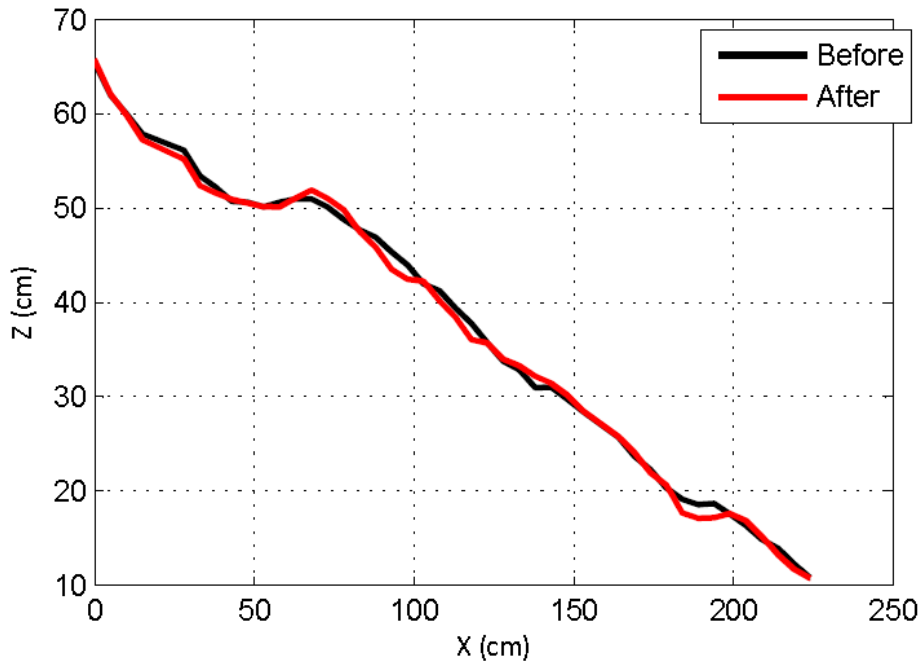

Figure 4.2: Average profile measurement graph for Set-2 of Model 1

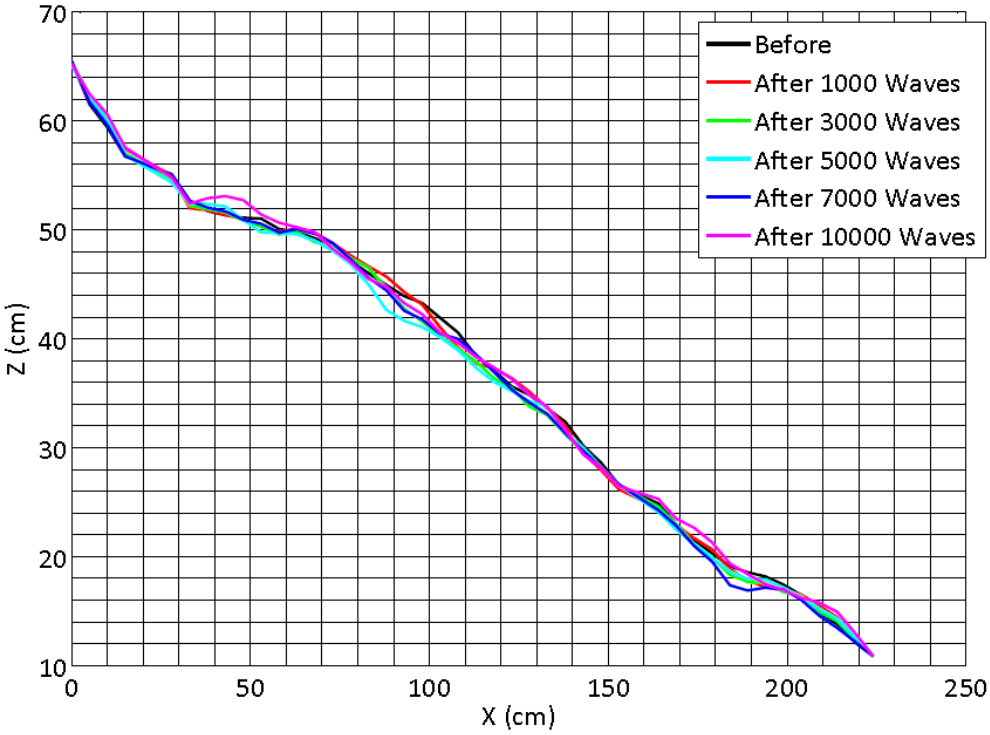

Figure 4.3: Average profile measurement graph for Set-3 of Model 1

Table 4.1: Damage parameters and recession values for Model 1

Name	Set No	Number of Waves	Damage Parameter, S	Rec_{meas} (m)	Rec_{cal} (m)
Model 1 (12-15 tons)	Set-1	1000	3.5	1.53	2.35
	Set-2	1000	5.2	2.15	2.35
	Set-3	1000	2.5	1.12	2.35
		3000	4.5	1.66	3.47
		5000	5.9	2.03	3.47
		7000	7.2	2.68	3.47
		10000	7.3	2.71	3.47

Figure 4.1 and Figure 4.2 indicate that there is not much difference between the profile measurements taken before and after the test which means the structure

protects its original cross-section after 1000 waves. Moreover, it can be seen from Figure 4.3 that the structure protects its original shape even after 10000 waves. According to Table 4.1, the damage parameters and recession values for 1000 waves are close to each other for all sets. Set-3 damage parameter and recession results present us the cumulative damage development of Model 1. Damage parameter and recession values of Set-3 show that damage on the structure is not affected considerably after 7000 waves. Furthermore, measured recession values are compatible with the calculated recession values.

Figure 4.4, Figure 4.5, and Figure 4.6 show the average profile measurement graphs for Set-1, Set-2, and Set-3 of Model 2, respectively. Moreover, damage parameters, calculated and measured recession values obtained from the profile measurement method for Model 2 are presented in Table 4.2.

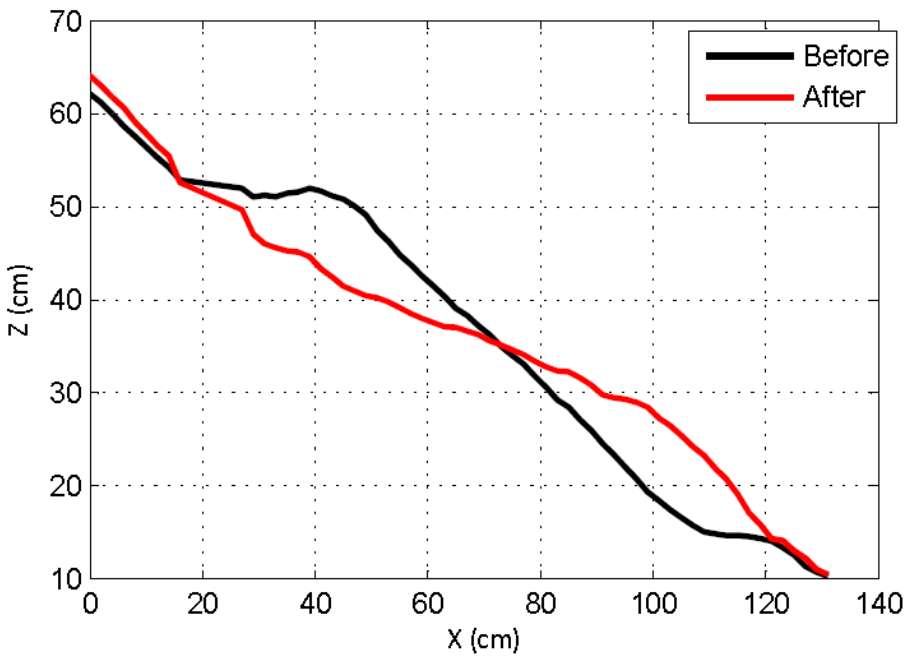

Figure 4.4: Average profile measurement graph for Set-1 of Model 2

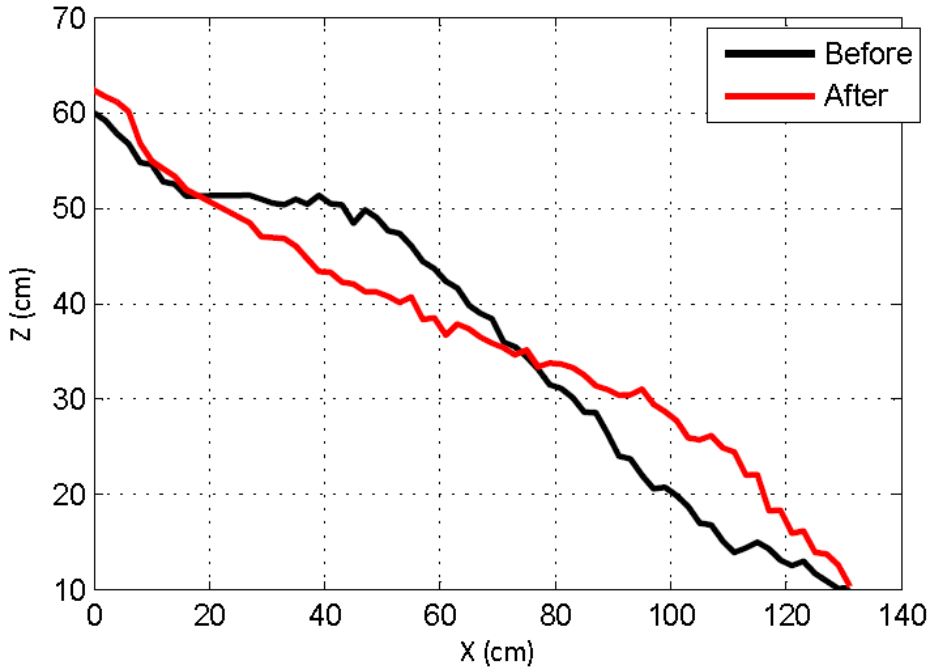

Figure 4.5: Average profile measurement graph for Set-2 of Model 2

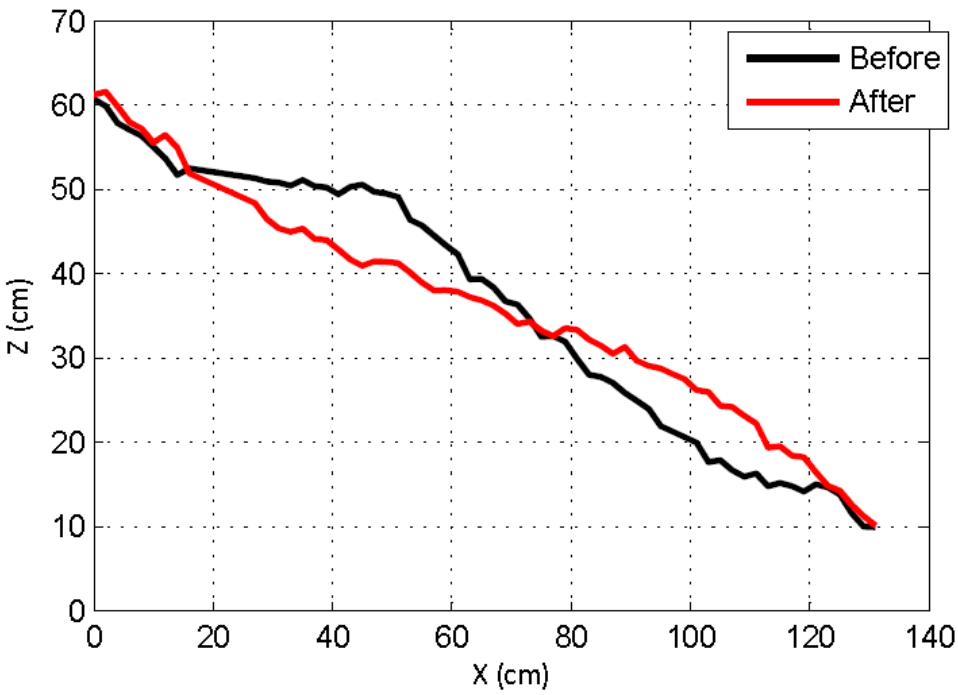

Figure 4.6: Average profile measurement graph for Set-3 of Model 2

Table 4.2: Damage parameters and recession values for Model 2

Name	Set No	Number of Waves	Damage Parameter, S	Rec_{meas} (m)	Rec_{cal} (m)
Model 2 (2-4 tons B=11.5m)	Set-1	1000	32.9	8.06	8.29
	Set-2	1000	31.8	8.25	8.29
	Set-3	1000	34.2	8.87	8.29

It can be seen from Figure 4.4, Figure 4.5, and Figure 4.6 that the structure gets S-shaped damage. Since Model 2 is designed as reshaping berm breakwater, S-shaped damage is not the governing parameter if the structure provides other design conditions. According to Table 4.2, the damage parameters and recession values for 1000 waves are close to each other for all sets. In addition, measured recession values are compatible with calculated recession values.

Figure 4.7 shows the average profile measurement graph for Set-1 of Model 3, and Figure 4.8 shows the average profile measurement graph for Set-2 of Model 3 including cumulative damage. Moreover, damage parameters, calculated and measured recession values obtained from the profile measurement method for Model 3 are presented in Table 4.3.

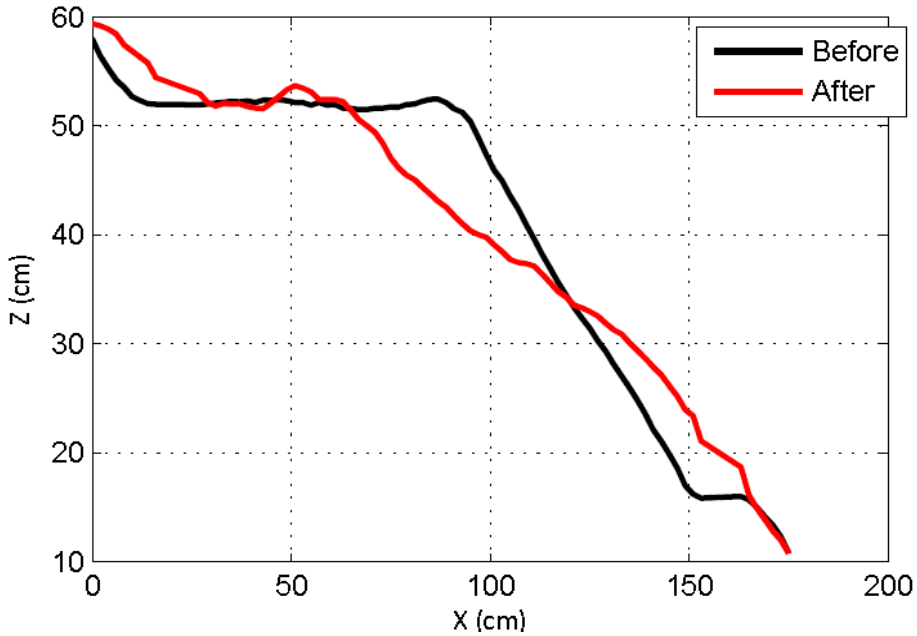

Figure 4.7: Average profile measurement graph for Set-1 of Model 3

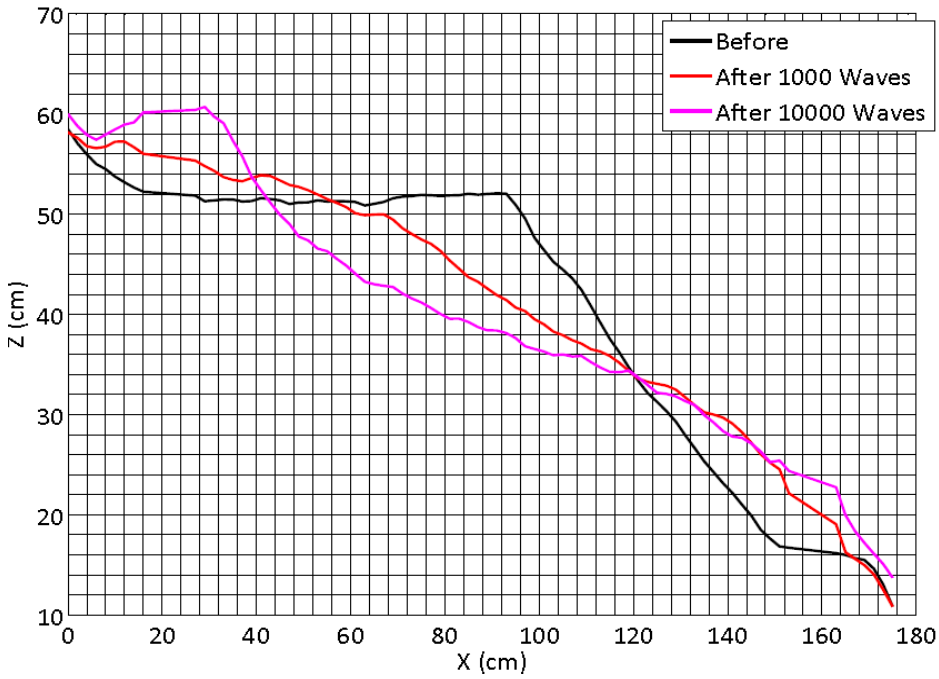

Figure 4.8: Average profile measurement graph for Set-2 of Model 3

Table 4.3: Damage parameters and recession values for Model 3

Name	Set No	Number of Waves	Damage Parameter, S	Rec_{meas} (m)	Rec_{cal} (m)
Model 3 (2-4 tons B=26m)	Set-1	1000	38.8	7.58	8.29
	Set-2	1000	41.3	8.53	8.29
		10000	80.0	16.58	10.67

Figure 4.7 indicates that the structure takes S-shaped damage. Furthermore, reshaping of the structure is shown in Figure 4.8. It can be seen from Figure 4.8 that while the berm is being eroded the stones are accumulated in front of the crest. According to Table 4.3, the damage parameters and recession values for 1000 waves are close to each other. However, Set-2 recession result presents that measured recession value is not compatible with the calculated recession value for 10000 waves.

Figure 4.9 and Figure 4.10 show the average profile measurement graphs for Set-1 and Set-2 of Model 4, respectively. Figure 4.11 shows the average profile measurement graph for Set-3 of Model 4 including cumulative damage. Moreover, damage parameters, calculated and measured recession values obtained from the profile measurement method for Model 4 are presented in Table 4.4.

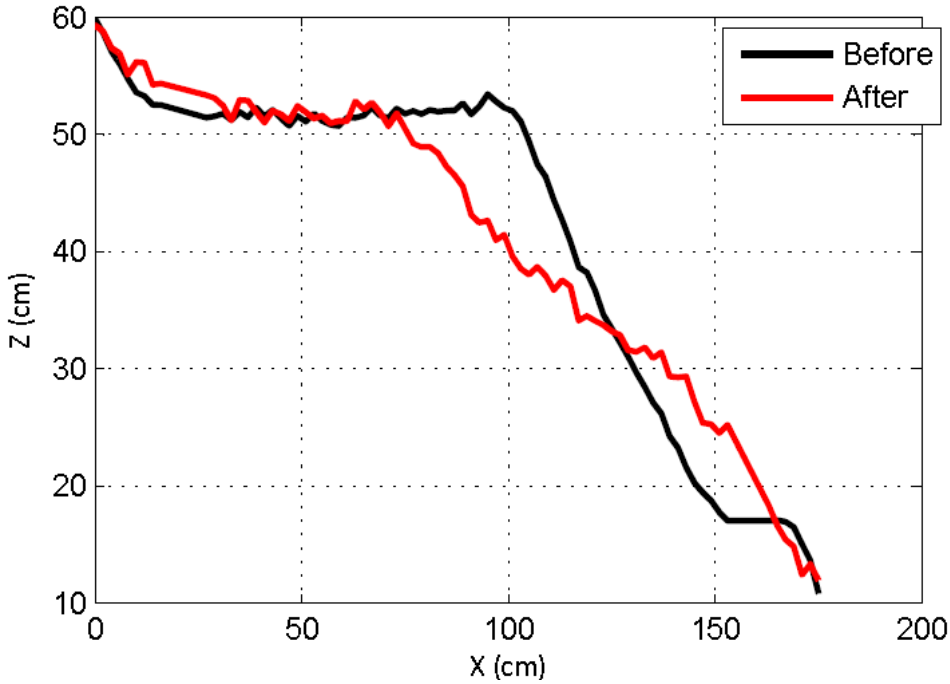

Figure 4.9: Average profile measurement graph for Set-1 of Model 4

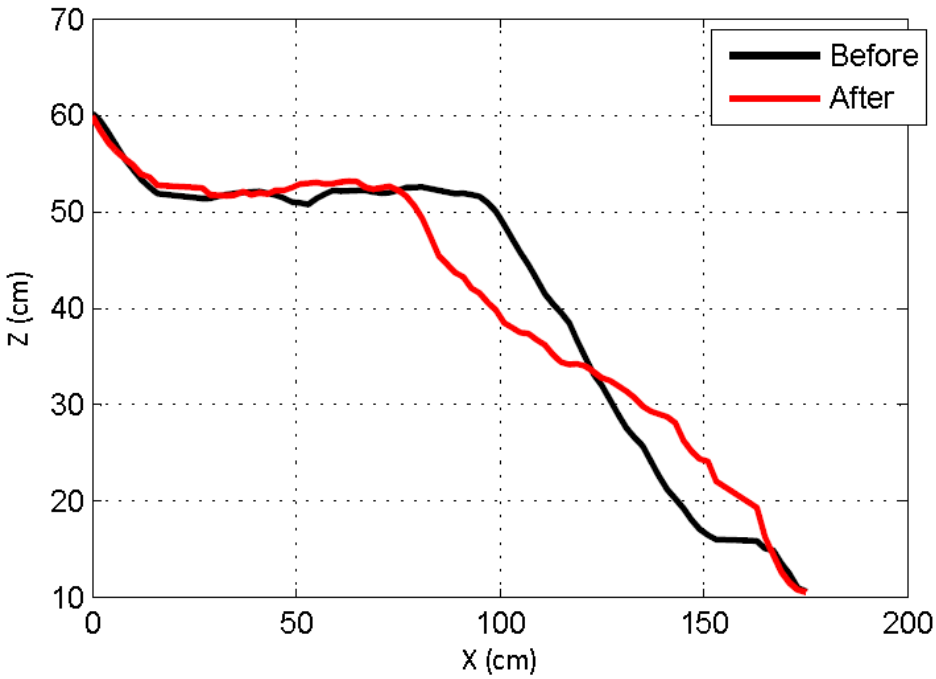

Figure 4.10: Average profile measurement graph for Set-2 of Model 4

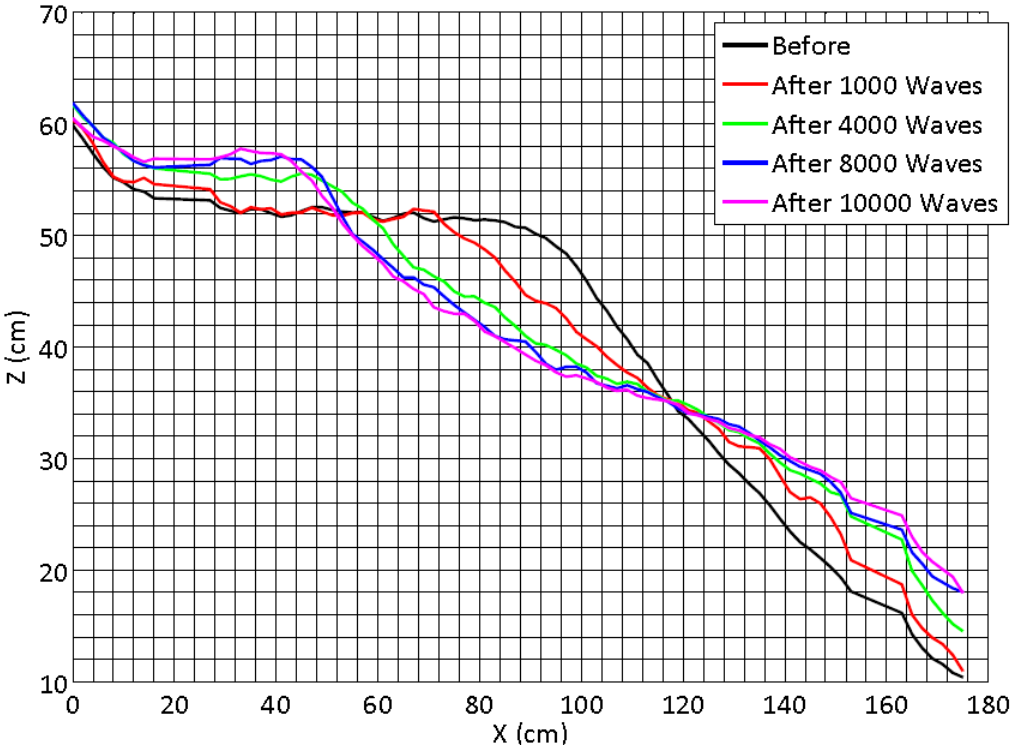

Figure 4.11: Average profile measurement graph for Set-3 of Model 4

Table 4.4: Damage parameters and recession values for Model 4

Name	Set No	Number of Waves	Damage Parameter, S	Rec_{meas} (m)	Rec_{cal} (m)
Model 4 (2-8 tons)	Set-1	1000	31.9	6.91	6.65
	Set-2	1000	28.0	6.72	6.65
	Set-3	1000	21.4	5.82	6.65
		4000	31.8	10.56	8.66
		8000	39.4	13.04	8.66
		10000	42.5	14.10	8.66

Figure 4.9 and Figure 4.10 indicate that the structure takes S-shaped damage as it is foreseen in the design period. Moreover, it can be seen from Figure 4.11 that while

the berm is being eroded the stones are accumulated in front of the crest. According to Table 4.4, there is not considerable difference between the damage parameters and recession values for 1000 waves. Set-3 damage parameter and recession results present the cumulative damage development of Model 4. Damage parameter and recession values of Set-3 show that damage on the structure is not affected considerably after 8000 waves. Furthermore, measured recession values are compatible with calculated recession values for 1000 waves; on the other hand, in the cumulative damage analysis, measured recession values are not compatible with calculated recession values.

Figure 4.12 shows the average profile measurement graph for Set-1 of Model 5 including cumulative damage, and Figure 4.13 shows the average profile measurement graph for Set-2 of Model 5. Moreover, damage parameters, calculated and measured recession values obtained from the profile measurement method for Model 5 are presented in Table 4.5.

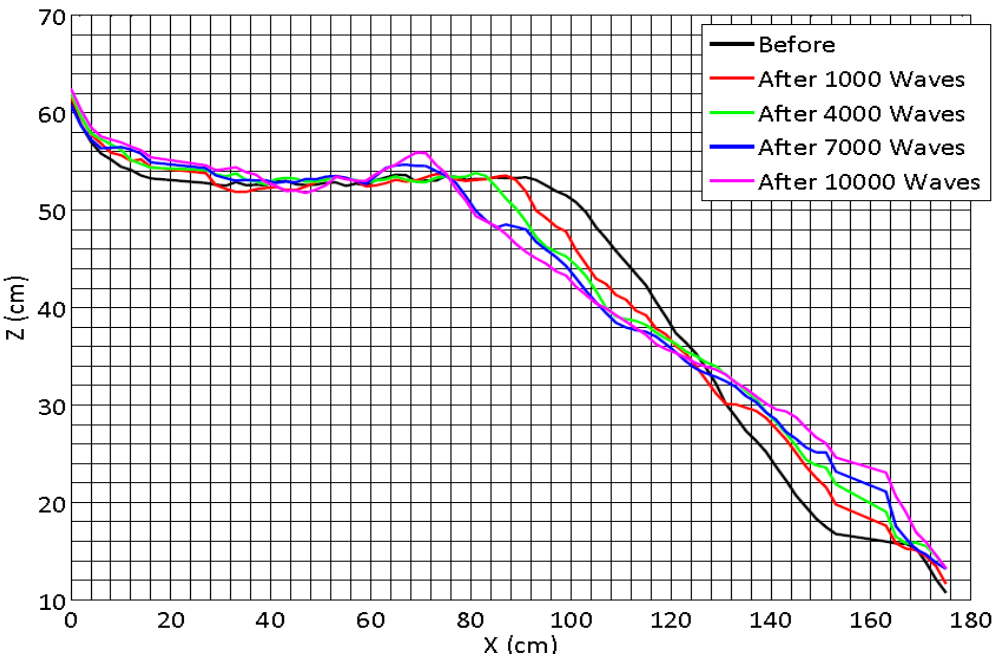

Figure 4.12: Average profile measurement graph for Set-1 of Model 5

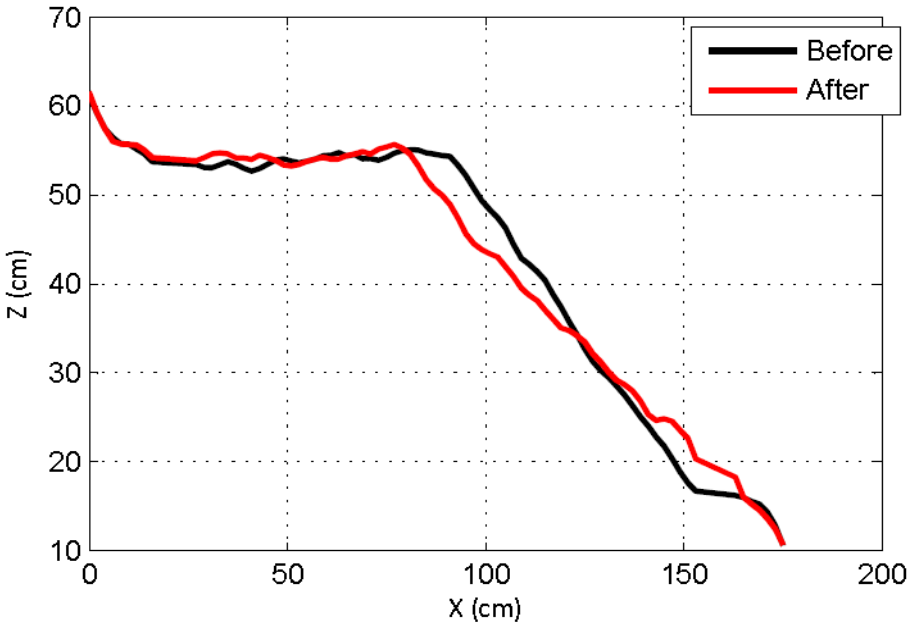

Figure 4.13: Average profile measurement graph for Set-2 of Model 5

Table 4.5: Damage parameters and recession values for Model 5

Name	Set No	Number of Waves	Damage Parameter, S	Rec_{meas} (m)	Rec_{cal} (m)
Model 5 (6-10 tons)	Set-1	1000	9.2	2.03	4.56
		4000	12.1	3.49	6.11
		7000	16.5	6.19	6.11
		10000	18.5	6.81	6.11
	Set-2	1000	11.3	3.46	4.56

Figure 4.12 and Figure 4.13 indicate that the structure takes S-shaped damage; however, reshaping does not cause accumulation in front of the crest. According to Table 4.5, there is not considerable difference between the damage parameters and recession values for 1000 waves. Set-1 damage parameter and recession results present the cumulative damage development of Model 5. Damage parameter and

recession values of Set-1 show that damage on the structure is not affected considerably after 7000 waves. Furthermore, measured recession values are compatible with calculated recession values. The compatibility of the measured and calculated recession values is based on the type of berm breakwater. Since Model 5 is designed as partly reshaping berm breakwater, the structure provides the recession values even in the cumulative damage condition.

4.1.2. Video Recording Analysis for Stability Investigation

In this study, it is aimed to investigate the relationship between cumulative damage and wave overtopping. However, profile measurements are not taken at the end of each 500 waves although the overtopping results are recorded since profile measurements are more time-consuming compared to overtopping measurements. Therefore, to establish a reliable relationship between cumulative damage and wave overtopping using overtopping measurements at the end of each 500 waves, the missing damage parameters and recession values resulted in profile are determined by processing the images in the video recordings taken during the experiments. Analyses of video recordings are only carried out for the cumulative damage sets of 10000 waves of alternative sections namely, Model 3, Model 4, and Model 5.

In the cumulative damage analysis for alternative models (Model 3, Model 4, and Model 5), number of waves of the damage parameters which are determined by video recording method are given in Table 4.6.

Table 4.6: Number of waves for alternative models

Model 3	Model 4	Model 5
500	500	500
-	-	-
1500	1500	1500
2000	2000	2000
2500	2500	2500
3000	3000	3000
3500	3500	3500
4000	-	-
4500	4500	4500
5000	5000	5000
5500	5500	5500
6000	6000	6000
6500	6500	6500
7000	7000	-
7500	7500	7500
8000	-	8000
8500	8500	8500
9000	9000	9000
9500	9500	9500
-	-	-

In the physical model experiments before the tests, photos of the models are taken when the section has no damage. Similarly, after the tests the photos of the models are taken to comprehend the damage visually. Moreover, during the experiments, video recordings are taken from the side of the section for all models. As a first step of the analysis of video recording method, screen shot is taken at the beginning of each video record. First screen shot has to be taken from the undamaged section in order to scale the image appropriately. Moreover, due to the angle of the video camera the rotation of the screen shots has to be adjusted. After the adequate adjustments are completed, damage parameter and recession are computed from scaled images.

Figure 4.14 shows an example of video recording analysis procedure for Model 3.

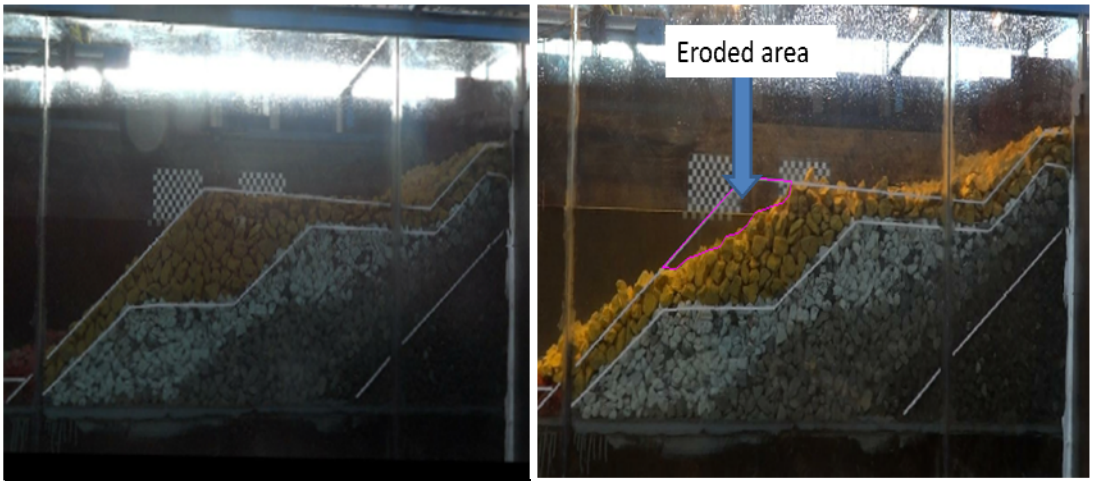

Figure 4.14: Undamaged and damaged cross-section after 500 waves for Model 3

Since the analyses of video recordings are conducted for only the side view of the cross-section, the results may be influenced by boundary effect. In the profile measurement technique the boundary effect is eliminated by averaging the measurements of three lines; however, in video recording method the averaging cannot be applied. Therefore, damage parameter and recession results obtained by the video recording are compared to damage parameter and recession results obtained by profile measurement whether they are compatible with each other or not. The results of the measurements for both methods are presented in the successive section.

It can be clearly seen from the profile measurements that in the cumulative damage analysis of Model 3 and Model 4, after the section is exposed to recession, stones are accumulated in front of the crest. In this study, the amount of accumulation is described by its height (h), and this parameter is used to examine the effect on cumulative damage and wave overtopping.

Table 4.7 shows damage parameter and recession results obtained from video recordings for Model 3.

Table 4.7: Video recording results for Model 3

Name	Number of Waves	h (m)	Rec_m (m)	Rec_p (m)	$A_{e(m)}$ (m^2)	$Dn_{50(m)}$ (m)	S
Model 3 (2-4 tons)	500	0.043	0.159	5.225	0.023	0.028	29.3
	1000	0.050	0.273	8.971	0.033	0.028	42.1
	1500	0.052	0.290	9.530	0.038	0.028	48.5
	2000	0.062	0.434	14.262	0.044	0.028	56.1
	2500	0.069	0.434	14.262	0.045	0.028	57.4
	3000	0.070	0.439	14.427	0.046	0.028	58.7
	3500	0.075	0.442	14.525	0.047	0.028	59.9
	4000	0.078	0.469	15.413	0.051	0.028	65.1
	4500	0.083	0.478	15.708	0.052	0.028	65.7
	5000	0.086	0.480	15.774	0.055	0.028	70.2
	5500	0.088	0.484	15.905	0.056	0.028	70.8
	6000	0.091	0.488	16.037	0.056	0.028	71.4
	6500	0.091	0.488	16.037	0.056	0.028	71.4
	7000	0.092	0.490	16.103	0.058	0.028	74.0
	7500	0.092	0.491	16.119	0.061	0.028	77.8
	8000	0.092	0.491	16.135	0.062	0.028	79.1
	8500	0.092	0.491	16.135	0.063	0.028	79.7
	9000	0.092	0.491	16.135	0.064	0.028	81.6
	9500	0.092	0.491	16.135	0.064	0.028	81.6
	10000	0.092	0.491	16.135	0.064	0.028	81.6

Table 4.8 shows damage parameters and recession results obtained from video recordings for Model 4.

Table 4.8: Video recording results for Model 4

Name	Number of Waves	h (m)	Rec_m (m)	Rec_p (m)	$A_{e(m)}$ (m^2)	$Dn_{50(m)}$ (m)	S
Model 4 (2-8 tons)	500	0.010	0.075	2.465	0.010	0.033	9.2
	1000	0.019	0.142	4.666	0.022	0.033	20.2
	1500	0.026	0.184	6.047	0.025	0.033	23.0
	2000	0.030	0.197	6.474	0.029	0.033	26.6
	2500	0.032	0.251	8.248	0.030	0.033	27.5
	3000	0.037	0.293	9.629	0.031	0.033	28.5
	3500	0.040	0.326	10.713	0.032	0.033	29.4
	4000	0.043	0.338	11.108	0.034	0.033	31.2
	4500	0.044	0.358	11.765	0.035	0.033	32.1
	5000	0.046	0.369	12.126	0.036	0.033	33.1
	5500	0.049	0.389	12.784	0.037	0.033	34.0
	6000	0.052	0.407	13.375	0.038	0.033	34.9
	6500	0.054	0.420	13.802	0.040	0.033	36.3
	7000	0.055	0.430	14.131	0.041	0.033	37.6
	7500	0.057	0.440	14.460	0.043	0.033	39.0
	8000	0.058	0.445	14.624	0.044	0.033	40.4
	8500	0.059	0.450	14.788	0.045	0.033	41.3
	9000	0.060	0.450	14.788	0.047	0.033	43.2
	9500	0.060	0.450	14.788	0.048	0.033	44.1
	10000	0.060	0.450	14.788	0.048	0.033	44.1

Table 4.9 shows damage parameters and recession results obtained from video recordings for Model 5.

Table 4.9: Video recording results for Model 5

Name	Number of Waves	h (m)	Rec_m (m)	Rec_p (m)	$A_{e(m)}$ (m^2)	$Dn_{50(m)}$ (m)	S
Model 5 (6-10 tons)	500	0.005	0.032	1.052	0.011	0.039	7.2
	1000	0.008	0.045	1.479	0.014	0.039	9.1
	1500	0.009	0.048	1.577	0.014	0.039	9.3
	2000	0.010	0.069	2.268	0.015	0.039	9.9
	2500	0.011	0.084	2.760	0.015	0.039	10.1
	3000	0.012	0.092	3.023	0.016	0.039	10.4
	3500	0.012	0.095	3.122	0.016	0.039	10.8
	4000	0.014	0.098	3.221	0.017	0.039	11.2
	4500	0.015	0.112	3.681	0.018	0.039	11.5
	5000	0.017	0.125	4.108	0.018	0.039	12.0
	5500	0.019	0.145	4.765	0.019	0.039	12.5
	6000	0.021	0.154	5.061	0.020	0.039	13.2
	6500	0.023	0.163	5.357	0.022	0.039	14.1
	7000	0.024	0.173	5.685	0.023	0.039	15.1
	7500	0.026	0.188	6.178	0.025	0.039	16.4
	8000	0.028	0.195	6.408	0.026	0.039	17.1
	8500	0.029	0.198	6.507	0.027	0.039	17.8
	9000	0.030	0.200	6.573	0.028	0.039	18.1
	9500	0.030	0.200	6.573	0.028	0.039	18.4
	10000	0.030	0.200	6.573	0.028	0.039	18.4

4.1.3. Comparison of the Results of Profile Measurements and Analyses of Video Recordings

In this section, comparison of the results obtained from profile measurements and analyses of video recordings is performed. The common number of waves in both profile measurements (PM), and video recording analyses (VR) are determined, and the stability analyses of the models are checked for both methods to observe whether there are any significant differences between them or not.

Table 4.10 shows the common number of waves in profile measurement and video recording analysis for Model 3. Damage parameter and recession results are also given in Table 4.10.

Table 4.10: Damage parameter and recession results for Model 3

Name	Set No	Number of Waves	S (PM)	S (VR)	Rec (m) (PM)	Rec (m) (VR)
Model 3 (2-4 tons)	Set-2	1000	41.3	42.1	8.53	8.97
		10000	80.0	81.6	16.58	16.14

Table 4.11 shows the common number of waves in profile measurement and video recording analysis for Model 4. Damage parameter and recession results are also given in Table 4.11.

Table 4.11: Damage parameter and recession results for Model 4

Name	Set No	Number of Waves	S (PM)	S (VR)	Rec (m) (PM)	Rec (m) (VR)
Model 4 (2-8 tons)	Set-3	1000	21.4	20.2	5.82	4.67
		4000	31.8	31.2	10.56	11.11
		8000	39.4	40.4	13.04	14.62
		10000	42.5	44.1	14.10	14.79

Table 4.12 shows the common number of waves in profile measurement and video recording analysis for Model 5. Damage parameter and recession results are also given in Table 4.12.

Table 4.12: Damage parameter and recession results for Model 5

Name	Set No	Number of Waves	S (PM)	S (VR)	Rec (m) (PM)	Rec (m) (VR)
Model 5 (6-10 tons)	Set-1	1000	9.2	9.1	2.03	1.48
		4000	12.1	11.2	3.49	3.22
		7000	16.5	15.1	6.19	5.69
		10000	18.5	18.4	6.81	6.57

Table 4.10, Table 4.11, and Table 4.12 show that the damage parameters and recession results obtained from the analyses of video recordings are close to damage parameters and recession results obtained from profile measurement for all alternative models tested for the observation of cumulative damage development. Therefore, boundary effect of the glass of inner channel does not have an important effect on the results of this study and the results come from the analyses of video recordings can be considered as reliable in terms of damage parameters and recession.

Relationship between the results of analyses of video recordings and profile measurements are summarized with Figure 4.15, Figure 4.16, and Figure 4.17 for Model 3, Model 4, and Model 5, respectively.

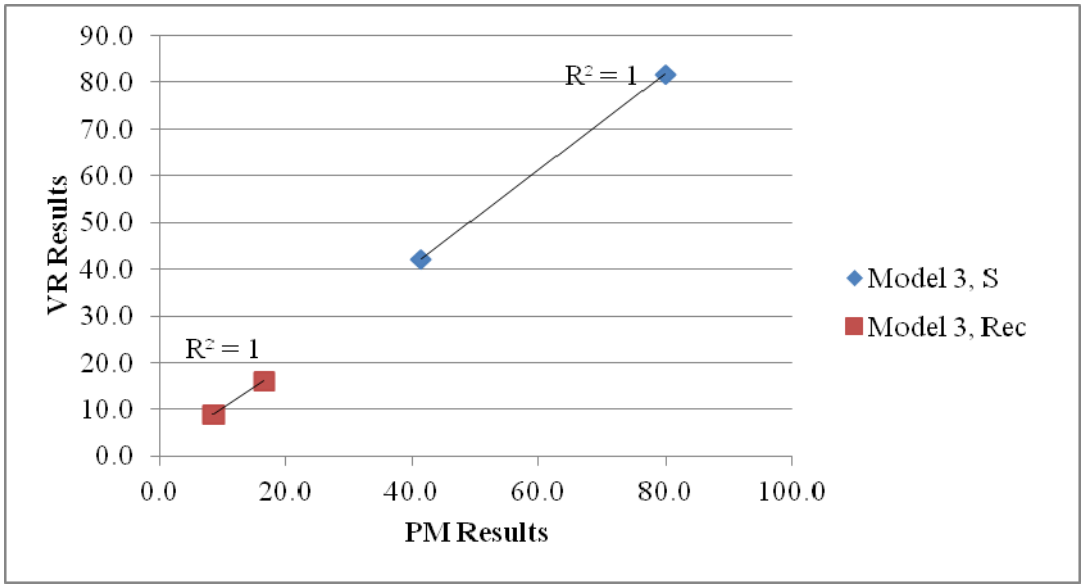

Figure 4.15: Relationship between the results of video recordings and profile measurements for Model 3

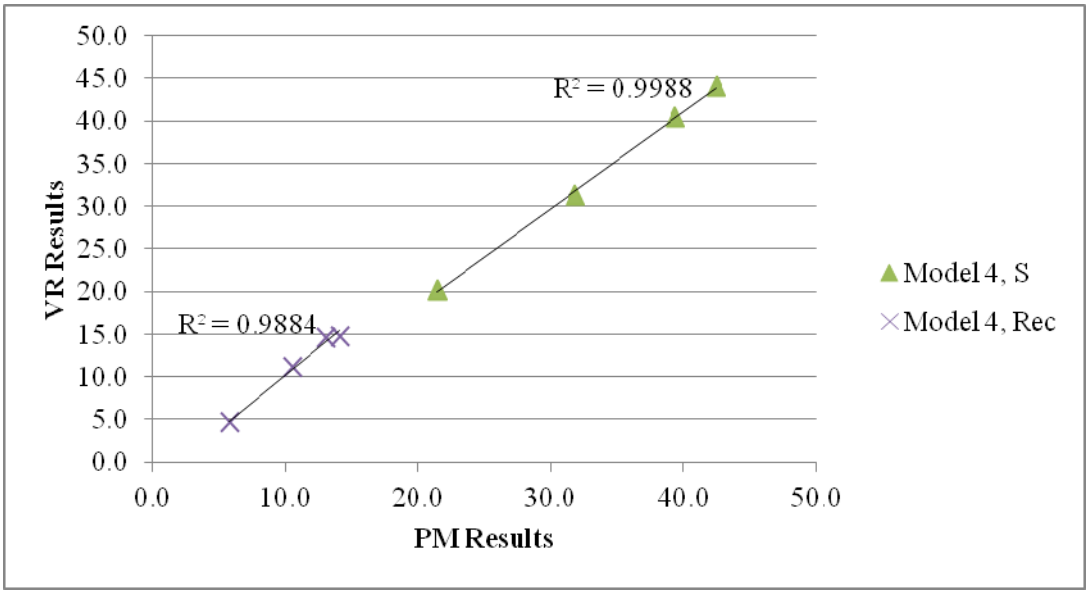

Figure 4.16: Relationship between the results of video recordings and profile measurements for Model 4

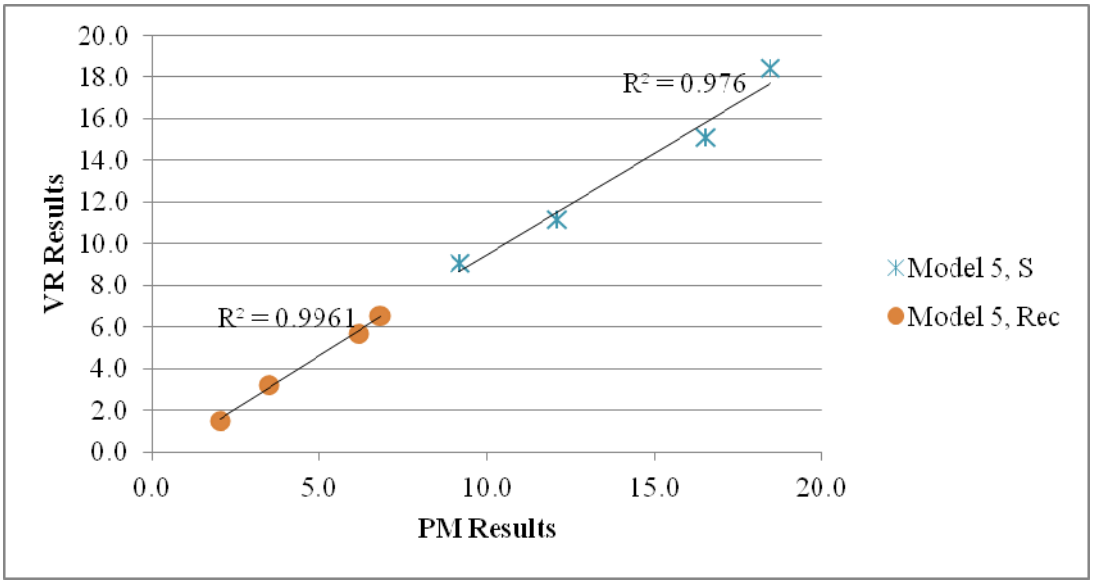

Figure 4.17: Relationship between the results of video recordings and profile measurements for Model 5

The correlation factor of Model 3 is 1 for both damage parameter and recession due to the lack of mutual number of waves among the profile measurements and video recording analysis. Therefore, establishment of a reliable comparison is quite difficult. However, the correlation factors for Model 4 and Model 5 show that the results obtained from the analyses of video recordings are compatible with the results obtained from profile measurements.

4.1.4. Discussion of Results of Stability Analyses

In this section, it is aimed to present the stability results of berm breakwater models, and compare the stability parameters between constructed section and alternative sections.

Damage Parameters

In this study, Ordu-Giresun berm breakwater is taken as a basis for proposing alternative fully and partly reshaping berm breakwaters. Therefore, it is tested in the physical model experiments as Model 1. Ordu-Giresun berm breakwater is designed as hardly reshaping berm breakwater with a stone range of 12-15 tons, and according to the classification given by Sigurdarson and Van der Meer (2012), the breakwater has to fulfil some conditions. The conditions have to be fulfilled by hardly reshaping berm breakwater are taken from Table 2.2. According to Table 2.2, damage parameter has to be in the range of 2-8. Damage parameters obtained from the experiments for Model 1 are presented in Table 4.13. Furthermore, Figure 4.18 and Figure 4.19 are given as examples in order to observe the damage visually for Set-1 of Model 1 before the test and after the test, respectively.

Table 4.13: Damage results for Model 1

Experiment Damage Results				**Literature Check**		
Name	**Set No**	**Number of Waves**	**S**	**Breakwater Type**	**S Range**	**Status**
Model 1 (12-15 tons)	Set-1	1000	3.5	HR	2-8	**Ok**
	Set-2	1000	5.2	HR	2-8	**Ok**
	Set-3	1000	2.5	HR	2-8	**Ok**
		3000	4.5	HR	2-8	**Ok**
		5000	5.9	HR	2-8	**Ok**
		7000	7.2	HR	2-8	**Ok**
		10000	7.3	HR	2-8	**Ok**

Figure 4.18: Set-1 of Model 1 cross-section before the test

Figure 4.19: Set-1 of Model 1 cross-section after the test

Table 4.13 shows that Ordu-Giresun berm breakwater fulfils the requirements of being hardly reshaping berm breakwater in terms of damage parameter condition. Set-3 of Model 1 implies that even if the structure is not got maintenance after approximately 30 hours storm (10000 waves); it protects its stability and hardly reshaping condition. Furthermore, the visual comparison between Figure 4.18 and Figure 4.19 reveals that there are only a small number of moving stones on the armour layer of the cross-section.

Model 2 is the minimum alternative section in terms of geometry and stone range instead of the Ordu-Giresun berm breakwater cross-section. Stone range of the cross-section is 2-4 tons. Since it has the minimum volume and smaller stone range, the section is quite important if it provides all the conditions of design. Model 2 is designed as fully reshaping berm breakwater, and thus, damage parameter should be higher than 20 as stated in Table 2.2. Damage parameters obtained from the experiments for Model 2 is presented in Table 4.14. Moreover, Figure 4.20 and Figure 4.21 are given as examples in order to observe the damage visually for Set-1 of Model 2 before the test and after the test, respectively.

Table 4.14: Damage results for Model 2

Experiment Damage Results				**Literature Check**		
Name	**Set No**	**Number of Waves**	**S**	**Breakwater Type**	**S Range**	**Status**
Model 2 (2-4 tons B=11.5m)	Set-1	1000	32.9	FR	>20	**Ok**
	Set-2	1000	31.8	FR	>20	**Ok**
	Set-3	1000	34.2	FR	>20	**Ok**

Figure 4.20: Set-1 of Model 2 cross-section before the test

Figure 4.21: Set-1 of Model 2 cross-section after the test

Since Model 2 is designed as a fully reshaping berm breakwater, there is not upper limit for damage parameter. However, lower limit for damage parameter is 20 and Table 4.14 presents that all damage parameters are higher than 20.

Model 3 is also designed as fully reshaping berm breakwater with a stone range 2-4 tons, and thus, damage parameter should be higher than 20 as stated in Table 2.2. Damage parameters obtained from the experiments for Model 3 is presented in Table 4.15. Moreover, Figure 4.22 and Figure 4.23 are given as examples in order to observe the damage visually for Set-1 of Model 3 before the test and after the test, respectively.

Table 4.15: Damage results for Model 3

Experiment Damage Results				**Literature Check**		
Name	**Set No**	**Number of Waves**	**S**	**Breakwater Type**	**S Range**	**Status**
Model 3 (2-4 tons B=26m)	Set-1	1000	38.8	FR	>20	**Ok**
	Set-2	1000	41.3	FR	>20	**Ok**
		10000	80.0	FR	>20	**Ok**

Figure 4.22: Set-1 of Model 3 cross-section before the test

Figure 4.23: Set-1 of Model 3 cross-section after the test

Table 4.15 shows that damage parameters of Model 3 are appropriate for fully reshaping berm breakwater condition. Moreover, Figure 4.23 shows the S-shaped damage on the armour layer. Since Model 2 and Model 3 are designed with the same conditions, the difference in the damage parameter results may occur due to the difference in the berm width.

Model 4 is designed with a wide range of stones which is 2-8 tons. According to design calculations, Model 4 is classified as fully reshaping berm breakwater. Therefore, damage parameter range is same with Model 2 and Model 3. Damage parameters obtained from the experiments for Model 4 is presented in Table 4.16. Moreover, Figure 4.24 and Figure 4.25 are given as examples in order to observe the damage visually for Set-1 of Model 4 before the test and after the test, respectively.

Table 4.16: Damage results for Model 4

Experiment Damage Results				**Literature Check**		
Name	**Set No**	**Number of Waves**	**S**	**Breakwater Type**	**S Range**	**Status**
Model 4 (2-8 tons)	Set-1	1000	31.9	FR	>20	**Ok**
	Set-2	1000	28.0	FR	>20	**Ok**
	Set-3	1000	21.4	FR	>20	**Ok**
		4000	31.8	FR	>20	**Ok**
		8000	39.4	FR	>20	**Ok**
		10000	42.5	FR	>20	**Ok**

Figure 4.24: Set-1 of Model 4 cross-section before the test

Figure 4.25: Set-1 of Model 4 cross-section after the test

Model 4 is different from Model 2 and Model 3 in terms of stone gradation even though they are all designed as fully reshaping berm breakwater. The median stone diameter of Model 2 and Model 3 is 3 tons; however, the median stone diameter is 5 tons. This difference between the models results in different damage parameters. Damage parameter of the higher median stone diameter gets lower than the lower median stone diameter. It can be observed more clearly in the cumulative damage process, such as at the end of 10000 waves, damage parameter of Model 4 is much smaller than Model 3. Moreover, the damage differences on the armour layer of Model 4 and Model 3 can be seen easily from Figure 4.25 and Figure 23.

Model 5 is designed with a wide range of stones which is 6-10 tons. According to design calculations, Model 5 is classified as partly reshaping berm breakwater. Therefore, damage parameter must be in the range of 10-20 as stated in Table 2.2. Damage parameters obtained from the experiments for Model 5 is presented in Table 4.17. Moreover, Figure 4.26 and Figure 4.27 are given as examples in order to observe the damage visually for Set-2 of Model 5 before the test and after the test, respectively.

Table 4.17: Damage results for Model 5

Experiment Damage Results				**Literature Check**		
Name	**Set No**	**Number of Waves**	**S**	**Breakwater Type**	**S Range**	**Status**
Model 5 (6-10 tons)	Set-1	1000	9.2	PR	10-20	**Ok**
		4000	12.1	PR	10-20	**Ok**
		7000	16.5	PR	10-20	**Ok**
		10000	18.5	PR	10-20	**Ok**
	Set-2	1000	11.3	PR	10-20	**Ok**

Figure 4.26: Set-2 of Model 5 cross-section before the test

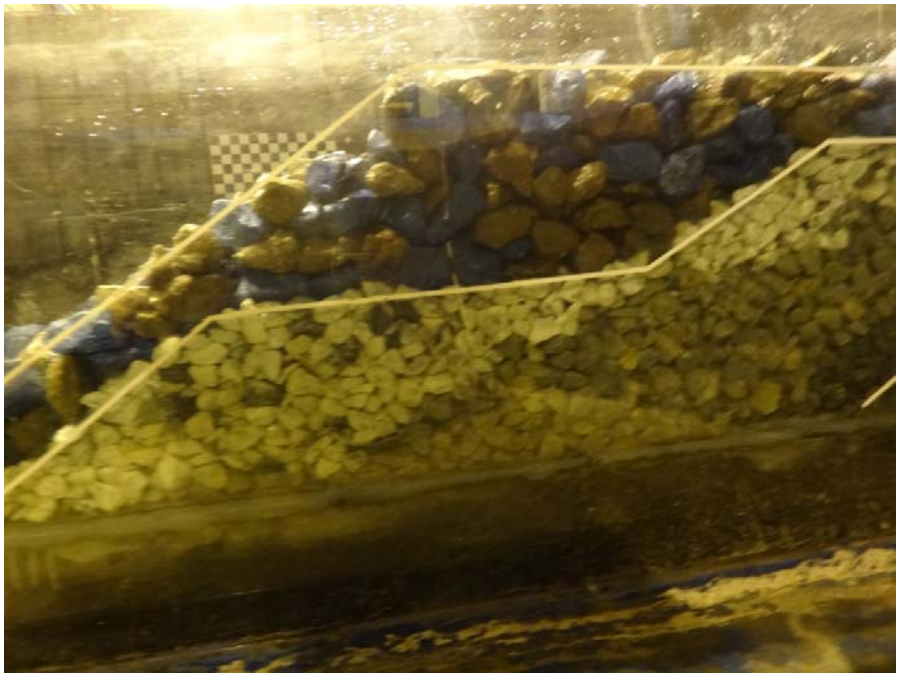

Figure 4.27: Set-2 of Model 5 cross-section after the test

Table 4.17 implies that Model 5 fulfils the damage requirements of being partly reshaping berm breakwater. Moreover, the section covers its stability even after approximately 30 hour storm (10000 waves). Furthermore, the visual comparison between Figure 4.26 and Figure 4.27 reveals that there are only a small number of moving stones on the armour layer of the cross-section.

Recession

Another important parameter on the classification of the berm breakwaters is recession. In the model experiments, recession is measured for all sets including cumulative damage investigation. Moreover, recession calculations are conducted according to Lykke Andersen et al. (2014) and classification results are controlled whether they are compatible with damage parameter results or not. The classification check is conducted according to the conditions given in Table 2.2 determined by Sigurdarson and Van der Meer (2012).

Recession results obtained from the experiments and calculated from the equations for Model 1 is presented in Table 4.18.

Table 4.18: Recession results for Model 1

Experiment Damage Results					**Literature Check**		
Name	**Set No**	**Number of Waves**	**Rec/Dn_{50} meas**	**Rec/Dn_{50} calc**	**Breakwater Type**	**Rec/Dn_{50}**	**Status**
Model 1 (12-15 tons)	Set-1	1000	0.88	1.35	HR	0.5-2	**Ok**
	Set-2	1000	1.23	1.35	HR	0.5-2	**Ok**
	Set-3	1000	0.64	1.35	HR	0.5-2	**Ok**
		3000	0.95	1.99	HR	0.5-2	**Ok**
		5000	1.16	1.99	HR	0.5-2	**Ok**
		7000	1.53	1.99	HR	0.5-2	**Ok**
		10000	1.56	1.99	HR	0.5-2	**Ok**

Model 1 is compatible with hardly reshaping berm breakwater conditions in terms of recession. Cross-section provides the requirements even after approximately 30 hour storm without providing any maintenance to the structure. Moreover, measured recession values are also compatible with the calculated results. Model 1 fulfils the conditions of being hardly reshaping berm breakwater both damage parameter and recession conditions.

Recession results obtained from the experiments and calculated from the equations for Model 2 is presented in Table 4.19.

Table 4.19: Recession results for Model 2

Experiment Damage Results					Literature Check		
Name	**Set No**	**Number of Waves**	**Rec/Dn_{50} meas**	**Rec/Dn_{50} calc**	**Breakwater Type**	**Rec/Dn_{50}**	**Status**
Model 2 (2-4 tons B=11.5m)	Set-1	1000	7.63	7.86	FR	3-10	**Ok**
	Set-2	1000	7.81	7.86	FR	3-10	**Ok**
	Set-3	1000	8.40	7.86	FR	3-10	**Ok**

Model 2 recession values both obtained from the calculations and measurements are in the range of 3-10. Therefore, Model 2 provides the requirements of being fully reshaping berm breakwater in terms of recession. Moreover, measured and calculated recession results are quite close to each other.

Recession results obtained from the experiments and calculated from the equations for Model 3 is presented in Table 4.20.

Table 4.20: Recession results for Model 3

Experiment Damage Results					Literature Check		
Name	**Set No**	**Number of Waves**	**Rec/Dn_{50} meas**	**Rec/Dn_{50} calc**	**Breakwater Type**	**Rec/Dn_{50}**	**Status**
Model 3 (2-4 tons B=26m)	Set-1	1000	7.18	7.86	FR	3-10	**Ok**
	Set-2	1000	8.08	7.86	FR	3-10	**Ok**
		10000	15.70	10.10	FR	3-10	**Not Ok**

Model 3 recession values show that in the cumulative damage analysis, the recession parameter does not fit in the allowable range for fully reshaping berm breakwater. However, recession values after 1000 waves are in the allowable range for fully reshaping berm breakwater. Moreover, it should be kept in mind that the classification determined by Sigurdarson and Van der Meer (2012) covers the results for 1000 waves. Even if the cumulative damage recession values do not fit the allowable range for the classification, one should take into account of recession values at the end of 1000 waves. Therefore, we can conclude that Model 3 is compatible with the design purpose.

Recession results obtained from the experiments and calculated from the equations for Model 4 is presented in Table 4.21.

Table 4.21: Recession results for Model 4

Experiment Damage Results					Literature Check		
Name	**Set No**	**Number of Waves**	**Rec/Dn_{50} meas**	**Rec/Dn_{50} calc**	**Breakwater Type**	**Rec/Dn_{50}**	**Status**
Model 4 (2-8 tons)	Set-1	1000	5.52	5.32	FR	3-10	**Ok**
	Set-2	1000	5.37	5.32	FR	3-10	**Ok**
	Set-3	1000	4.65	5.32	FR	3-10	**Ok**
		4000	8.43	6.92	FR	3-10	**Ok**
		8000	10.42	6.92	FR	3-10	**Not Ok**
		10000	11.26	6.92	FR	3-10	**Not Ok**

Recession results acquired at the end of cumulative damage analysis for Model 4 show similar properties as Model 3. Table 4.21 shows that at the end of 8000 waves, recession limit is exceeded. However, recession values at the end of 1000 waves for all sets are in the allowable range. Therefore, we can conclude that Model 4 is compatible with the design purpose.

Recession results obtained from the experiments and calculated from the equations for Model 5 is presented in Table 4.22.

Table 4.22: Recession results for Model 5

Experiment Damage Results					Literature Check		
Name	**Set No**	**Number of Waves**	**Rec/Dn_{50} meas**	**Rec/Dn_{50} calc**	**Breakwater Type**	**Rec/Dn_{50}**	**Status**
Model 5 (6-10 tons)	Set-1	1000	1.39	3.12	PR	1-5	**Ok**
		4000	2.38	4.17	PR	1-5	**Ok**
		7000	4.23	4.17	PR	1-5	**Ok**
		10000	4.65	4.17	PR	1-5	**Ok**
	Set-2	1000	2.36	3.12	PR	1-5	**Ok**

Recession values of Model 5 show that the structure satisfies the recession criteria of partly reshaping berm breakwater. Moreover, even in the cumulative damage analysis, the structure satisfies the recession criteria as Model 1.

According to the tables given above it can be said that in the cumulative damage analysis, fully reshaping berm breakwater exceed the recession criteria of the breakwater classification. However, hardly and partly reshaping berm breakwaters do not exceed the recession criteria even in the cumulative damage analysis.

From the stability perspective, all alternative models satisfy the conditions of berm breakwater classification determined by Sigurdarson and Van der Meer (2012).

Moreover, it can be seen from the tables given in Section 4.1.4, Ordu-Giresun hardly reshaping berm breakwater, which is Model 1, can be constructed as partly or fully reshaping berm breakwater since all alternative models fulfil the stability condition.

Cumulative Damage

In the physical model experiments, alternative models to Ordu-Giresun berm breakwater are tested for cumulative damage analysis. Model 2 is not tested for cumulative damage since it does not satisfy all design conditions. On the other hand, Model 3, Model 4, and Model 5 are tested under the cumulative damage condition. Cumulative damage measurements are conducted by the analyses of video recordings as stated in Section 4.1.2. Damage parameters for models tested under the cumulative damage are also checked according to Sigurdarson and Van der Meer (2012).

Damage parameters obtained from the analyses of video recordings under the cumulative damage for Model 3 are presented in Table 4.23.

Table 4.23: Damage parameters for Model 3

Video Recording Results					Literature Check		
Name	**Number of Waves**	**$A_{e(m)}$ (m^2)**	**$Dn_{50(m)}$ (m)**	**S**	**Breakwater Type**	**S Range**	**Status**
Model 3 (2-4 tons)	500	0.0230	0.028	29.3	FR	>20	**Ok**
	1000	0.0330	0.028	42.1	FR	>20	**Ok**
	1500	0.0380	0.028	48.5	FR	>20	**Ok**
	2000	0.0440	0.028	56.1	FR	>20	**Ok**
	2500	0.0450	0.028	57.4	FR	>20	**Ok**
	3000	0.0460	0.028	58.7	FR	>20	**Ok**
	3500	0.0470	0.028	59.9	FR	>20	**Ok**
	4000	0.0510	0.028	65.1	FR	>20	**Ok**
	4500	0.0515	0.028	65.7	FR	>20	**Ok**
	5000	0.0550	0.028	70.2	FR	>20	**Ok**
	5500	0.0555	0.028	70.8	FR	>20	**Ok**
	6000	0.0560	0.028	71.4	FR	>20	**Ok**
	6500	0.0560	0.028	71.4	FR	>20	**Ok**
	7000	0.0580	0.028	74.0	FR	>20	**Ok**
	7500	0.0610	0.028	77.8	FR	>20	**Ok**
	8000	0.0620	0.028	79.1	FR	>20	**Ok**
	8500	0.0625	0.028	79.7	FR	>20	**Ok**
	9000	0.0640	0.028	81.6	FR	>20	**Ok**
	9500	0.0640	0.028	81.6	FR	>20	**Ok**
	10000	0.0640	0.028	81.6	FR	>20	**Ok**

Table 4.23 shows that damage parameters obtained from the analyses of video recordings for Model 3 is compatible with both damage parameters obtained from profile measurement and the limitations for the classification.

Damage parameters obtained from the analyses of video recordings under the cumulative damage for Model 4 are presented in Table 4.24.

Table 4.24: Damage parameters for Model 4

Video Recording Results					Literature Check		
Name	**Number of Waves**	**$A_{e(m)}$ (m^2)**	**$Dn_{50(m)}$ (m)**	**S**	**Breakwater Type**	**S Range**	**Status**
Model 4 (2-8 tons)	500	0.0100	0.033	9.2	FR	>20	**Ok**
	1000	0.0220	0.033	20.2	FR	>20	**Ok**
	1500	0.0250	0.033	23.0	FR	>20	**Ok**
	2000	0.0290	0.033	26.6	FR	>20	**Ok**
	2500	0.0300	0.033	27.5	FR	>20	**Ok**
	3000	0.0310	0.033	28.5	FR	>20	**Ok**
	3500	0.0320	0.033	29.4	FR	>20	**Ok**
	4000	0.0340	0.033	31.2	FR	>20	**Ok**
	4500	0.0350	0.033	32.1	FR	>20	**Ok**
	5000	0.0360	0.033	33.1	FR	>20	**Ok**
	5500	0.0370	0.033	34.0	FR	>20	**Ok**
	6000	0.0380	0.033	34.9	FR	>20	**Ok**
	6500	0.0395	0.033	36.3	FR	>20	**Ok**
	7000	0.0410	0.033	37.6	FR	>20	**Ok**
	7500	0.0425	0.033	39.0	FR	>20	**Ok**
	8000	0.0440	0.033	40.4	FR	>20	**Ok**
	8500	0.0450	0.033	41.3	FR	>20	**Ok**
	9000	0.0470	0.033	43.2	FR	>20	**Ok**
	9500	0.0480	0.033	44.1	FR	>20	**Ok**
	10000	0.0480	0.033	44.1	FR	>20	**Ok**

Table 4.24 shows that damage parameters obtained from the analyses of video recordings for Model 4 is compatible with both damage parameters obtained from profile measurement and the limitations for the classification.

Damage parameters obtained from the analyses of video recordings under the cumulative damage for Model 5 are presented in Table 4.25.

Table 4.25: Damage parameters for Model 5

Video Recording Results					Literature Check		
Name	**Number of Waves**	**$A_{e(m)}$ (m^2)**	**$Dn_{50(m)}$ (m)**	**S**	**Breakwater Type**	**S Range**	**Status**
Model 5 (6-10 tons)	500	0.0110	0.039	7.2	PR	10-20	**Ok**
	1000	0.0138	0.039	9.1	PR	10-20	**Ok**
	1500	0.0141	0.039	9.3	PR	10-20	**Ok**
	2000	0.0150	0.039	9.9	PR	10-20	**Ok**
	2500	0.0153	0.039	10.1	PR	10-20	**Ok**
	3000	0.0158	0.039	10.4	PR	10-20	**Ok**
	3500	0.0164	0.039	10.8	PR	10-20	**Ok**
	4000	0.0170	0.039	11.2	PR	10-20	**Ok**
	4500	0.0175	0.039	11.5	PR	10-20	**Ok**
	5000	0.0182	0.039	12.0	PR	10-20	**Ok**
	5500	0.0190	0.039	12.5	PR	10-20	**Ok**
	6000	0.0200	0.039	13.1	PR	10-20	**Ok**
	6500	0.0215	0.039	14.1	PR	10-20	**Ok**
	7000	0.0230	0.039	15.1	PR	10-20	**Ok**
	7500	0.0250	0.039	16.4	PR	10-20	**Ok**
	8000	0.0260	0.039	17.1	PR	10-20	**Ok**
	8500	0.0270	0.039	17.8	PR	10-20	**Ok**
	9000	0.0275	0.039	18.1	PR	10-20	**Ok**
	9500	0.0280	0.039	18.4	PR	10-20	**Ok**
	10000	0.0280	0.039	18.4	PR	10-20	**Ok**

Table 4.25 shows that damage parameters obtained from the analyses of video recordings for Model 5 is compatible with both damage parameters obtained from profile measurement and the limitations for the classification.

In addition to damage parameters, recession values for models tested under the cumulative damage are also checked according to Sigurdarson and Van der Meer (2012).

Recession values obtained from the analyses of video recordings under the cumulative damage for Model 3 is presented in Table 4.26.

Table 4.26: Recession values for Model 3

Video Recording Results					Literature Check		
Name	**Number of Waves**	**Rec_m (m)**	**Rec_p (m)**	**Rec/Dn_{50} meas**	**Breakwater Type**	**Rec/Dn_{50}**	**Status**
Model 3 (2-4 tons)	500	0.1590	5.23	4.95	FR	3-10	**Ok**
	1000	0.2730	8.97	8.50	FR	3-10	**Ok**
	1500	0.2900	9.53	9.02	FR	3-10	**Ok**
	2000	0.4340	14.26	13.51	FR	3-10	**Not Ok**
	2500	0.4340	14.26	13.51	FR	3-10	**Not Ok**
	3000	0.4390	14.43	13.66	FR	3-10	**Not Ok**
	3500	0.4420	14.53	13.75	FR	3-10	**Not Ok**
	4000	0.4690	15.41	14.60	FR	3-10	**Not Ok**
	4500	0.4780	15.71	14.88	FR	3-10	**Not Ok**
	5000	0.4800	15.77	14.94	FR	3-10	**Not Ok**
	5500	0.4840	15.91	15.06	FR	3-10	**Not Ok**
	6000	0.4880	16.04	15.19	FR	3-10	**Not Ok**
	6500	0.4880	16.04	15.19	FR	3-10	**Not Ok**
	7000	0.4900	16.10	15.25	FR	3-10	**Not Ok**
	7500	0.4905	16.12	15.26	FR	3-10	**Not Ok**
	8000	0.4910	16.14	15.28	FR	3-10	**Not Ok**
	8500	0.4910	16.14	15.28	FR	3-10	**Not Ok**
	9000	0.4910	16.14	15.28	FR	3-10	**Not Ok**
	9500	0.4910	16.14	15.28	FR	3-10	**Not Ok**
	10000	0.4910	16.14	15.28	FR	3-10	**Not Ok**

Model 3 recession values obtained from the analyses of video recordings are similar to recession values obtained from profile measurement. Table 4.26 shows that in the cumulative damage analysis, the recession parameter does not fit in the allowable range for fully reshaping berm breakwater. In Table 4.20, it is presented that at the end of 10000 waves the recession exceeds the limits since there are not any profile measurements before 10000 waves for cumulative damage. However, in Table 4.26, it can be easily observed that the recession values exceed the limitations after 2000 waves.

Recession values obtained from the analyses of video recordings under the cumulative damage for Model 4 is presented in Table 4.27.

Table 4.27: Recession values for Model 4

Video Recording Results					Literature Check		
Name	**Number of Waves**	**Rec_m (m)**	**Rec_p (m)**	**Rec/Dn_{50} meas**	**Breakwater Type**	**Rec/Dn_{50}**	**Status**
Model 4 (2-8 tons)	500	0.0750	2.46	1.97	FR	3-10	**Ok**
	1000	0.1420	4.67	3.73	FR	3-10	**Ok**
	1500	0.1840	6.05	4.83	FR	3-10	**Ok**
	2000	0.1970	6.47	5.17	FR	3-10	**Ok**
	2500	0.2510	8.25	6.59	FR	3-10	**Ok**
	3000	0.2930	9.63	7.69	FR	3-10	**Ok**
	3500	0.3260	10.71	8.56	FR	3-10	**Ok**
	4000	0.3380	11.11	8.87	FR	3-10	**Ok**
	4500	0.3580	11.76	9.40	FR	3-10	**Ok**
	5000	0.3690	12.13	9.69	FR	3-10	**Ok**
	5500	0.3890	12.78	10.21	FR	3-10	**Not Ok**
	6000	0.4070	13.38	10.68	FR	3-10	**Not Ok**
	6500	0.4200	13.80	11.02	FR	3-10	**Not Ok**
	7000	0.4300	14.13	11.29	FR	3-10	**Not Ok**
	7500	0.4400	14.46	11.55	FR	3-10	**Not Ok**
	8000	0.4450	14.62	11.68	FR	3-10	**Not Ok**
	8500	0.4500	14.79	11.81	FR	3-10	**Not Ok**
	9000	0.4500	14.79	11.81	FR	3-10	**Not Ok**
	9500	0.4500	14.79	11.81	FR	3-10	**Not Ok**
	10000	0.4500	14.79	11.81	FR	3-10	**Not Ok**

Model 4 recession values obtained from the analyses of video recordings are similar to recession values obtained from profile measurement. Table 4.27 shows that in the cumulative damage analysis, the recession parameter does not fit in the allowable range for fully reshaping berm breakwater. In Table 4.21, it can be observed that

between 4000 and 8000 waves the recession value exceeds the allowable recession. This range is determined easily with the help of Table 4.27. According to video recording analysis results, recession exceeds the allowable limits at the end of 5500 waves for Model 4 whereas 2000 waves for Model 3. This difference occurs due to the difference in median stone diameter.

Recession values obtained from the analyses of video recordings under the cumulative damage for Model 5 is presented in Table 4.28.

Table 4.28: Recession values for Model 5

Video Recording Results					**Literature Check**		
Name	**Number of Waves**	**Rec_m (m)**	**Rec_p (m)**	**Rec/Dn_{50} meas**	**Breakwater Type**	**Rec/Dn_{50}**	**Status**
Model 5 (6-10 tons)	500	0.0320	1.05	0.72	PR	1-5	**Ok**
	1000	0.0450	1.48	1.01	PR	1-5	**Ok**
	1500	0.0480	1.58	1.08	PR	1-5	**Ok**
	2000	0.0690	2.27	1.55	PR	1-5	**Ok**
	2500	0.0840	2.76	1.89	PR	1-5	**Ok**
	3000	0.0920	3.02	2.07	PR	1-5	**Ok**
	3500	0.0950	3.12	2.13	PR	1-5	**Ok**
	4000	0.0980	3.22	2.20	PR	1-5	**Ok**
	4500	0.1120	3.68	2.51	PR	1-5	**Ok**
	5000	0.1250	4.11	2.81	PR	1-5	**Ok**
	5500	0.1450	4.77	3.25	PR	1-5	**Ok**
	6000	0.1540	5.06	3.46	PR	1-5	**Ok**
	6500	0.1630	5.36	3.66	PR	1-5	**Ok**
	7000	0.1730	5.69	3.88	PR	1-5	**Ok**
	7500	0.1880	6.18	4.22	PR	1-5	**Ok**
	8000	0.1950	6.41	4.38	PR	1-5	**Ok**
	8500	0.1980	6.51	4.44	PR	1-5	**Ok**
	9000	0.2000	6.57	4.49	PR	1-5	**Ok**
	9500	0.2000	6.57	4.49	PR	1-5	**Ok**
	10000	0.2000	6.57	4.49	PR	1-5	**Ok**

Table 4.28 indicates that Model 5 recession results acquired from the analyses of video recordings are compatible to recession results acquired from profile measurement. Both Table 4.22 and Table 4.28 show that Model 5 recession results are in the allowable range for partly reshaping berm breakwater.

In the cumulative damage analysis, it is aimed to examine the relationship between damage and number of waves. Main damage on the structure occurs after which wave, and how many waves after the structure stabilizes are the main questions in the cumulative damage investigation. Therefore, damage parameter results and number of waves are drawn on a graph for Model 3, Model 4, and Model 5.

Figure 4.28 presents the relationship between damage and number of waves for Model 3, Model 4, and Model 5.

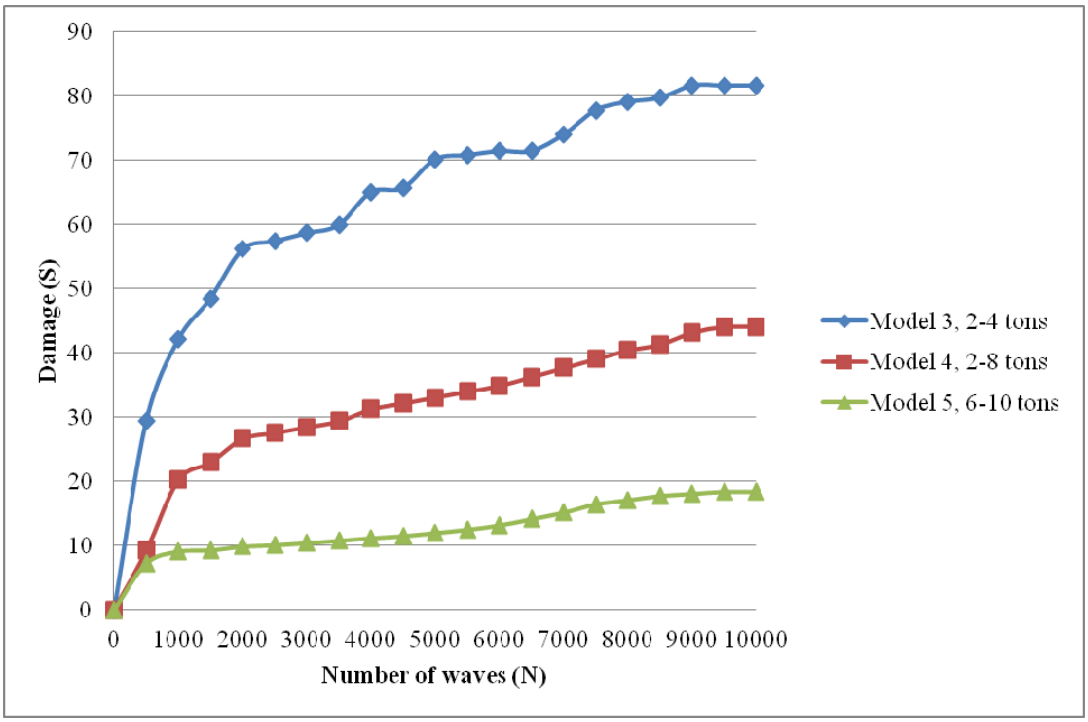

Figure 4.28: Cumulative damage analysis for alternative models

It can be said according to Figure 4.28 that the structures take most of the damage at the end of first 1000 waves. After 1000 waves, the structure takes damage with in a slowly increasing way until it reaches the equilibrium. This might be the reason of testing models under 1000 waves since the model gets most of the damage at the end of 1000 waves. Furthermore, the structures reach equilibrium approximately at the end of 8000 waves according to Figure 4.28.

4.2. Serviceability of the Structures

Another important parameter on the design of breakwaters is serviceability of the structure. Serviceability of the structure is governed by wave overtopping. Since the structure under consideration is a breakwater protecting an airport, wave overtopping has a vital importance. In the design calculations, the allowable mean overtopping discharge has been determined as 10 l/s/m for Ordu-Giresun berm breakwater. Therefore, the same condition is taken as the upper limit for mean overtopping discharge of alternative models.

Wave overtopping is measured for all models at the end of each 500 waves by weighing the water collected in a tank and then, converted into mean overtopping discharge. After measuring the mean overtopping discharge, the structure is controlled whether it satisfies the serviceability condition or not.

Wave overtopping measurements for Model 1 are presented in Table 4.29.

Table 4.29: Overtopping results for Model 1

Experiment Overtopping Results					Literature Check	
Name	**Set No**	**Number of Waves**	**Model Quantity**	**Prototype Quantity**	**Overtopping Range**	**Status**
Model 1 (12-15 tons)	Set-1	0-500	3792 grams	3.17 l/s/m	< 10 l/s/m	**Ok**
		500-1000	3096 grams	2.59 l/s/m	< 10 l/s/m	**Ok**
	Set-2	0-500	1434 grams	1.20 l/s/m	< 10 l/s/m	**Ok**
		500-1000	1196 grams	1.00 l/s/m	< 10 l/s/m	**Ok**
	Set-3	0-500	2846 grams	2.38 l/s/m	< 10 l/s/m	**Ok**
		500-1000	2624 grams	2.20 l/s/m	< 10 l/s/m	**Ok**
		1000-1500	3218 grams	2.69 l/s/m	< 10 l/s/m	**Ok**
		1500-2000	4622 grams	3.87 l/s/m	< 10 l/s/m	**Ok**
		2000-2500	4026 grams	3.37 l/s/m	< 10 l/s/m	**Ok**
		2500-3000	3950 grams	3.31 l/s/m	< 10 l/s/m	**Ok**
		3000-3500	3934 grams	3.29 l/s/m	< 10 l/s/m	**Ok**
		3500-4000	3002 grams	2.51 l/s/m	< 10 l/s/m	**Ok**
		4000-4500	3486 grams	2.92 l/s/m	< 10 l/s/m	**Ok**
		4500-5000	3574 grams	2.99 l/s/m	< 10 l/s/m	**Ok**
		5000-5500	4624 grams	3.87 l/s/m	< 10 l/s/m	**Ok**
		5500-6000	4580 grams	3.83 l/s/m	< 10 l/s/m	**Ok**
		6000-6500	3714 grams	3.11 l/s/m	< 10 l/s/m	**Ok**
		6500-7000	3780 grams	3.16 l/s/m	< 10 l/s/m	**Ok**
		7000-7500	3262 grams	2.73 l/s/m	< 10 l/s/m	**Ok**
		7500-8000	2701 grams	2.26 l/s/m	< 10 l/s/m	**Ok**
		8000-8500	2638 grams	2.21 l/s/m	< 10 l/s/m	**Ok**
		8500-9000	2566 grams	2.15 l/s/m	< 10 l/s/m	**Ok**
		9000-9500	2928 grams	2.45 l/s/m	< 10 l/s/m	**Ok**
		9500-10000	2580 grams	2.16 l/s/m	< 10 l/s/m	**Ok**

Table 4.29 shows that all overtopping measurements are in the allowable range for Model 1 even in the cumulative damage situation. Therefore, it can be concluded that Ordu-Giresun berm breakwater fulfils both stability and serviceability requirements.

Wave overtopping measurements for Model 2 are presented in Table 4.30.

Table 4.30: Overtopping results for Model 2

Experiment Overtopping Results					Literature Check	
Name	**Set No**	**Number of Waves**	**Model Quantity**	**Prototype Quantity**	**Overtopping Range**	**Status**
Model 2 (2-4 tons B=11.5m)	Set-1	0-500	73094 grams	61.20 l/s/m	< 10 l/s/m	**Not Ok**
		500-1000	54945 grams	46.00 l/s/m	< 10 l/s/m	**Not Ok**
	Set-2	0-500	95080 grams	79.61 l/s/m	< 10 l/s/m	**Not Ok**
		500-1000	110264 grams	92.32 l/s/m	< 10 l/s/m	**Not Ok**
	Set-3	0-500	87920 grams	73.61 l/s/m	< 10 l/s/m	**Not Ok**
		500-1000	99920 grams	83.66 l/s/m	< 10 l/s/m	**Not Ok**

As it can be seen from Table 4.30, Model 2 does not satisfy the serviceability requirements. Therefore, Model 2 is not tested for cumulative damage although it satisfies the stability condition.

Wave overtopping measurements for Model 3 are presented in Table 4.31.

Table 4.31: Overtopping results for Model 3

Experiment Overtopping Results					Literature Check	
Name	**Set No**	**Number of Waves**	**Model Quantity**	**Prototype Quantity**	**Overtopping Range**	**Status**
Model 3 (2-4 tons B=26m)	Set-1	0-500	6862 grams	5.75 l/s/m	< 10 l/s/m	**Ok**
		500-1000	6704 grams	5.61 l/s/m	< 10 l/s/m	**Ok**
	Set-2	0-500	9844 grams	8.24 l/s/m	< 10 l/s/m	**Ok**
		500-1000	8764 grams	7.34 l/s/m	< 10 l/s/m	**Ok**
		1000-1500	5480 grams	4.59 l/s/m	< 10 l/s/m	**Ok**
		1500-2000	5650 grams	4.73 l/s/m	< 10 l/s/m	**Ok**
		2000-2500	5914 grams	4.95 l/s/m	< 10 l/s/m	**Ok**
		2500-3000	6325 grams	5.30 l/s/m	< 10 l/s/m	**Ok**
		3000-3500	7452 grams	6.24 l/s/m	< 10 l/s/m	**Ok**
		3500-4000	8544 grams	7.15 l/s/m	< 10 l/s/m	**Ok**
		4000-4500	9794 grams	8.20 l/s/m	< 10 l/s/m	**Ok**
		4500-5000	9184 grams	7.69 l/s/m	< 10 l/s/m	**Ok**
		5000-5500	8460 grams	7.08 l/s/m	< 10 l/s/m	**Ok**
		5500-6000	7290 grams	6.10 l/s/m	< 10 l/s/m	**Ok**
		6000-6500	8456 grams	7.08 l/s/m	< 10 l/s/m	**Ok**
		6500-7000	6358 grams	5.32 l/s/m	< 10 l/s/m	**Ok**
		7000-7500	6262 grams	5.24 l/s/m	< 10 l/s/m	**Ok**
		7500-8000	6194 grams	5.19 l/s/m	< 10 l/s/m	**Ok**
		8000-8500	8658 grams	7.25 l/s/m	< 10 l/s/m	**Ok**
		8500-9000	8207 grams	6.87 l/s/m	< 10 l/s/m	**Ok**
		9000-9500	8252 grams	6.91 l/s/m	< 10 l/s/m	**Ok**
		9500-10000	7988 grams	6.69 l/s/m	< 10 l/s/m	**Ok**

After testing Model 2, it is observed that stability condition is satisfied; on the other hand, serviceability condition is not satisfied. Therefore, Model 3 is tested with same stone range and a longer berm in order to decrease the wave overtopping. According to Table 4.31, serviceability condition is provided by Model 3 even in the cumulative damage situation by increasing the berm width.

Wave overtopping measurements for Model 4 are presented in Table 4.32.

Table 4.32: Overtopping results for Model 4

Experiment Overtopping Results					Literature Check	
Name	**Set No**	**Number of Waves**	**Model Quantity**	**Prototype Quantity**	**Overtopping Range**	**Status**
Model 4 (2-8 tons)	Set-1	0-500	9494 grams	7.95 l/s/m	< 10 l/s/m	**Ok**
		500-1000	9390 grams	7.86 l/s/m	< 10 l/s/m	**Ok**
	Set-2	0-500	6362 grams	5.33 l/s/m	< 10 l/s/m	**Ok**
		500-1000	4838 grams	4.05 l/s/m	< 10 l/s/m	**Ok**
	Set-3	0-500	8652 grams	7.24 l/s/m	< 10 l/s/m	**Ok**
		500-1000	7776 grams	6.51 l/s/m	< 10 l/s/m	**Ok**
		1000-1500	7570 grams	6.34 l/s/m	< 10 l/s/m	**Ok**
		1500-2000	4770 grams	3.99 l/s/m	< 10 l/s/m	**Ok**
		2000-2500	4696 grams	3.93 l/s/m	< 10 l/s/m	**Ok**
		2500-3000	5672 grams	4.75 l/s/m	< 10 l/s/m	**Ok**
		3000-3500	4968 grams	4.16 l/s/m	< 10 l/s/m	**Ok**
		3500-4000	4626 grams	3.87 l/s/m	< 10 l/s/m	**Ok**
		4000-4500	5687 grams	4.76 l/s/m	< 10 l/s/m	**Ok**
		4500-5000	6070 grams	5.08 l/s/m	< 10 l/s/m	**Ok**
		5000-5500	5338 grams	4.47 l/s/m	< 10 l/s/m	**Ok**
		5500-6000	5778 grams	4.84 l/s/m	< 10 l/s/m	**Ok**
		6000-6500	6242 grams	5.23 l/s/m	< 10 l/s/m	**Ok**
		6500-7000	6362 grams	5.33 l/s/m	< 10 l/s/m	**Ok**
		7000-7500	5355 grams	4.48 l/s/m	< 10 l/s/m	**Ok**
		7500-8000	5691 grams	4.76 l/s/m	< 10 l/s/m	**Ok**
		8000-8500	4960 grams	4.15 l/s/m	< 10 l/s/m	**Ok**
		8500-9000	6834 grams	5.72 l/s/m	< 10 l/s/m	**Ok**
		9000-9500	5682 grams	4.76 l/s/m	< 10 l/s/m	**Ok**
		9500-10000	4872 grams	4.08 l/s/m	< 10 l/s/m	**Ok**

Table 4.32 shows that all overtopping measurements are in the allowable range for Model 4 even in the cumulative damage situation.

Wave overtopping measurements for Model 5 are presented in Table 4.33.

Table 4.33: Overtopping results for Model 5

Experiment Overtopping Results					Literature Check	
Name	**Set No**	**Number of Waves**	**Model Quantity**	**Prototype Quantity**	**Overtopping Range**	**Status**
Model 5 (6-10 tons)	Set-1	0-500	1808 grams	1.51 l/s/m	< 10 l/s/m	**Ok**
		500-1000	2286 grams	1.91 l/s/m	< 10 l/s/m	**Ok**
		1000-1500	2084 grams	1.74 l/s/m	< 10 l/s/m	**Ok**
		1500-2000	2684 grams	2.25 l/s/m	< 10 l/s/m	**Ok**
		2000-2500	2430 grams	2.03 l/s/m	< 10 l/s/m	**Ok**
		2500-3000	2457 grams	2.06 l/s/m	< 10 l/s/m	**Ok**
		3000-3500	1412 grams	1.18 l/s/m	< 10 l/s/m	**Ok**
		3500-4000	1658 grams	1.39 l/s/m	< 10 l/s/m	**Ok**
		4000-4500	1908 grams	1.60 l/s/m	< 10 l/s/m	**Ok**
		4500-5000	1586 grams	1.33 l/s/m	< 10 l/s/m	**Ok**
		5000-5500	2170 grams	1.82 l/s/m	< 10 l/s/m	**Ok**
		5500-6000	2496 grams	2.09 l/s/m	< 10 l/s/m	**Ok**
		6000-6500	2188 grams	1.83 l/s/m	< 10 l/s/m	**Ok**
		6500-7000	2294 grams	1.92 l/s/m	< 10 l/s/m	**Ok**
		7000-7500	2670 grams	2.24 l/s/m	< 10 l/s/m	**Ok**
		7500-8000	2488 grams	2.08 l/s/m	< 10 l/s/m	**Ok**
		8000-8500	2774 grams	2.32 l/s/m	< 10 l/s/m	**Ok**
		8500-9000	2565 grams	2.15 l/s/m	< 10 l/s/m	**Ok**
		9000-9500	2448 grams	2.05 l/s/m	< 10 l/s/m	**Ok**
		9500-10000	3046 grams	2.55 l/s/m	< 10 l/s/m	**Ok**
	Set-2	0-500	1760 grams	1.47 l/s/m	< 10 l/s/m	**Ok**
		500-1000	1988 grams	1.66 l/s/m	< 10 l/s/m	**Ok**

As it can be seen from Table 4.33, Model 5 satisfies the serviceability condition for all sets.

Moreover, in the literature, several methods are given by design manuals to compute mean overtopping discharge. The mean overtopping discharge of the models are calculated as presented in Chapter 2 according to CLASH (Verhaeghe et al., 2005), TAW (2002), and formulas proposed by Sigurdarson and Van der Meer (2012). Measured mean overtopping discharges are compared to the calculated discharges.

Calculated and measured mean overtopping discharges for Model 1 are compared in Table 4.34.

Table 4.34: Overtopping comparison for Model 1

Experiment Overtopping Results				Literature Check		
Name	**Set No**	**Number of Waves**	**Prototype Quantity**	**CLASH Results**	**TAW Results**	**EUROTOP (by S&WdM) Results**
Model 1 (12-15 tons)	Set-1	0-500	3.17 l/s/m	1.62 l/s/m	7.01 l/s/m	2.06 l/s/m
		500-1000	2.59 l/s/m			
	Set-2	0-500	1.20 l/s/m			
		500-1000	1.00 l/s/m			
	Set-3	0-500	2.38 l/s/m			
		500-1000	2.20 l/s/m			
		1000-1500	2.69 l/s/m			
		1500-2000	3.87 l/s/m			
		2000-2500	3.37 l/s/m			
		2500-3000	3.31 l/s/m			
		3000-3500	3.29 l/s/m			
		3500-4000	2.51 l/s/m			
		4000-4500	2.92 l/s/m			
		4500-5000	2.99 l/s/m			
		5000-5500	3.87 l/s/m			
		5500-6000	3.83 l/s/m			
		6000-6500	3.11 l/s/m			
		6500-7000	3.16 l/s/m			
		7000-7500	2.73 l/s/m			
		7500-8000	2.26 l/s/m			
		8000-8500	2.21 l/s/m			
		8500-9000	2.15 l/s/m			
		9000-9500	2.45 l/s/m			
		9500-10000	2.16 l/s/m			

Table 4.34 indicates that measured overtopping values are close to results which are calculated by CLASH (Verhaeghe et al., 2005) and modified EurOtop formulas given by Sigurdarson and Van der Meer (2012). In addition, TAW (2002) gives higher overtopping results for Model 1. Although calculated and measured wave overtopping results are different, they are all in the allowable limits of serviceability.

Calculated and measured mean overtopping discharges for Model 2 are compared in Table 4.35.

Table 4.35: Overtopping comparison for Model 2

Experiment Overtopping Results				**Literature Check**		
Name	**Set No**	**Number of Waves**	**Prototype Quantity**	**CLASH Results**	**TAW Results**	**EUROTOP (by S&WdM) Results**
Model 2 (2-4 tons B=11.5m)	Set-1	0-500	61.20 l/s/m	9.86 l/s/m	121.10 l/s/m	12.46 l/s/m
		500-1000	46.00 l/s/m			
	Set-2	0-500	79.61 l/s/m			
		500-1000	92.32 l/s/m			
	Set-3	0-500	73.61 l/s/m			
		500-1000	83.66 l/s/m			

Model 2 wave overtopping results are close to TAW (2002) results which do not provide the serviceability criteria. Even though most of the overtopping measurements are compatible with CLASH (Verhaeghe et al., 2005) results, this case does not fulfil any requirement. Moreover, the results calculated by CLASH (Verhaeghe et al., 2005) and modified EurOtop formulas given by Sigurdarson and Van der Meer (2012) are close to each other similar to Model 1.

Calculated and measured mean overtopping discharges for Model 3 are compared in Table 4.36.

Table 4.36: Overtopping comparison for Model 3

Experiment Overtopping Results				Literature Check		
Name	**Set No**	**Number of Waves**	**Prototype Quantity**	**CLASH Results**	**TAW Results**	**EUROTOP (by S&WdM) Results**
Model 3 (2-4 tons B=26m)	Set-1	0-500	5.75 l/s/m	2.76 l/s/m	121.10 l/s/m	12.46 l/s/m
		500-1000	5.61 l/s/m			
	Set-2	0-500	8.24 l/s/m			
		500-1000	7.34 l/s/m			
		1000-1500	4.59 l/s/m			
		1500-2000	4.73 l/s/m			
		2000-2500	4.95 l/s/m			
		2500-3000	5.30 l/s/m			
		3000-3500	6.24 l/s/m			
		3500-4000	7.15 l/s/m			
		4000-4500	8.20 l/s/m			
		4500-5000	7.69 l/s/m			
		5000-5500	7.08 l/s/m			
		5500-6000	6.10 l/s/m			
		6000-6500	7.08 l/s/m			
		6500-7000	5.32 l/s/m			
		7000-7500	5.24 l/s/m			
		7500-8000	5.19 l/s/m			
		8000-8500	7.25 l/s/m			
		8500-9000	6.87 l/s/m			
		9000-9500	6.91 l/s/m			
		9500-10000	6.69 l/s/m			

Table 4.36 indicates that the results calculated by TAW (2002) and modified EurOtop formulas given by Sigurdarson and Van der Meer (2012) are not affected by the change between Model 2 and Model 3. However, CLASH (Verhaeghe et al., 2005) result is decreased due to the difference between Model 2 and Model 3.

Calculated and measured mean overtopping discharges for Model 4 are compared in Table 4.37.

Table 4.37: Overtopping comparison for Model 4

Experiment Overtopping Results				Literature Check		
Name	**Set No**	**Number of Waves**	**Prototype Quantity**	**CLASH Results**	**TAW Results**	**EUROTOP (by S&WdM) Results**
Model 4 (2-8 tons)	Set-1	0-500	7.95 l/s/m	2.76 l/s/m	121.10 l/s/m	12.46 l/s/m
		500-1000	7.86 l/s/m			
	Set-2	0-500	5.33 l/s/m			
		500-1000	4.05 l/s/m			
	Set-3	0-500	7.24 l/s/m			
		500-1000	6.51 l/s/m			
		1000-1500	6.34 l/s/m			
		1500-2000	3.99 l/s/m			
		2000-2500	3.93 l/s/m			
		2500-3000	4.75 l/s/m			
		3000-3500	4.16 l/s/m			
		3500-4000	3.87 l/s/m			
		4000-4500	4.76 l/s/m			
		4500-5000	5.08 l/s/m			
		5000-5500	4.47 l/s/m			
		5500-6000	4.84 l/s/m			
		6000-6500	5.23 l/s/m			
		6500-7000	5.33 l/s/m			
		7000-7500	4.48 l/s/m			
		7500-8000	4.76 l/s/m			
		8000-8500	4.15 l/s/m			
		8500-9000	5.72 l/s/m			
		9000-9500	4.76 l/s/m			
		9500-10000	4.08 l/s/m			

Table 4.37 indicates that measured overtopping values are close to results which are calculated by CLASH (Verhaeghe et al., 2005). Measured and calculated by CLASH (Verhaeghe et al., 2005) wave overtopping results are in the allowable limits of serviceability; however, the results calculated by TAW (2002) and modified EurOtop formulas given by Sigurdarson and Van der Meer (2012) do not provide the serviceability requirement.

Calculated and measured mean overtopping discharges for Model 5 are compared in Table 4.38.

Table 4.38: Overtopping comparison for Model 5

Experiment Overtopping Results				Literature Check		
Name	**Set No**	**Number of Waves**	**Prototype Quantity**	**CLASH Results**	**TAW Results**	**EUROTOP (by S&WdM) Results**
Model 5 (6-10 tons)	Set-1	0-500	1.51 l/s/m	2.76 l/s/m	121.10 l/s/m	4.46 l/s/m
		500-1000	1.91 l/s/m			5.38 l/s/m
		1000-1500	1.74 l/s/m			5.79 l/s/m
		1500-2000	2.25 l/s/m			5.89 l/s/m
		2000-2500	2.03 l/s/m			6.61 l/s/m
		2500-3000	2.06 l/s/m			7.16 l/s/m
		3000-3500	1.18 l/s/m			7.47 l/s/m
		3500-4000	1.39 l/s/m			7.59 l/s/m
		4000-4500	1.60 l/s/m			7.70 l/s/m
		4500-5000	1.33 l/s/m			8.29 l/s/m
		5000-5500	1.82 l/s/m			8.85 l/s/m
		5500-6000	2.09 l/s/m			9.77 l/s/m
		6000-6500	1.83 l/s/m			10.20 l/s/m
		6500-7000	1.92 l/s/m			10.65 l/s/m
		7000-7500	2.24 l/s/m			11.17 l/s/m
		7500-8000	2.08 l/s/m			11.97 l/s/m
		8000-8500	2.32 l/s/m			12.36 l/s/m
		8500-9000	2.15 l/s/m			12.53 l/s/m
		9000-9500	2.05 l/s/m			12.63 l/s/m
		9500-10000	2.55 l/s/m			12.63 l/s/m
	Set-2	0-500	1.47 l/s/m			4.46 l/s/m
		500-1000	1.66 l/s/m			

Table 4.38 indicates that the results calculated by TAW (2002) and CLASH (Verhaeghe et al., 2005) are not affected to the change between Model 4 and Model 5. Because the geometry of the models are same and the formulations of TAW (2002) and CLASH (Verhaeghe et al., 2005) do not include the effect of reshaping while modified EurOtop formulas given by Sigurdarson and Van der Meer (2012)

include. Moreover, in Model 5 reshaping of the section is examined under cumulative damage situation. As it can be seen from Table 4.38, overtopping results calculated by modified EurOtop formulas given by Sigurdarson and Van der Meer (2012) increase due to reshaping and results are in the allowable range at the end of 6000 waves. Furthermore, results calculated by CLASH (Verhaeghe et al., 2005) are more compatible with the measured overtopping values.

4.3. Discussion of Relation between Stability and Serviceability of Models

In this study, it is aimed to investigate the cumulative damage in reshaping breakwaters and its effect to wave overtopping. In order to find a relationship, the stability conditions including damage parameter and recession are determined by the analyses of video recordings as described in Section 4.1.2. In addition, wave overtopping measurements are determined for every model as described in Section 4.2.

The parameters that are used in the investigation of the relation between stability and serviceability for Model 3, Model 4, and Model 5 are given in Table 4.39, Table 4.40, and Table 4.41, respectively.

Table 4.39: Parameters obtained from video recordings for Model 3

Name	Number of Waves	S	h/Rec	q (l/s/m)	$q/(g*H_{mo}^3)^{0.5}$
Model 3 (2-4 tons)	500	29.3	0.270	8.24	0.152
	1000	42.1	0.183	7.34	0.136
	1500	48.5	0.179	4.59	0.085
	2000	56.1	0.143	4.73	0.087
	2500	57.4	0.159	4.95	0.092
	3000	58.7	0.159	5.30	0.098
	3500	59.9	0.170	6.24	0.115
	4000	65.1	0.166	7.15	0.132
	4500	65.7	0.174	8.20	0.152
	5000	70.2	0.179	7.69	0.142
	5500	70.8	0.182	7.08	0.131
	6000	71.4	0.186	6.10	0.113
	6500	71.4	0.186	7.08	0.131
	7000	74.0	0.188	5.32	0.098
	7500	77.8	0.188	5.24	0.097
	8000	79.1	0.187	5.19	0.096
	8500	79.7	0.187	7.25	0.134
	9000	81.6	0.187	6.87	0.127
	9500	81.6	0.187	6.91	0.128
	10000	81.6	0.187	6.69	0.124

Table 4.40: Parameters obtained from video recordings for Model 4

Name	Number of Waves	S	h/Rec	q (l/s/m)	$q/(g*H_{mo}^{3})^{0.5}$
Model 4 (2-8 tons)	500	9.2	0.133	7.24	0.134
	1000	20.2	0.134	6.51	0.120
	1500	23.0	0.141	6.34	0.117
	2000	26.6	0.152	3.99	0.074
	2500	27.5	0.127	3.93	0.073
	3000	28.5	0.126	4.75	0.088
	3500	29.4	0.123	4.16	0.077
	4000	31.2	0.126	3.87	0.072
	4500	32.1	0.123	4.76	0.088
	5000	33.1	0.125	5.08	0.094
	5500	34.0	0.125	4.47	0.083
	6000	34.9	0.128	4.84	0.089
	6500	36.3	0.129	5.23	0.097
	7000	37.6	0.128	5.33	0.099
	7500	39.0	0.130	4.48	0.083
	8000	40.4	0.130	4.76	0.088
	8500	41.3	0.131	4.15	0.077
	9000	43.2	0.133	5.72	0.106
	9500	44.1	0.133	4.76	0.088
	10000	44.1	0.133	4.08	0.075

Table 4.41: Parameters obtained from video recordings for Model 5

Name	Number of Waves	S	h/Rec	q (l/s/m)	$q/(g*H_{mo}^{3})^{0.5}$
Model 5 (6-10 tons)	500	7.2	0.156	1.51	0.028
	1000	9.1	0.178	1.91	0.035
	1500	9.3	0.188	1.74	0.032
	2000	9.9	0.145	2.25	0.042
	2500	10.1	0.131	2.03	0.038
	3000	10.4	0.130	2.06	0.038
	3500	10.8	0.126	1.18	0.022
	4000	11.2	0.143	1.39	0.026
	4500	11.5	0.134	1.60	0.030
	5000	12.0	0.132	1.33	0.025
	5500	12.5	0.131	1.82	0.034
	6000	13.1	0.136	2.09	0.039
	6500	14.1	0.141	1.83	0.034
	7000	15.1	0.139	1.92	0.036
	7500	16.4	0.138	2.24	0.041
	8000	17.1	0.144	2.08	0.039
	8500	17.8	0.146	2.32	0.043
	9000	18.1	0.150	2.15	0.040
	9500	18.4	0.150	2.05	0.038
	10000	18.4	0.150	2.55	0.047

According to the previous tables, Figure 4.29 - Figure 4.32 are drawn in order to find a relationship between stability and serviceability.

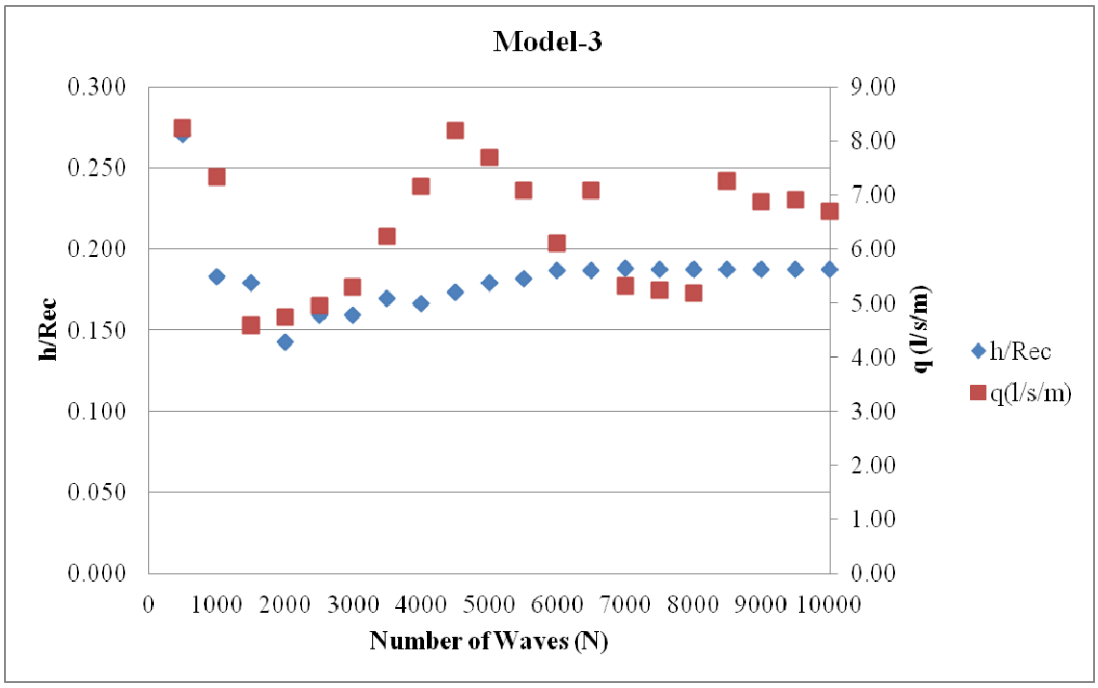

Figure 4.29: Damage vs. overtopping under cumulative damage for Model 3

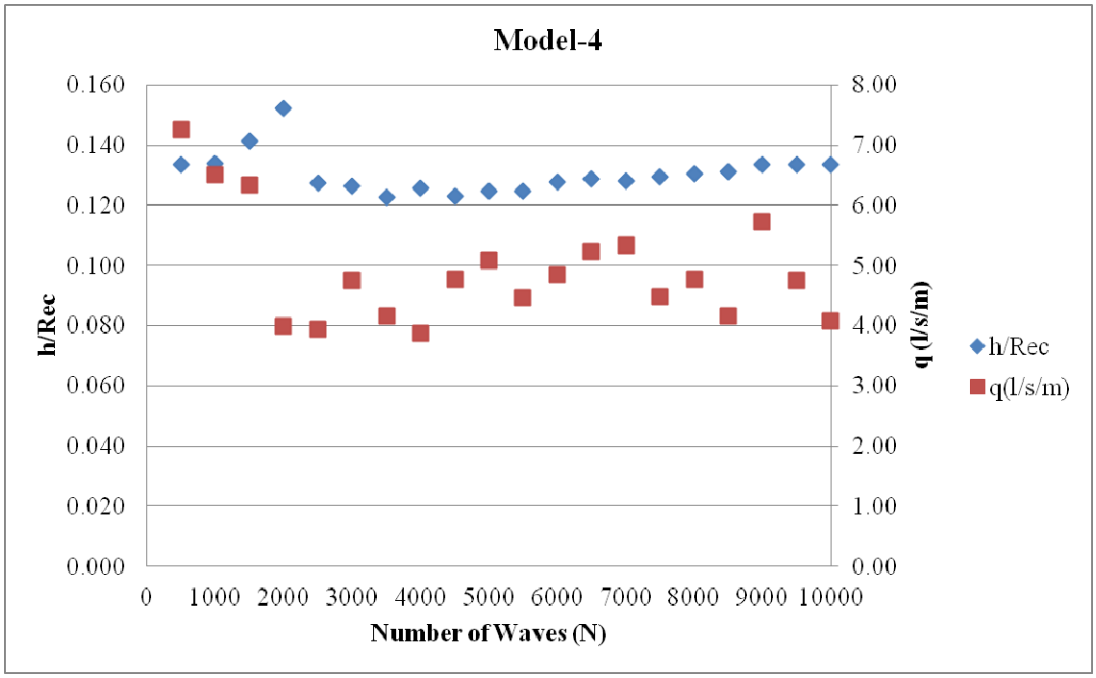

Figure 4.30: Damage vs. overtopping under cumulative damage for Model 4

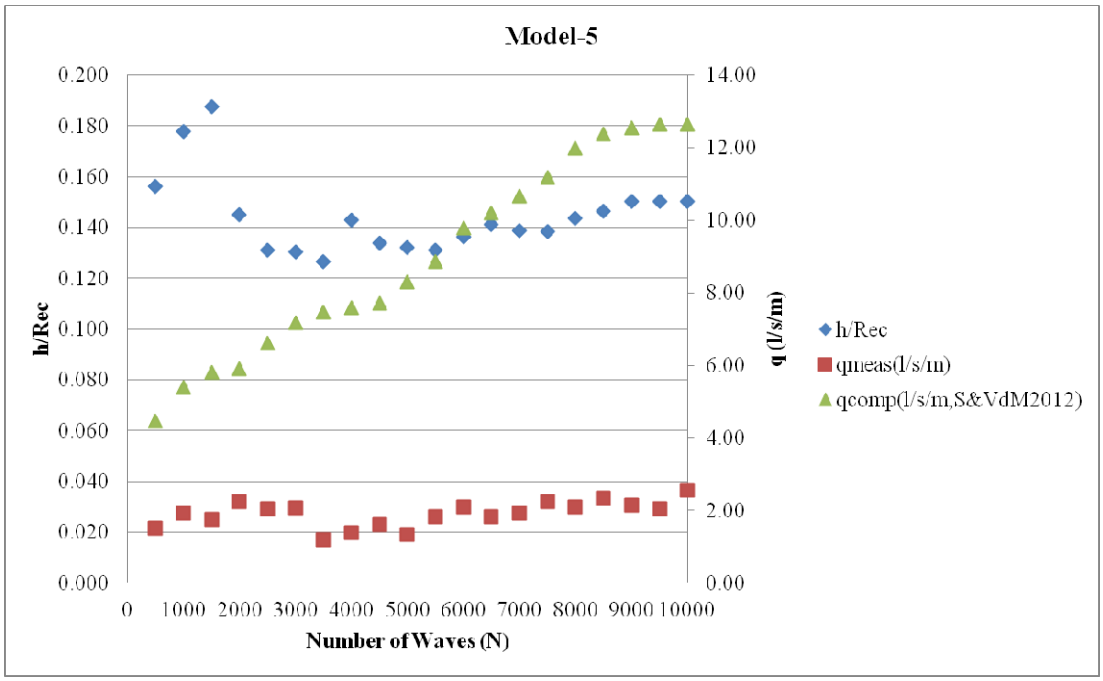

Figure 4.31: Damage vs. overtopping under cumulative damage for Model 5

Figure 4.29, Figure 4.30, and Figure 4.31 indicate that h/Rec parameter for all models remains approximately constant with number of waves (N) even though the damage on the structure increases. Moreover, Figure 4.31 also states that the overtopping results calculated by the Sigurdarson and Van der Meer (2012) formula have an increasing trend with number of waves whereas overtopping measurements obtained from the model experiments have a steady trend.

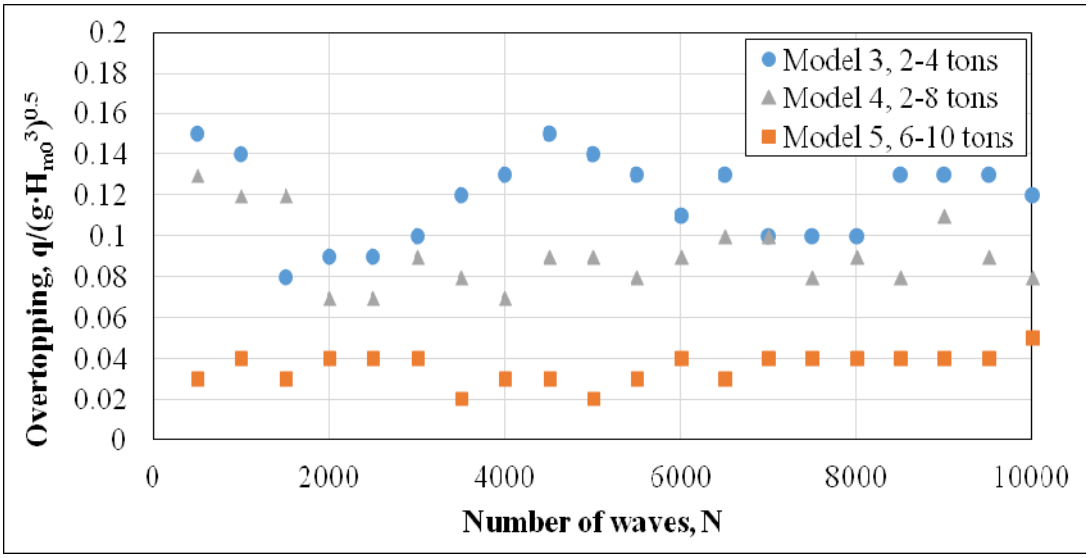

Figure 4.32: Number of waves vs. overtopping under cumulative damage

Figure 4.32 presents that overtopping measurements ($q/(g*H_{mo}^3)^{0.5}$) do not increase considerably with increasing number of waves (N) even though the damage on the structure increases. These results may be observed since the accumulation in front of the crest (h) increases while the berm width is exposed to recession. Therefore, significant changes are not observed in the overtopping measurements.

Figures given below indicate that all models show similar behaviour under the damage. The damage of the cross-sections is compared to each other and it can be said that when the damage increases on the structure, overtopping discharges do not change significantly.

Table 4.42 shows the summary of the stability and overtopping performances for the studied cross-sections.

Table 4.42: Summary of stability and overtopping performances

Name	Type of Reshaping	Theoretical Damage Parameter Range	Armour Stone Weight (tons)	Berm Width (m)	Total Volume of Cross-section (m^3/m)	Measured Average Damage Parameter After 1000 Waves	Measured Mean Overtopping Discharge (l/s/m)
Model 1	HR	2-8	12-15	15	1091.8	3.7	2.1
Model 2	FR	>20	2-4	11.5	774.3	32.9	72.7
Model 3	FR	>20	2-4	26	979.5	40.1	6.7
Model 4	FR	>20	2-8	26	981.7	27.1	6.5
Model 5	PR	10-20	6-10	26	984.9	10.2	1.6

Table 4.42 presents that measured damage parameters after 1000 waves of all models are compatible with the theoretical damage parameters. The effect of berm width on the mean overtopping discharge can be observed from the measured discharge values for Model 2 and Model 3. Moreover, Table 4.42 shows that Ordu-Giresun hardly reshaping berm breakwater might be designed as a reshaping berm breakwater with the same stability and serviceability conditions.

CHAPTER 5

CONCLUSION

In this study, Ordu-Giresun berm breakwater is investigated by testing the constructed cross-section and designed alternative sections with smaller stone sizes in order to make a comparison between the constructed section and alternative sections in terms of stability and serviceability conditions. All cross-sections are tested by physical model experiments, conducted in the wave flume of Middle East Technical University Coastal and Harbour Engineering Laboratory.

Stability of cross-sections is tested in terms of damage parameter and recession. Damage parameters and recession are obtained from both profile measurements and the analyses of video recordings. Damage parameters are calculated according to the formula given by Van der Meer (1988), and recession values are calculated according to the formula given by Lykke Andersen et al. (2014).

Serviceability of the cross-sections is tested by wave overtopping discharge. Results obtained from physical model experiments are compared to well-known wave overtopping manuals, which are TAW (2002), CLASH (Verhaeghe, et al., 2005), and the formula proposed by Sigurdarson and Van der Meer (2012).

Moreover, relationship between damage and wave overtopping is discussed.

Results of this study can be summarized as follows:

- Model 1, constructed Ordu-Giresun berm breakwater, has been designed as a hardly reshaping berm breakwater with an armour stone range of 12-15 tons in prototype scale. Both damage parameter and recession results indicate that

Model 1 fulfils the requirements of hardly reshaping berm breakwaters given by Sigurdarson and Van der Meer (2012). Moreover, measured wave overtopping discharge is in the allowable design overtopping range (<10 l/s/m).

- Model 2 is designed as a fully reshaping berm breakwater with an armour stone range of 2-4 tons and with a berm width (B) of 11.5 m in prototype scale. Both damage parameter and recession results indicate that Model 2 fulfils the requirements of fully reshaping berm breakwaters given by Sigurdarson and Van der Meer (2012). On the other hand, the cross-section does not satisfy the wave overtopping requirement; thus, Model 2 is not an appropriate alternative for Ordu-Giresun berm breakwater even the stability condition is satisfied.
- Model 3 is designed as a fully reshaping berm breakwater with an armour stone range of 2-4 tons and with a berm width (B) of 26 m in prototype scale. Both damage parameter and recession results indicate that Model 3 fulfils the requirements of fully reshaping berm breakwaters given by Sigurdarson and Van der Meer (2012). Furthermore, Overtopping requirements are satisfied compared to Model 2 with the increase in berm width.
- Model 4 is designed as fully reshaping berm breakwater with a stone range of 2-8 tons. Both damage parameter and recession results indicate that Model 4 fulfils the requirements of fully reshaping berm breakwaters given by Sigurdarson and Van der Meer (2012). Since the median stone diameter of Model 4 increases compared to Model 2 and Model 3, damage on the armour layer decreases even though they are all fully reshaping berm breakwaters. In addition, overtopping measurements are in the allowable range.
- Model 5, is designed as partly reshaping berm breakwater with a stone range of 6-10 tons. Both damage parameter and recession results indicate that Model 5 fulfils the requirements of partly reshaping berm breakwaters given by Sigurdarson and Van der Meer (2012). Moreover, measured wave overtopping discharge is in the allowable overtopping range.

- Cumulative damage analysis of alternative models, Model 3, Model 4, and Model 5, show that cross-sections get most of the damage within 1000 waves and after that damage follows a slowly decreasing path until they reach equilibrium. According to cumulative damage analysis, cross-sections reach equilibrium approximately at the end of 8000 waves.
- Overtopping calculations are compared to each other and it is seen that the results calculated by TAW (2002) are the highest values among three manuals and the measured quantities. Overtopping results calculated by CLASH (Verhaeghe et al., 2005) and by Sigurdarson and Van der Meer (2012) are more compatible with the measured overtopping results.
- In the literature, most of the design formulations do not include parameters regarding the number of waves in scope of wave overtopping. Similarly, after examining the results of this study it can be said that when the damage increases on the structure, overtopping discharges do not change significantly. This could be due to the fact as the damage progresses on the structure, the berm height increases obstructing wave overtopping and the berm width decreases promoting it.
- The results of this study show that Ordu-Giresun hardly reshaping berm breakwater might be designed as a reshaping berm breakwater with the same stability and serviceability conditions.

This study forms a base for future studies in order to have a better understanding on the design of berm breakwaters. However, there are certainly more questions on the design of berm type rubble mound breakwaters. These questions are left as future studies which are given as:

- Since limited number of physical model experiments is conducted in this study, model tests should be extended for future studies in order to validate the relationship between grading (and therefore porosity and resulting surface roughness of the structure) and wave overtopping.

- In order to observe the effect of material size in core and filter, different core and filter material which will have effect on the permeability of the structure can be used in future studies.
- Moreover, in order to observe the effect of toe structure, different alternative sections without toe structure should be investigated for future studies.

REFERENCES

Andersen, T. L., and Burcharth, H. F. (2010), *"A New Formula for Front Slope Recession of Berm Breakwaters",* Coastal Engineering*,* 57, 359-374.

Andersen, T. L., Meer, J. W., Burcharth, H. F., and Sigurdarson, S. (2012), "*Stability of Hardly Reshaping Berm Breakwaters",* Proc., Int. Conf. on Coastal Engineering, ASCE, Santander, Spain.

Andersen, T. L., Moghim, M. N., and Burcharth, H. F. (2014), *"Revised Recession of Reshaping Berm Breakwaters",* Proc., Int. Conf. on Coastal Engineering, ASCE, Seoul, Korea.

CE 593 Lecture Notes, (2014), METU, Ankara, Turkey.

Dalyrmple, R. A. (1985), "*Physical Modelling in Littoral Processes",* Recent Advances in Hydraulic Physical Modelling, R. Martins, Ed., Kluwer Academic Publishers, Dordrecht, the Netherlands.

Ergin, A., Günbak A. R., and Yanmaz, M. (1989), "*Rubble-mound Breakwaters with S-shape Design.",* J. Waterway, Port, Coastal, and Ocean Eng., 115.5, 579-593.

EurOtop Manual, (2007), Overtopping Manual, Wave Overtopping of Sea Defences and Related Structures, Assessment Manual.

Gent, M. R., Boogaard, H. F., Pozueta, B., and Medina, J. R. (2007), *"Neural Network Modelling of Wave Overtopping at Coastal Structures", Coastal Engineering, 54*(8), 586-593.

Goda, Y., Suzuki, Y. (1976), *"Estimation of Incident and Reflected Waves in Random Wave Experiments",* Proceedings of 15th International Conference on Coastal Engineering, Honolulu, Hawaii, USA

Günbak, A.R., Güler I., and Gökçe, T. (1988), *"Samandağ Balıkçı Barınağı Araştırması Sonuç Raporu",* 87-03-03-04. Middle East Technical University Civil Engineering Department Coastal and Harbor Engineering Laboratory, Ankara.

Hudson, R. Y. (1959), *"Laboratory Investigations of Rubble Mound Breakwaters",* J. Waterways & Harbors Division, ASCE, Vol 85, No WW3, Paper No 2171, pp 93-121.

Hudson, R. Y., Hermann, F. A., Sager, R. A., Whalin, R. W., Keulegan, G. H., Chatham, C. E., and Hales, L. Z. (1979), *"Coastal Hydraulic Models",* Special Report No.5, US Army Engineer Waterways Experiment Station, Vicksburg, Missisippi

Hughes, S. A. (1993), *"Physical Models and Laboratory Techniques in Coastal Engineering",* Advanced Series on Ocean Engineering, Vol 7, World Scientific, Singapore

Kamphius, J. W. (1991), *"Physical Modeling",* Handbook of Coastal and Ocean Engineering, J. B. Herbich, Ed., Vol 2, Gulf Publishing Company, Houstan, Texas, USA

Le Mehaute, B. (1990), *"Similitude",* Ocean Engineering Science, B. Le Mehaute, Ed., Vol 9, Part B in the series The Sea, John Wiley and Sons, New York, pp 955-980.

Moghim, M., Shafieefar, M., Tørum, A., and Chegini, V. (2011), *"A New Formula for the Sea State and Structural Parameters Influencing the Stability of Homogenous Reshaping Berm Breakwaters",* Coastal Engineering*,* 58.8, 706-721.

PIANC, (2003), *"State-of-the-Art of Designing and Constructing Berm Breakwaters",* WG40.

Shekari, M. R. and Shafieefar, M., (2012), *"An Experimental Study on the Reshaping of Berm Breakwaters Under Irregular Wave Attacks",* Applied Ocean Research, 42, 16-23.

Sigurdarson, S., Mocke, R., Primmer, M., and Gretarsson, S. (2011), *"The Icelandic-type Berm Breakwater",* Proceedings of the 20th Australasian Coastal and Ocean Engineering Conference and the 13th Australasian Port and Harbour Conference. Barton, A.C.T.: Engineers Australia, 676-681.

Sigurdarson, S., Smarason, O.B., and Vigosson, G. (2006), *"Berm breakwater" Port engineering,* 5th ed., P. Bruun.

TAW (2002), *"Wave Run-Up and Wave Overtopping at Dikes",* Technical Report, Technical Advisory Committee on Flood Defense, Delft.

TDG Scientific Measuring Ltd., (2016).

Tørum A. and Krogh, S. R., (2000), *"Berm Breakwaters",* Stone Quality. Civil and Enviromental Engineering, 2000.

Van der Meer, J. W. (1988), *"Rock Slopes and Gravel Beaches under Wave Attack",* Ph. D. Thesis, Delft University, the Netherlands.

Van der Meer, J. W., and Sigurdarson, S. (2012), *"Wave Overtopping at Berm Breakwaters in line with EurOtop", Proc., Int. Conf. on Coastal Engineering,* ASCE, Santander, Spain.

Van der Meer, J. W., and Sigurdarson, S. (2014), "*Geometrical Design of Berm Breakwaters", Proc., Int. Conf. on Coastal Engineering,* Seoul, Korea.

Verhaeghe, H., (2005), "*Neural Network Prediction of Wave Overtopping at Coastal Structures",* Ph.D. Thesis, Universiteit Gent, Gent, Belgium.

Figure 2.1. The Sirevåg berm breakwater. (2012), *"Armourstone for the icelandic-type berm breakwater.",* Retrieved from https://www.researchgate.net/figure/266260481_fig4_Figure-5-The-Sirevag-berm-breakwater (Agu. 3, 2016).

Figure 2.2. Ordu-Giresun Havalimanı. Retrieved from http://www.dhmi.gov.tr/fotogaleri.aspx?hv=54# (Agu. 1, 2016).

Figure 2.4. Input parameters for wave overtopping in CLASH. Retrieved from http://www.nn-overtopping.deltares.nl (Agu. 1, 2016).

APPENDICES

A) WAVE PARAMETERS MEASURED IN THE MODEL EXPERIMENTS

Table A.1: Wave parameters in the physical model experiments for Model 1

Name	Set No	Number of Waves	Wave Calibration (Empty Channel) Experiments		Structure Experiments			
			H_s (m)	T_s (s)	$H_{s,\ toe}$ (m)	$T_{s,\ toe}$ (s)	$H_{s,\ empty}$ (m)	$T_{s,\ empty}$ (s)
Model 1 (12-15 tons)	Set-1	500	6.39	11.04	6.89	11.12	6.93	10.88
		1000	6.37	11.09	6.85	11.22	6.86	10.88
	Set-2	500	6.20	10.94	6.46	10.99	6.80	11.06
		1000	6.17	11.01	6.44	11.11	6.79	11.09
	Set-3	500	6.52	11.20	6.65	11.17	6.27	11.04
		1000	6.40	11.27	6.59	11.07	6.22	11.05
		1500	6.52	11.18	6.64	11.09	6.30	11.02
		2000	6.73	11.24	6.71	11.12	6.97	11.00
		2500	6.69	11.31	6.62	11.12	6.95	11.06
		3000	6.68	11.28	6.66	11.12	6.91	11.05
		3500	6.60	11.23	6.82	11.09	6.79	11.02
		4000	6.54	11.25	6.79	11.09	6.74	11.12
		4500	6.60	11.28	6.82	11.03	6.77	11.07
		5000	6.55	11.30	6.80	11.14	6.74	11.07
		5500	6.55	11.15	6.83	11.04	6.76	11.06
		6000	6.48	11.23	6.76	11.11	6.71	11.09
		6500	6.50	11.21	6.77	11.00	6.69	11.07
		7000	6.52	11.28	6.84	11.17	6.75	11.10
		7500	6.09	11.22	6.73	11.12	6.72	11.03
		8000	5.99	11.17	6.64	11.06	6.66	11.02
		8500	5.97	11.29	6.64	11.04	6.65	11.06
		9000	5.93	11.26	6.61	11.06	6.65	11.10
		9500	5.95	11.21	6.62	11.11	6.66	11.07
		10000	6.04	11.23	6.69	11.17	6.73	11.04

Table A.2: Wave parameters in the physical model experiments for Model 2

Name	Set No	Number of Waves	Wave Calibration (Empty Channel) Experiments		Structure Experiments			
			H_s (m)	T_s (s)	$H_{s,\ toe}$ (m)	$T_{s,\ toe}$ (s)	$H_{s,\ empty}$ (m)	$T_{s,\ empty}$ (s)
Model 2 (2-4 tons B=11.5m)	Set-1	500	6.85	11.05	6.75	11.15	6.93	11.05
		1000	6.76	10.88	6.72	11.26	6.85	11.02
	Set-2	500	6.69	11.01	6.69	11.26	6.79	10.90
		1000	6.57	11.03	6.61	11.24	6.76	10.92
	Set-3	500	6.22	11.21	6.17	11.08	6.18	11.13
		1000	6.16	11.15	6.12	11.06	6.11	11.12

Table A.3: Wave parameters in the physical model experiments for Model 3

Name	Set No	Number of Waves	Wave Calibration (Empty Channel) Experiments		Structure Experiments			
			H_s (m)	T_s (s)	$H_{s,\ toe}$ (m)	$T_{s,\ toe}$ (s)	$H_{s,\ empty}$ (m)	$T_{s,\ empty}$ (s)
Model 3 (2-4 tons B=26m)	Set-1	500	6.61	10.99	6.65	11.05	6.40	11.01
		1000	6.52	11.01	6.63	11.10	6.40	11.04
	Set-2	500	6.41	11.13	6.43	11.33	6.83	10.90
		1000	6.27	11.19	6.45	11.30	6.81	10.89
		1500	6.30	11.06	6.56	11.26	6.61	10.89
		2000	6.25	11.04	6.51	11.30	6.62	10.95
		2500	6.55	11.13	6.73	11.29	6.94	10.90
		3000	6.48	11.07	6.66	11.22	6.89	10.85
		3500	6.50	11.09	6.61	11.30	6.92	10.88
		4000	6.50	11.13	6.67	11.24	6.93	10.92
		4500	6.67	11.09	6.68	11.23	6.88	10.89
		5000	6.63	11.10	6.56	11.31	6.81	10.87
		5500	6.67	11.12	6.61	11.28	6.84	10.87
		6000	6.60	11.11	6.57	11.25	6.85	10.88
		6500	6.79	11.10	6.90	11.33	7.16	10.91
		7000	6.80	11.05	6.91	11.31	7.15	10.87
		7500	6.79	11.14	6.94	11.24	7.20	10.93
		8000	6.81	11.07	6.89	11.31	7.18	10.93
		8500	6.40	11.03	6.56	11.21	6.42	10.90
		9000	6.38	11.02	6.55	11.30	6.37	10.83
		9500	6.38	11.04	6.50	11.19	6.35	10.86
		10000	6.37	11.13	6.54	11.32	6.35	10.91

Table A.4: Wave parameters in the physical model experiments for Model 4

Name	Set No	Number of Waves	Wave Calibration (Empty Channel) Experiments		Structure Experiments			
			H_s (m)	T_s (s)	$H_{s,\ toe}$ (m)	$T_{s,\ toe}$ (s)	$H_{s,\ empty}$ (m)	$T_{s,\ empty}$ (s)
Model 4 (2-8 tons)	Set-1	500	6.70	10.99	6.61	10.98	6.61	10.98
		1000	6.61	10.99	6.64	11.12	6.59	11.09
	Set-2	500	7.28	11.08	7.09	11.24	7.25	11.00
		1000	7.18	11.09	7.08	11.23	7.19	10.98
	Set-3	500	6.64	11.27	6.71	11.23	5.53	12.27
		1000	6.64	11.23	6.71	11.17	5.52	12.59
		1500	6.80	11.28	6.81	11.21	6.70	11.03
		2000	6.71	11.31	6.75	11.17	6.66	11.05
		2500	6.72	11.30	6.82	11.20	6.66	11.04
		3000	6.56	11.25	6.65	11.23	6.54	11.08
		3500	6.63	11.30	6.76	11.13	6.55	11.05
		4000	6.61	11.29	6.67	11.22	6.56	11.07
		4500	6.61	11.28	6.69	11.21	6.66	11.07
		5000	6.64	11.27	6.67	11.26	6.67	11.06
		5500	6.63	11.31	6.63	11.20	6.64	11.06
		6000	6.64	11.38	6.69	11.27	6.69	11.10
		6500	6.60	11.25	6.62	11.15	6.65	11.12
		7000	6.56	11.24	6.58	11.21	6.59	11.06
		7500	6.62	11.30	6.68	11.23	6.62	11.07
		8000	6.64	11.27	6.63	11.21	6.62	11.13
		8500	6.56	11.30	6.77	11.20	7.01	11.12
		9000	6.49	11.23	6.73	11.20	6.97	11.10
		9500	6.49	11.23	6.73	11.22	7.01	11.15
		10000	6.54	11.28	6.75	11.18	6.96	11.09

Table A.5: Wave parameters in the physical model experiments for Model 5

Name	Set No	Number of Waves	Wave Calibration (Empty Channel) Experiments		Structure Experiments			
			H_s (m)	T_s (s)	$H_{s,\ toe}$ (m)	$T_{s,\ toe}$ (s)	$H_{s,\ empty}$ (m)	$T_{s,\ empty}$ (s)
Model 5 (6-10 tons)	Set-1	500	6.77	11.13	6.61	11.29	6.17	11.10
		1000	6.77	11.05	6.61	11.30	6.17	11.16
		1500	7.03	11.09	6.99	11.23	7.00	11.01
		2000	6.98	11.07	6.94	11.24	6.93	11.04
		2500	6.97	11.06	6.98	11.28	6.95	11.07
		3000	7.01	11.14	6.98	11.20	6.97	10.98
		3500	6.92	11.11	6.95	11.32	6.96	11.09
		4000	6.91	11.11	6.96	11.23	6.93	11.08
		4500	6.74	11.08	6.73	11.30	6.56	10.99
		5000	6.69	11.12	6.72	11.23	6.53	10.89
		5500	6.75	11.18	6.76	11.22	6.55	10.94
		6000	6.71	11.13	6.74	11.26	6.57	11.08
		6500	6.72	11.10	6.75	11.21	6.57	11.04
		7000	6.73	11.10	6.77	11.24	6.54	11.03
		7500	6.52	11.06	6.84	11.30	6.82	10.95
		8000	6.50	11.13	6.83	11.21	6.80	10.98
		8500	6.48	11.08	6.81	11.21	6.85	11.03
		9000	6.53	11.07	6.88	11.21	6.81	10.95
		9500	6.44	11.07	6.76	11.23	6.76	10.95
		10000	6.46	11.06	6.81	11.32	6.83	10.98
	Set-2	500	6.70	11.12	6.62	11.29	6.65	11.05
		1000	6.65	11.14	6.62	11.27	6.70	11.02